Optimization of Off-grid Photovoltaic Systems

by

Dongjin Cho

A dissertation submitted to the Graduate Faculty of
Auburn University
in partial fulfillment of the
requirements for the Degree of
Doctor of Philosophy

Auburn, Alabama
May 2, 2020

Key words: Off-grid PV system, PV array capacity, Battery capacity, Stochastic optimization, Mixed integer programming, Energy consumption scheduling

Approved by

Jorge Valenzuela, Chair, Professor of Industrial and Systems Engineering
Dianne Hall, Professor of Information Systems and Business Analytics
Kang Bok Lee, Associate Professor of Information Systems and Business Analytics
Alexsandr Vinel, Assistant Professor of Industrial and Systems Engineering

Abstract

Among various renewable energy sources, solar energy is considered one of the most effective solutions because it is abundant, eco-friendly, sustainable energy resources to address the energy shortage of the present and future. Electricity generation by an off-grid photovoltaic (PV) system is particularly effective in isolated areas where there is no access to any other source of electricity. However, it makes difficult to estimate the cost-effective capacity of an off-grid energy system under the inherent nature of solar irradiance, unexpected climate changes and energy demand uncertainty. The objective of the dissertation is to develop mathematical optimization models that assist and improve the decision-making process in designing the optimal capacity of a residential off-grid PV-battery system under uncertainties. In the first chapter, a mathematical model for energy consumption scheduling of an off-grid PV-battery system problem is proposed. It is a mixed-integer programming problem that considers energy consumption patterns and appliance priorities. The model pre-schedules appliance operation that maximizes the operation of higher priority appliances given the forecasted solar irradiance. It is represented how it can be solved on case studies based on region and season. The results demonstrate that the proposed model provides optimal schedules for operating the higher-priority appliances. In the second chapter, an off-grid PV system design approach that considers energy consumption scheduling and system operation under solar irradiance uncertainty is developed. The solution method combined the Nelder-Mead algorithm, mixed-integer programming, and Monte Carlo simulation. The day-ahead schedule

obtained by the energy consumption scheduling model is executed on a Monte Carlo simulation that considers the uncertainty of solar irradiance. The performance of the algorithm is tested using solar irradiance data at two locations in the USA. Based on the simulation results, the algorithm finds the cost-efficient capacity of the energy system at a minimum annual equivalent cost (AEC). Finally, in the third chapter, a stochastic optimization model that simultaneously considers scenarios to represent the uncertainty of solar irradiance and energy consumption scheduling is studied. The resulting model is a complicated multi-objective mixed integer programming problem. The model aims to determine the optimal PV array and battery capacity to supply the energy demand at minimum AEC of the energy system in variation of solar irradiance occurrences. Experimental results confirm that the stochastic optimization model better estimates the energy system capacity at minimum AEC than the non-optimized deterministic model. Moreover, 20-scenario model is more effective than less-scenario models since the solution obtained by 20-scenario model satisfies energy demand under all number of scenarios considered.

Acknowledgments

First, and most of all, I am deeply grateful to my advisor Dr. Jorge Valenzuela for his encouragement and advice during the Ph.D. program at Auburn University. His feedback on my research, academic expertise and mentorship made it possible to complete my journey to Ph.D.

I thank Dr. Dianne Hall, Dr. Kangbok Lee, and Dr. Alexander Vinel for serving on my dissertation committee. The instruction and feedback that I received were invaluable. Also, I am thankful to Dr. Timothy McDonald for reviewing my dissertation as a university reader.

I would like to thank the friends I have made during the Ph.D. program: Dr. Kyoungsun Kim, Dr. Hyuncheol Baik, Chanok Han, Dr. Nasrin Mohabbati-Kalejahi, and Dr. LuAnn Carpenter. Particularly, a special thanks to an old friend of mine, Dr. Sahnah Lim, an assistant professor at NYU for proofreading and reviewing my dissertation and published papers.

As a military officer who has been supported by the Republic of Korean Army, I would like to thank the government of the Republic of Korea. Also, I deeply appreciate my senior officer Col. Ikhyun Kim (Dr.) for his warm encouragement as a mentor

I would like to thank my parents in heaven and relatives for their endless love and encouragement. Special thanks to my beloved wife - Mijung (Kelly) - and two lovely daughters - Yerin (Irene), Serene (Eva) - for their dedicated love and support throughout my life. None of this would have been possible without you all. I love you all from the bottom of my heart.

Finally, I give the Lord all my glory, and thanks.

List of Tables

List of Figures

List of Abbreviations

PV	Photovoltaic
GHG	Greenhouse Gas
CO2	Carbon Dioxide
MILP	Mixed Integer Linear Programming
PAR	Peak-to-Average-Ratio
SOC	State of Charge
STC	Standard Test Condition
OECD	Organization for Economic Co-operation and Development
AEC	Annual Equivalent Cost
EIA	U.S Energy Information Administration
LSLP	Loss of Power Supply Probability

Table of Contents

Introduction

Today, energy resources are one of the most important factors for sustainable human development. However, fossil fuels, on which humans have been depending heavily during several decades, are confronted with the serious problem of depletion. Industrialization and growing population size bring about the rapid growth in electricity usage, which is generated by conventional natural resources such as oil, coal, and gas. These processes also contribute to an increase in greenhouse gas (GHG) and carbon dioxide (CO2) emission, which have a hazardous influence on the atmosphere of the earth. In particular, global warming caused by the greenhouse gas effect is associated with the extreme weather phenomenon, posing a great threat to human survival. For these reasons, developing eco-friendly renewable energy sources becomes a crucial factor in the sustainable prosperity of human beings. In recent years, power generation technologies for renewable energy sources such as solar, wind, biomass, and tide have been studied. These renewable energy sources have gained popularity since it is clean, environmentally friendly and abundant, and can reduce dependence on conventional fossil fuels.

Among various renewable energy resources, solar energy has great potential to meet the future needs of the world. Several solar energy generating methods have been developed so far; the photovoltaic (PV) energy system directly converts solar irradiance into electricity via PV arrays and is one of the most popular renewable energy systems. It has a longer life cycle than other renewable energy systems, is easy to operate and maintain, and offers flexible installing based on

the geographical features or user energy demand since it is composed of several modules. In particular, the deployment of a standalone PV-battery energy system in isolated areas such as islands or rural areas where the grid network cannot be constructed will be useful in solving energy deficiency problems in those areas and can become a promising solution to deal with the increasing energy demand of the world in the future. However, in an off-grid PV-battery system, optimal energy management is required because the sun is the only energy source to generate electricity, which is time-dependent and limited to day hours. An effort to find an optimal capacity of the energy system is also needed to satisfy user energy demand within a limited budget. With such characteristics of an off-grid PV energy system in mind, in this dissertation, we have developed optimization models to determine energy consumption schedules and the energy system capacity under uncertainties.

The remainder of this dissertation is organized as follows. Chapter 1 presents an optimization model to find daily optimal schedules of home appliances to maximize the usage of high-priority appliances given PV array and battery capacities. Chapter 2 proposes a Nelder-Mead algorithm for designing a residential off-grid PV system. Chapter 3 describes a stochastic optimization model for determining the capacity of a residential off-grid PV-battery system considering solar irradiance uncertainty and hourly energy consumption patterns.

Chapter 1 Scheduling Energy Consumption for Residential Off-grid Photovoltaic Systems

1.1 Abstract

Among various renewable energy sources, solar energy is considered an effective solution to the shortage of energy in the future. A stand-alone photovoltaic (PV) system can be particularly impactful in an isolated area where access to the grid is limited or unavailable. Because solar energy generation primarily depends on the availability of solar irradiance over time, energy management is crucial, which in turn can also satisfy user comfort and system efficiency. In this paper, we propose an energy consumption scheduling model for a residential house with a stand-alone PV system and battery. We develop a mixed-integer optimization model that uses consumption patterns and appliance priority to schedule the use of appliances. We test our model under four scenarios based on region and season. The results demonstrate that the proposed model provides optimal schedules for operating the appliances. In addition, we conduct a sensitivity analysis on PV array and battery capacities. We compare the optimized case with the non-optimized case.

Keywords: Stand-alone PV system, Optimal Energy Scheduling, Battery Capacity, Mixed-Integer Programming

1.2 Introduction

A recent report from the United Nations shows that 1.1 billion people around the world do not have access to electricity and another one billion more have limited access only to an unreliable electrical grid [1]. For an isolated area where access to the grid is limited or nonexistent, an off-grid energy system that uses renewable energy sources such as solar and wind is a promising solution to the shortage of reliable electric energy [2]. Among various renewable energy sources, solar energy is a particularly attractive solution due to its inherent features since it is abundant, cost-free, sustainable and eco-friendly [3]. However, the amount and availability of solar irradiance depend on several factors such as the time of the day, season, and geographic area. The time-dependence is the main difficulty that an isolated PV system faces [4]. To cope with these complications, a stand-alone system would require the use of a battery to store the energy. The battery can provide continuous and reliable power to guarantee satisfaction from the demand side. But energy storage is costly and can make the operation of a stand-alone energy system more complicated [5]. To address these challenges, we propose an optimal energy management model to achieve higher system efficiency and user comfort.

In recent years, various algorithms and methodologies have been proposed to optimize energy in residential areas by reducing operational costs and maximizing user comfort. In [6], the authors examined flexible convex programming optimization for automatic load management of various home appliances to reduce the operating cost and user discomfort. In [7], a Mixed Integer Linear Programming (MILP) model and heuristic algorithm are used to schedule appliances by taking into consideration total cost and climatic factors. In [8], the authors used an integer linear programming approach to reduce total cost and optimize the use of the grid capacity. In [9], a simple linear programming model was formulated to adjust hourly load levels in response to hourly

electricity cost. In [10], a particle swarm optimization method was used to schedule distributed energy resources. In [11], the authors used a genetic algorithm approach to combine a real-time pricing model with an inclining block model to minimize total cost and peak-to-average ratio. In [12], a robust optimization methodology is used to minimize the operating costs of temperature-related appliances. Moreover, in [13], a two-stage pricing approach is used to reduce electricity costs while maintaining user comfort. In addition to these studies, mixed-integer programming is used in [14] to schedule appliances by minimizing total energy cost, and, in [15], the authors schedule energy to reduce total energy cost and peak-to-average-ratio (PAR) in load demand using the game theory approach. In the reviewed literature, the primary objective is to minimize the total cost of an on-grid renewable energy system under a dynamic pricing environment in which the price of the energy changes with every period. In contrast, our objective is to maximize the use of appliances by using the available solar energy. In our model, no energy from the grid is available, and no benefit is obtained from unused solar energy. Moreover, there are few studies that examine energy scheduling in an off-grid residential energy system with a single renewable energy source. We propose an energy management optimization model for an off-grid PV system with energy storage to achieve higher system efficiency and satisfy user comfort. The contributions of this paper are:

- A mathematical model to schedule operation times of appliances based on user consumption pattern

- An examination of effects for PV array and battery capacities on the user demand satisfaction

The remainder of this paper is organized as follows: Section 2 presents the proposed model. Section 3 discusses the case study and the results. Finally, section 4 ends with concluding remarks.

1.3 The proposed model

The proposed scheduling energy consumption model uses consumption patterns, priority usage of appliances, and solar irradiance daily forecast to pre-schedule the operation time of appliances with the objective to maximize the operation of higher priority appliances given the forecasted available energy. The model assumes that the energy generating system is an off-grid system consisting of a PV array, a battery, a PV charging controller, and an inverter to power all appliances in a rural home. The appliances are assumed to operate in a binary manner -- 'on' or 'off' (1 or 0). Figure 1.1 illustrates this energy system.

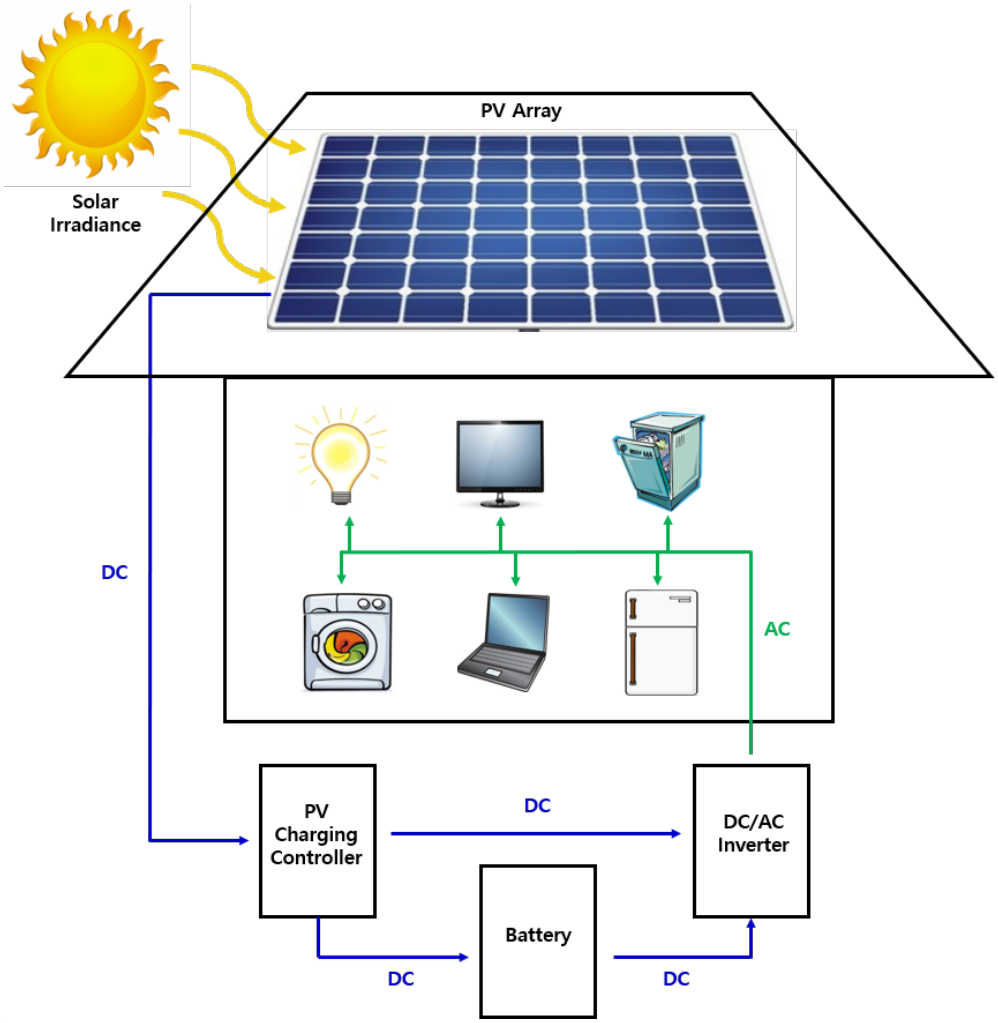

Figure 1.1 Proposed energy system

In Figure 1.1, the PV array converts the solar irradiance into electric energy during the daytime. Most of the energy is used to operate the appliances and the remaining energy (if any) is stored in the battery through the PV charging controller. The DC/AC inverter converts the DC power into AC power required to operate the appliances. The battery is used at nighttime and sometimes at daytime when there is not enough solar irradiance to operate the appliances. Temperature related appliances such as an air conditioner, heater, and a water boiler are not considered here because they usually consume a large amount of energy and a PV array may not be capable of powering them.

1.3.1 Operation cycle

We divide a day into L equal periods of length $\mathrm{T} = \frac{24}{\mathrm{L}}$ hours. All parameters and variables are measured at the end of a period. Thus, a period t starts from time $t-1$ and ends at time t. The operation cycle of an appliance in a day is determined by the required number of periods T_a. These values indicate that the user would like to operate the appliance as much as T_a periods.

1.3.2 Operation flexibility

We define two types of appliances, flexible and inflexible. For a flexible appliance, the operation cycle can be scheduled at any time during a day. A washing machine and a dishwasher are examples of flexible appliances. In contrast, an inflexible appliance must be scheduled as requested by the user. A television and a light bulb are examples of inflexible appliances.

1.3.3 Operation period preference

To represent the operation period preference, we use a binary matrix P. The entry $P_{a,t}$ of the matrix is equal to "1" if the user prefers to operate the appliance a during the period t. The matrix P does not represent the number of times the appliance is required to operate. Therefore, to model an appliance required to operate twice (or more) during a day, we replace it with two (or more) appliances. Figure 2 shows an example of matrix P for three appliances. We assume that $T_a = 2$ hours for all of the appliances. In Figure 1.2, Appliance 1 is flexible and can operate for two consecutive hours at any period. Appliance 2 is flexible and may operate either between 8 AM and 10 AM or between 6 PM and 8 PM. Appliance 3 is inflexible and is required to operate twice during the day for two hours each time. Appliance 3 is, therefore, represented by appliances 3-1 and 3-2.

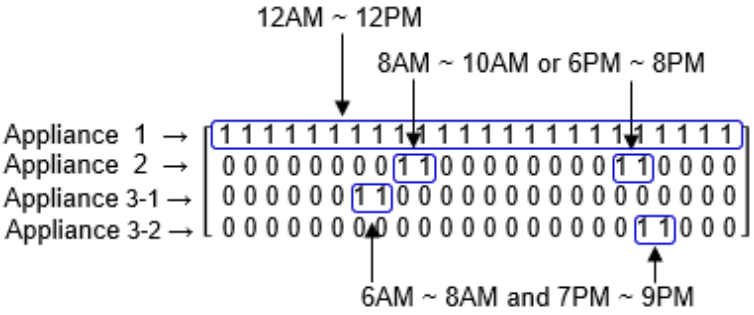

Figure 1.2 Operation period preference matrix

1.3.4 Operation priority

Considering that an off-grid energy system may not produce enough energy to operate all appliances as desired, we use the priority weight 1 - 10 to prioritize the operation of the appliances. A high priority weight indicates a high operation priority. We define matrix W to indicate the operation priority of the appliances. The entry W_a of the matrix indicates the priority of operating

appliance a during any given day. Figure 1.3 shows the entries of the operation priority matrix W for the three appliances mentioned above. In Figure 1.3, Appliance 1 has the highest operation priority, and Appliance 3-2 has the lowest operation priority on any given day.

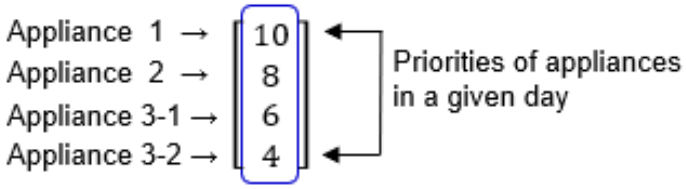

Figure 1.3 Operation priority matrix

1.3.5 Appliance sequence precedence

An appliance may require that another appliance completes its cycle before the appliance can start operating. For example, a dryer machine may not start unless the washing machine has ended its cycle. We define the set S to include all appliances that are preceded by at least one appliance and the set S_a to describes the appliances that precede a.

$$S_a = \{a_1, a_2, \dots a_s\} \text{ where } a_k \in \{1,2, \dots, A\} \text{ and } a \in S$$

1.3.6 Uninterruptible appliance

An appliance (i.e., a dishwasher) may require that its operation not stop before its cycle ends. We define the set U^{app} to group the uninterruptible appliances.

$$U^{app} = \{a_1, a_2, \dots a_s\} \text{ where } a_k \in \{1,2, \dots, A\}$$

1.3.7 Solar energy

The solar irradiance of period t, denoted by $\mathrm{S}_t^{\mathrm{PV}}$, is converted into solar energy $\mathrm{E}_t^{\mathrm{PV}}$ by an array of solar panels. The conversion function is given by Eq. (1.1) [16].

$$\mathrm{E}_t^{\mathrm{PV}} = \mathrm{S}_t^{\mathrm{PV}} * \mathrm{R}^{\mathrm{PV}} * \mathrm{A}^{\mathrm{PV}} \tag{1.1}$$

where R^{PV} and A^{PV}indicate efficiency and the area of the PV array, respectively. For the solar irradiance $\mathrm{S}_t^{\mathrm{PV}}$, we use the National Solar Radiation Database from the National Centers for Environmental Information of National Oceanic and Atmosphere Administration [17].

1.3.8 Model formulation

1.3.8.1 Objective function

The purpose of the optimization model is to schedule the use of limited solar energy for the operation of appliances based on their priority and period preference. The objective function is defined in Eq. (1.2).

$$\max. \sum_{t=1}^{\mathrm{T}} \sum_{a=1}^{\mathrm{A}} \mathrm{W}_a * x_{a,t}^{\mathrm{app\_state}} \tag{1.2}$$

Parameter W_a is the user-defined priority weight of the appliances and the decision binary variable $x_{a,t}^{\mathrm{app\_state}}$ represents the operation state of the appliances. Since the scheduling of the appliances is sensitive to the values of W_a, the values can be changed to force a solution more desirable to the user. The objective function is subject to the following constraints (1.3) - (1.18).

1.3.8.2 PV Energy Output

The constraint given in Eq. (1.3) states that the PV energy output ($\mathrm{E}_t^{\mathrm{PV}}$) equals, at any period t, the energy to operate the appliances ($e_t^{\mathrm{app\_pv}}$) plus the energy to charge the battery (e_t^{chr}), and plus the energy loss ($e_t^{\mathrm{loss\_pv}}$).

$$e_t^{\mathrm{app\_pv}} + e_t^{\mathrm{chr}} + e_t^{\mathrm{loss\_pv}} = \mathrm{E}_t^{\mathrm{PV}} \tag{1.3}$$

1.3.8.3 Total Energy Consumed

The constraint given in Eq. (1.4) states that the energy consumed by all appliances that are "on" is derived from the PV array ($e_t^{\mathrm{app\_pv}}$) and/or the battery ($e_t^{\mathrm{app\_bat}}$) at each period.

$$\sum_{a=1}^{\mathrm{A}} \mathrm{E}_a * x_{a,t}^{\mathrm{app\_state}} + \mathrm{E}_t^{\mathrm{M}} = (e_t^{\mathrm{app\_pv}} + e_t^{\mathrm{app\_bat}}) * \mathrm{R}^{\mathrm{INV}} \tag{1.4}$$

The parameter E_a is the energy consumption of an appliance and $\mathrm{E}_t^{\mathrm{M}}$ is extra energy for operating appliances occasionally.

1.3.8.4 Battery Charge and Discharge

The state of charge (SOC) of the battery is defined as the ratio of its current energy level to its nominal capacity. We assume that the battery starts with a SOC equal to 30%. The SOC at all periods is calculated by Eq. (1.5) [18].

$$s_t^{\mathrm{bat}} = s_{(t-1)}^{\mathrm{bat}} * (1 - \mathrm{R}^{\mathrm{DCH}}) + \frac{\left(e_t^{\mathrm{chr}} * \mathrm{R}^{\mathrm{CHR}}\right)}{\mathrm{C}^{\mathrm{BAT}}} - \frac{e_t^{\mathrm{app\_bat}}}{\mathrm{C}^{\mathrm{BAT}}} \tag{1.5}$$

To ensure enough SOC of the battery for the next day, the SOC of the battery at the last period (T) should be greater than or equal to S^{ESC} .

$$s_T^{bat} \geq S^{ESC} \tag{1.6}$$

To guarantee a durable life of the battery, the SOC should be between S^{MIN} and S^{MAX} at all periods.

$$S^{MIN} \leq s_t^{bat} \leq S^{MAX} \tag{1.7}$$

The Eq. (1.8) ensures that charging and discharging of the battery cannot occur at the same period.

$$y_t^{chr} + y_t^{dch} \leq 1 \tag{1.8}$$

where the variables y_t^{chr} and y_t^{dch} are binary and represent charging or discharging of the battery, respectively.

For technical specifications, the energy discharged from the battery must be less than or equal to the maximum discharging energy (R^{MDC}) at all periods.

$$e_t^{app\_bat} \leq y_t^{dch} * R^{MDC} \tag{1.9}$$

Similarly, the energy charged to the battery must be less than or equal to the maximum charging energy (R^{MCH}) at all periods.

$$e_t^{chr} \leq y_t^{chr} * R^{MCH} \tag{1.10}$$

1.3.8.5 Appliance Daily Operation

When there is not enough energy in the system, the Eq. (1.11) enforces that an appliance might not operate the number of operation periods defined by the user.

$$\sum_{t=1}^{T} x_{a,t}^{app\_state} \leq T_a \tag{1.11}$$

The Eq. (1.12) ensures that an uninterruptible appliance either operates the whole cycle T_a or it does not operate.

$$\sum_{t=1}^{T} x_{a,t}^{app\_state} = T_a * z_a \qquad \forall\, a \in U^{app} \tag{1.12}$$

Where variable z_a is a binary variable.

1.3.8.6 Operation Period Preference

Eq. (1.13) ensures that an appliance will only operate during a period that the user defined it as preferred.

$$x_{a,t}^{app\_state} \leq P_{a,t} \tag{1.13}$$

A value one of the binary parameter $P_{a,t}$ indicates that the appliance operates preferably during the preferred period t defined by the user.

1.3.8.7 Sequential Operation

Eq. (1.14) and Eq. (1.15) enforce the sequence precedence for appliances in the set S.

$$\mathrm{T}_{a^*} - \sum_{n=1}^{\mathrm{N}} x_{a^*,n}^{\text{app\_state}} \leq \mathrm{M} * \left(1 - x_{a,t+1}^{\text{app\_state}}\right) \quad \forall\, a \in \mathrm{S}, a^* \in \mathrm{S}_a, \text{and } \mathrm{N} = 1,2,..,t \quad (1.14)$$

$$x_{a,1}^{\text{app\_state}} = 0 \quad (1.15)$$

Where M is a big number. In Eq. (1.14), the operation of appliance a is preceded by appliance a^*. At each period t, when the left-hand side is equal to zero (appliance a^* finished its operation), appliance a can be "on" or "off" ($x_{a,t+1}^{\text{app\_state}}$= 1) at period $t+1$. If the left-hand side is positive (appliance a^* has not finished its operation), appliance a should be "off" ($x_{a,t+1}^{\text{app\_state}}$= 0) at period $t+1$. Defining M as a big number ensures that the constraint is satisfied when appliance a^* has not finished its operation. Eq. (1.15) enforces the operation status of appliance a ($x_{a,1}^{\text{app\_state}}$) to be "off" at period 1 since appliance a can only operate after appliance a^* completes its operation.

1.3.8.8 Uninterruptible Operation

To assure that an uninterruptible appliance will not be stopped after it begins its cycle, we include the constraints defined by Eq. (1.16) - (1.18) [14].

$$x_{a,t}^{\text{app\_state}} \leq 1 - x_{a,t}^{\text{app\_end}} \qquad \forall\, a \in \mathrm{U}^{\text{app}} \qquad (1.16)$$

$$x_{a,t-1}^{\text{app\_state}} - x_{a,t}^{\text{app\_state}} \leq x_{a,t}^{\text{app\_end}} \qquad \forall\, a \in \mathrm{U}^{\text{app}} \qquad (1.17)$$

$$x_{a,t-1}^{\text{app\_end}} \leq x_{a,t}^{\text{app\_end}} \qquad \forall\, a \in \mathrm{U}^{\text{app}} \qquad (1.18)$$

The binary variable $x_{a,t}^{\text{app\_end}}$ is valued at 1 when the appliance a has finished its cycle at time $t-1$. When $x_{a,t}^{\text{app\_end}} = 1$, the operation status of appliance a ($x_{a,t}^{\text{app\_state}}$) is changed from "on" (=1) to "off" (=0) in Eq. (1.16). This indicates that the operation of appliance a has completed at period

t. Finally, $x_{a,t}^{\text{app\_end}}$ must equal to 1 after $x_{a,t-1}^{\text{app\_end}}$ becomes 1 in Eq. (1.18) which specifies that the operation of appliance a cannot resume after period t.

1.3.8.9 Optimization model

The proposed energy consumption scheduling model can be summarized as

maximize benefit function (1.2)

subject to constraints (1.1), (1.3) - (1.18)

$$e_t^{\text{app\_bat}}, e_t^{\text{chr}}, e_t^{\text{loss\_pv}}, e_t^{\text{app\_pv}}, s_t^{\text{bat}} \geq 0, \qquad \forall\, t \tag{1.19}$$

$$y_t^{\text{chr}}, y_t^{\text{dch}}, x_{a,t}^{\text{app\_state}}, x_{a,t}^{\text{app\_end}}, z_a \in \{0,1\}, \qquad \forall\, a, t \tag{1.20}$$

This model represents a mixed-integer optimization problem. The solution to the problem provides the best operation periods for the appliances considering the forecasted solar energy and the required operation of the appliances. In the case studies, we solve the optimization model on a computer with a 3.2GHz Core i5 processor and 8GB of memory. In all cases, it takes less than two seconds to obtain the solutions.

1.4 Case Studies and Results

To verify the model, we create the following four scenarios:

Table 1.1 Four scenarios of the case study

Scenario	City	State	Season
AU-W	Auburn	Alabama	Winter
AU-S	Auburn	Alabama	Summer
PH-W	Phoenix	Arizona	Winter
PH-S	Phoenix	Arizona	Summer

1.4.1 System Data

In this case study, we consider a 3-bedroom and 2-bathroom house with a 4-person family. We divide a day into 24 equal periods of length $T = 1$ hour. It is assumed that during weekdays the family wakes up at 6AM (period 7), leaves for school and work at 8AM (period 9), returns home at 6PM (period 19), and goes to bed at 11PM (period 24).

In the house, there are 14 physical appliances. To represent appliances that operate more than once a day, we create 11 additional appliances. For example, the coffee machine is operated in the morning and in the evening. This fact is represented by two coffee machines. The appliances and their parameters are given in Table 1.2.

Table 1.2 Physical appliances

Label	Full name	Type	Energy used (kWh)
CLW	Clothes Washer (Warm wash, Cold rinse)	Flexible / Uninterruptible	2.300
CLD	Clothes Dryer (Light Load)	Flexible / Uninterruptible	2.500
DIW	Dish Washer	Flexible / Uninterruptible	1.200
CFB	CFL Bulb (11W)	Flexible / Uninterruptible	0.011
LEB	LED Bulb (10W)	Inflexible / Interruptible	0.010
HAB	Halogen Bulb (40W)	Inflexible / Interruptible	0.040
INB	Incandescent Bulb (40W)	Inflexible / Interruptible	0.050
REF	Refrigerator (16 cu. ft., AC)	Inflexible / Interruptible	0.050
EOR	Electric Oven / Range	Inflexible / Interruptible	2.300
TOO	Toaster Oven	Inflexible / Interruptible	0.750
COM	Coffee Machine (Brew, Warmer on)	Inflexible / Interruptible	0.400
DOL	Desktop or Laptop	Inflexible / Interruptible	0.300
TVD	LED TV / Satellite Dish	Inflexible / Interruptible	0.056
IMW	Internet Modem / Wireless Router	Inflexible / Interruptible	0.015
ENM	Energy Margin	Inflexible / Interruptible	0.500

In Table 1.3, we show the required operation of the appliances for a weekday. We arbitrarily create appliance consumption patterns and priorities for summer and winter seasons. Notice that the washer, dryer and dishwasher are flexible appliances which can shift their operation cycle based on the availability of energy. They are also uninterruptible appliances which cannot be

stopped until they complete their operation cycle. An energy margin of 0.5kW is assigned for occasional usage of appliances such as charging a cell phone or operating a vacuum cleaner.

Table 1.3 Appliance parameters (weekday)

Appliance	Qty	T_a (H)		$P_{a,t}$		W_a
		Summer	Winter	Summer	Winter	
CLW	1	2	2	1 - 24	1 - 24	8
CLD	1	1	1	1 - 24	1 - 24	6
DIW	1	2	2	1 - 24	1 - 24	7
CFB (Morning)	6	1	2	7	7 - 8	10
CFB (Morning)	6	1	2	7	7 - 8	3
LEB (Morning)	6	1	2	7	7 - 8	6
LEB (Morning)	6	1	2	7	7 - 8	3
HAB (Morning)	5	1	2	7	7 - 8	5
HAB (Morning)	5	1	2	7	7 - 8	3
INB (Morning)	5	1	2	7	7 - 8	4
INB (Morning)	5	1	2	7	7 - 8	3
CFB (Evening)	12	4	5	20 - 23	19 - 23	10
LEB (Evening)	12	4	5	20 - 23	19 - 23	8
HAB (Evening)	10	4	5	20 - 23	19 - 23	6
INB (Evening)	10	4	5	20 - 23	19 - 23	4
REF	1	24	24	1 - 24	1 - 24	10
EOR	1	1	1	19 - 20	19 - 20	9
TOO	1	1	1	7 - 8	7 - 8	9
COM (Morning)	1	1	1	7 - 8	7 - 8	6
COM (Evening)	1	1	1	20 - 21	20 - 21	5
DOL	1	7	7	7 - 8 or 19 - 23	7 - 8 or 19 - 23	7
TVD (Morning)	1	2	2	7 - 8	7 - 8	6
TVD (Evening)	1	5	5	19 - 23	19 - 23	8
IMW (Morning)	1	2	2	7 - 8	7 - 8	7
IMW (Evening)	1	5	5	19 - 23	19 - 23	7
ENM	1	7	7	7 - 8 and 19 - 23	7 - 8 and 19 - 23	N/A

The specifications of the PV system and the battery are listed in Table 1.4.

Table 1.4 Specifications of the PV system and battery

Parameter	Value	Description
A^{PV}	65.5m^2	Area of PV array
R^{PV}	17%	PV system efficiency
R^{INV}	99%	Inverter efficiency
C^{BAT}	9.8kWh	Battery capacity
S^{ISC} / S^{ESC}	30%	Initial SOC / End SOC
S^{MIN}	5%	Minimum SOC
S^{MAX}	95%	Maximum SOC
R^{CHR}	99%	Charging efficiency
R^{DCH}	0.139%	Self-discharging efficiency
R^{MCH} / R^{MDC}	5kWh	Maximum / Minimum discharging power

1.4.2 Forecasted Solar Irradiance

For the solar irradiance, we use the historical data from the National Solar Irradiation Database [17]. Although the data represents actual solar irradiance in Alabama and Arizona, for testing purposes, we assume that it corresponds to forecasted data. These data profiles are used to simulate a winter and a summer day in Auburn (Alabama) and Phoenix (Arizona). Figure 1.4 shows the hourly solar irradiance profiles in Auburn and Phoenix on Dec 1, 2005, and Jul 1, 2005.

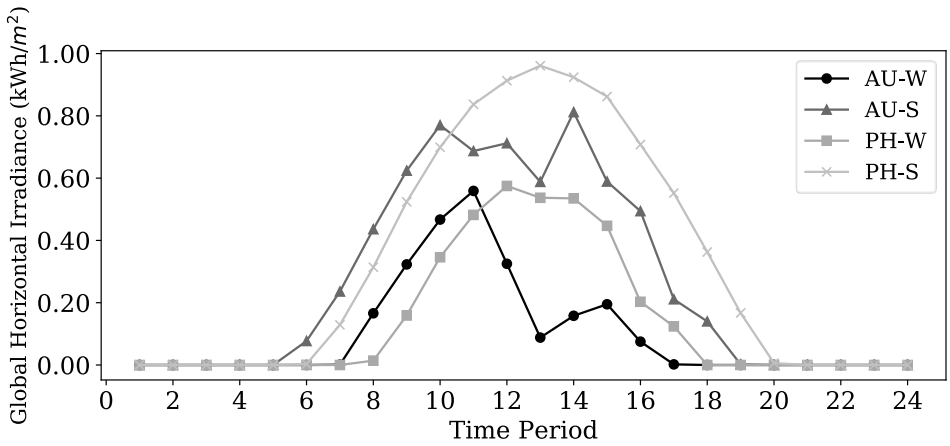

Figure 1.4 Hourly solar irradiance profile in Auburn and Phoenix

In Figure 1.5, we show the total energy generated by the PV array for each scenario. This is the summation of the parameter E_t^{PV} over the 24 hours. The figure also shows the total energy required by the appliances in summer (26.41kWh) and winter (28.3kWh). Notice that in Auburn, 270% more solar energy is generated under the scenario AU-S than the scenario AU-W. Similarly, in Phoenix, the ratio is 230%. In addition, under scenario AU-W, there is not enough solar energy to meet the required energy.

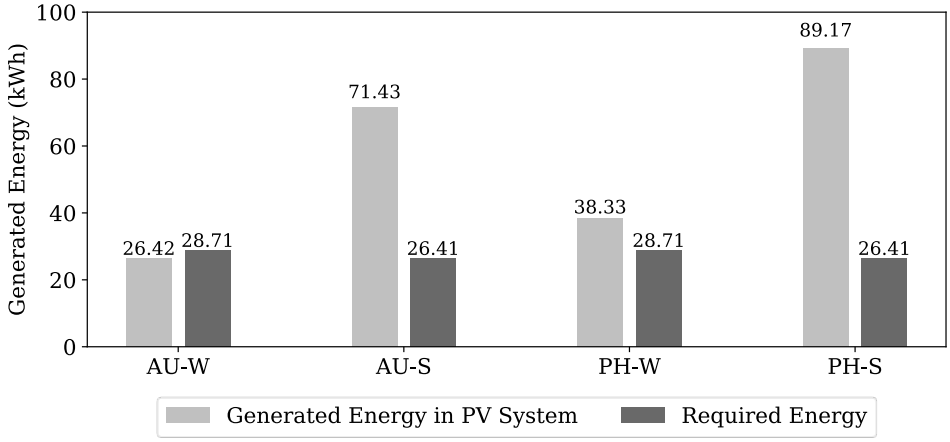

Figure 1.5 PV solar energy generated and required energy under four scenarios

1.4.3 Results

We assume that the model is run at 12:00 midnight, and at that hour, the SOC of the battery is 30%. At the end of the last period (12:00 midnight of the next day), the SOC is required to be greater than 30%, which will be used the next day. We run the appliance scheduling model for each of the scenarios. The results from the model are summarized in Tables 1.5-1.7 and Figures 1.6-1.7. Table 1.5 shows the appliance scheduling results for each scenario. The washer (CLW) and dishwasher (DIW) are scheduled to operate during two periods, and the dryer (CLD) is scheduled to operate during one period in all scenarios. All 14 appliances required to operate

during periods 7 to 8 are scheduled for operation in all summer scenarios. But, in winter scenarios AU-W and PH-W, there is not enough solar irradiance in Auburn and Phoenix the morning of Dec. 1. 2015 to operate all 14 appliances.

Table 1.5 Appliance scheduling results

Appliance	Scheduling results (periods)			
	AU-W	AU-S	PH-W	PH-S
CLW	10 - 11	10 - 11	12 - 13	11 - 12
CLD	14	13	15	14
DIW	12 - 13	9 – 10	12 - 13	10 - 11
CFB - Morning	7 - 8	7	7 - 8	7
CFB - Morning	7 - 8	7	7 - 8	7
LEB - Morning	7 - 8	7	7 - 8	7
LEB - Morning	7 - 8	7	7 - 8	7
HAB - Morning	7 - 8	7	7	7
HAB - Morning	-	7	-	7
INB - Morning	-	7	-	7
INB - Morning	-	7	-	7
CFB - Evening	19 - 23	20 - 23	19 - 23	20 - 23
LEB - Evening	19 - 23	20 - 23	19 - 23	20 - 23
HAB - Evening	-	-	-	20 - 22
INB - Evening	-	-	-	-
REF - Evening	1 - 24	1 - 24	1 - 24	1 - 24
EOR	-	-	-	-
TOO	8	7	-	8
COM - Morning	7	7	7	8
COM - Evening	-	-	-	-
DOL	7 - 8, 19 - 23	7 - 8, 19 - 22	7, 19 - 23	7 - 8, 19 - 23
TVD - Morning	7 - 8	7 - 8	7 - 8	7 - 8
TVD - Evening	19 - 23	19 – 23	19 – 23	19 - 23
IMW - Morning	7 - 8	7 - 8	7 - 8	7 - 8
IMW - Evening	19 - 23	19 - 23	19 - 23	19 - 23
ENM	7 - 8, 19 - 23	7 - 8, 19 - 23	7 - 8, 19 - 23	7 - 8, 19 - 23

The electric oven/range (EOR) is not scheduled for operation under all the scenarios, even though it has a higher priority than the other appliances during that period. The reason is that when there is insufficient energy, lower priority appliances that require less energy and longer operation periods such as the TV or computer are more likely to operate than higher priority appliances that

require more energy and shorter operating periods. A coffee machine (COM - Evening) also does not operate under all the scenarios since its priority-level is lower than that of other appliances. We notice that only in the scenario PH-S 10 halogen bulbs (HAB - Evening) are scheduled to operate during periods 20 to 22. This is due to the availability of 0.173kW of additional solar irradiance in Phoenix during periods 19 to 20 on Jul. 1. 2015.

In Figures 1.6 and 1.7, we show the hourly SOC of the battery profiles under all scenarios. We observe that the battery is charged/discharged during periods 1 to 19. Charging/Discharging periods are different in all the scenarios. However, the battery usually tries to maintain its maximum level (95%) at period 18 (AU-W, AU-S, PH-W) or 19 (PH-S) in order to operate as many required appliances in the evening. However, some appliances such as an electric oven/range (EOR) and coffee machine (COM - Evening) do not operate even though the SOC of the battery is at its maximum during period 18 or 19 since there is insufficient energy in the battery under all scenarios.

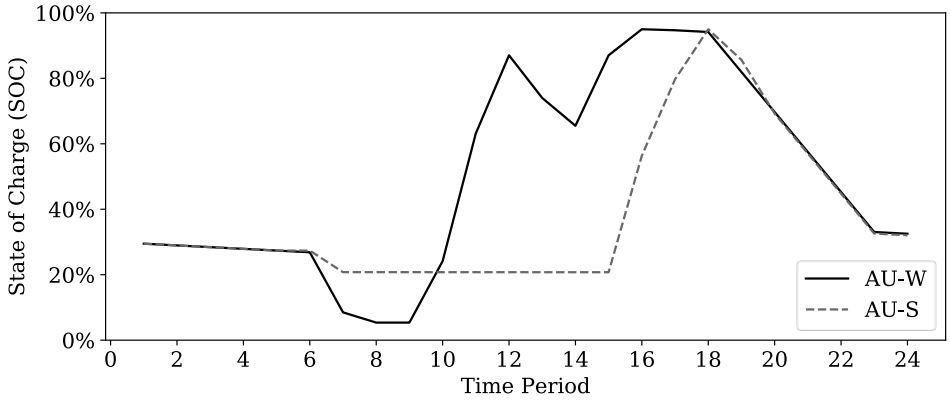

Figure 1.6 SOC of the battery under scenario AU-W and AU-S

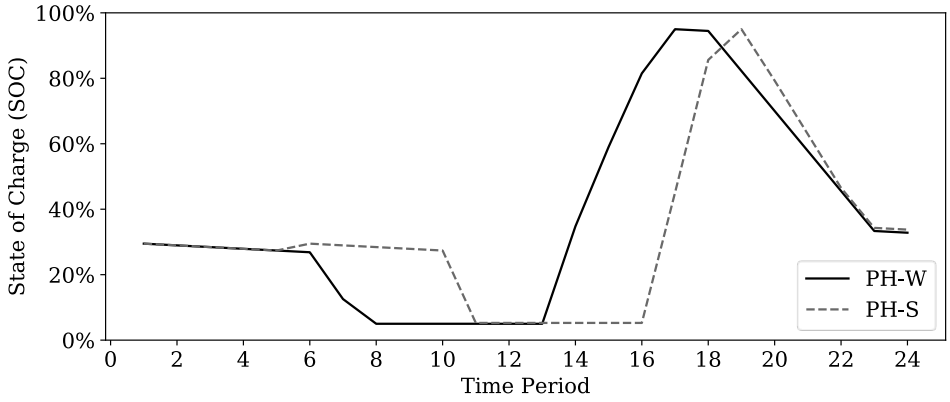

Figure 1.7 SOC of the battery under scenario PH-W and PH-S

In Table 1.6, we represent the demand satisfaction rate for all scenarios, which is the percentage of energy used to operate appliances compared with total energy demand for each of the scenarios. The average demand satisfaction for all scenarios is 73.17%. On average, it is 12% higher on a summer day than on a winter day and 1.36% higher in Auburn than in Phoenix. Even though there is enough PV energy under all scenarios except for scenario AU-W, it cannot satisfy 100% of the user's energy demand. The reason is that some appliances do not operate after period 18 when the battery has insufficient capacity to supply energy to all required appliances in the evening.

Table 1.6 Energy used by appliances (kWh) under four scenarios

Scenario	Total energy demand	Energy used by appliances	Demand satisfaction
AU-W	28.71kWh	20.11kWh	70.05%
AU-S	26.41kWh	20.51kWh	77.66%
PH-W	28.71kWh	18.46kWh	64.30%
PH-S	26.41kWh	21.31kWh	80.69%

In Table 1.7, we show a summary of the total energy used by the appliances under all scenarios. The average energy used by appliances is 20.09kWh of which 11.6kWh comes directly from the PV array and 8.49kWh comes from the battery. Notice that in Auburn, 1.95% more energy is used

in the summer than in the winter on weekdays in Auburn, while, on average, 13.33% more energy is used on weekdays in the summer than in the winter in Phoenix. An average of 0.51kWh is also used to convert energy from the PV array to the battery, the PV array to the appliances, the battery to the appliances, and to self-discharge the battery. Notably, on average, there is 46.27kWh more unused energy in the summer than in the winter since there is more solar irradiance in summer than in winter. This energy loss is the summation of surplus energy ($\sum e_t^{\text{loss\_pv}}$) at each period after operating appliances and charging the battery. Energy loss occurs during daytime periods since the amount of generated PV energy is much more than the energy required by appliances and the capacity of the battery.

Table 1.7 Total energy usage (kWh) under four scenarios

Scenario	Appliances from PV	Appliances from battery	Conversion losses	Unused energy
AU-W	9.69	10.42	0.54	5.53
AU-S	13.58	6.92	0.5	50.22
PH-W	10.1	8.36	0.48	19.11
PH-S	13.06	8.25	0.53	66.96

The scheduling results show that PV array and battery capacities should be increased under all scenarios to meet 100% of user energy demand. Increasing PV array and battery capacities allow for more available energy and storage to be used during the nighttime. Increasing both PV array and battery capacities also increases demand satisfaction.

1.5 Sensitivity Analysis

We conduct a sensitivity analysis to find a near-optimal PV array and battery capacities to fully satisfy the user energy demand. We add PV cells to the PV array (11.2kW) in increments of 2.8kW and capacity to the battery (9.8kWh) in increments of 20%. In Figures 1.8-1.11, we observe

that the demand can be fully satisfied under all scenarios by increasing the battery capacity, except for the AU-W scenario in Figure 1.8. Under the AU-W scenario and PV capacity of 11.2kW, the PV array does not generate sufficient energy to operate all required appliances. We also observe that the battery capacity has a higher impact on demand satisfaction than the PV array capacity. In Auburn, a 14kW of PV array with a 21.56kWh of battery is enough to meet the winter and summer demand. Similarly, in Phoenix, a system with a smaller PV array (11.2kW) and a larger battery (23.52kWh) is required.

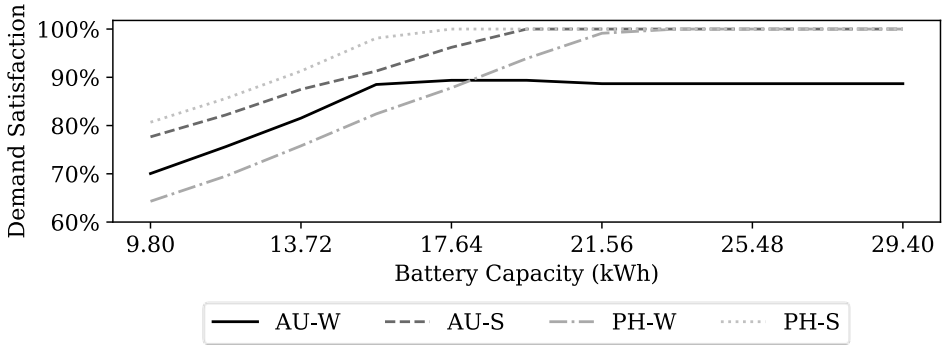

Figure 1.8 Impact of battery capacity on demand satisfaction (%) when PV capacity = 11.2kW

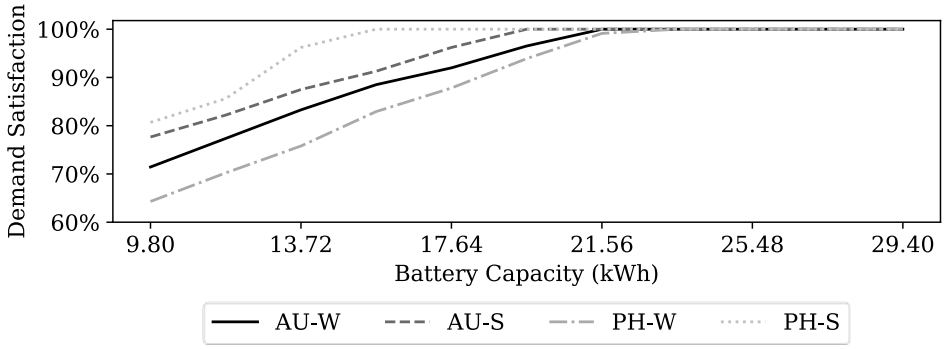

Figure 1.9 Impact of battery capacity on demand satisfaction (%) when PV capacity = 14.0kW

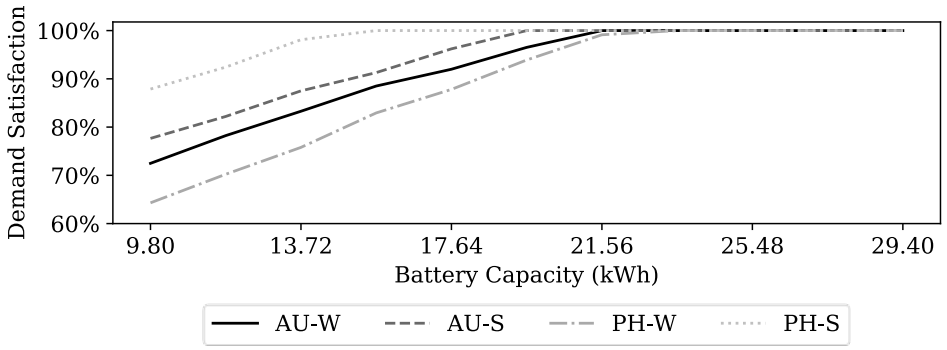

Figure 1.10 Impact of battery capacity on demand satisfaction (%) when PV capacity = 16.8kW

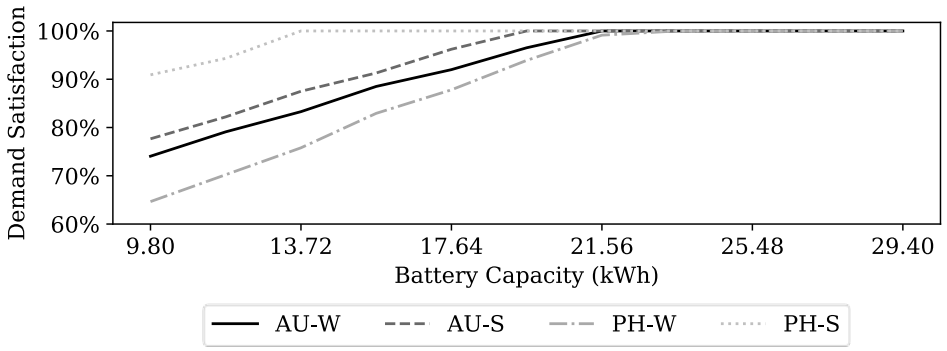

Figure 1.11 Impact of battery capacity on demand satisfaction (%) when PV capacity = 19.6kW

Figures 1.12-1.15 show that the amount of energy loss is increased under all scenarios when the PV capacity increases while this unused energy is decreased when the battery capacity increases. The amount of energy loss remains steadily constant when it reaches a 100% demand satisfaction because the battery is not required to store an additional amount of energy for the day.

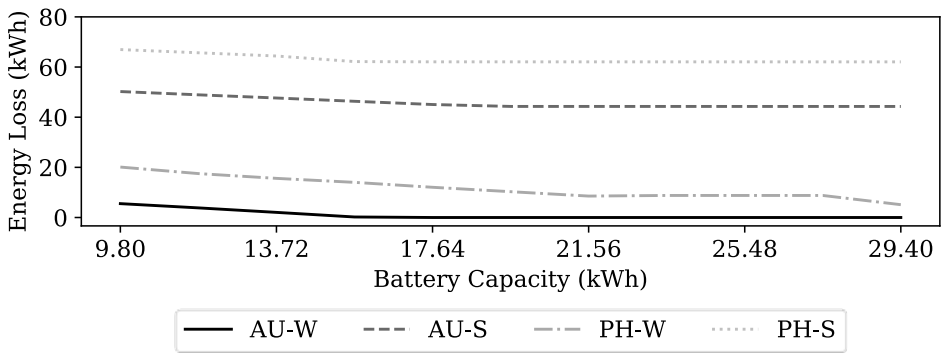

Figure 1.12 Impact of battery capacity on energy losses (kWh) when PV capacity = 11.2kW

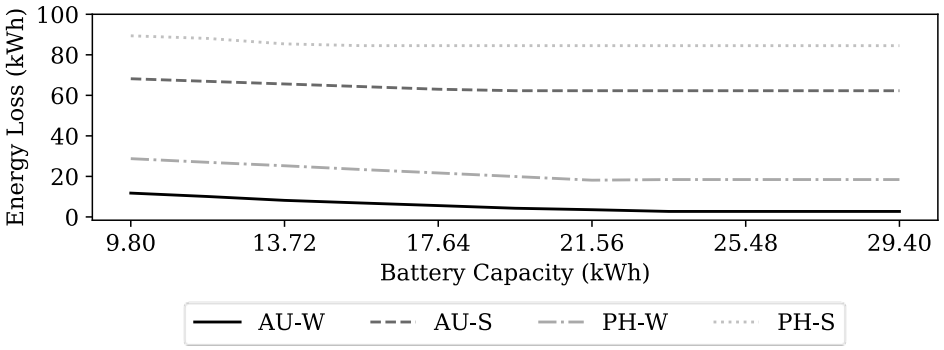

Figure 1.13 Impact of battery capacity on energy losses (kWh) when PV capacity = 14.0kW

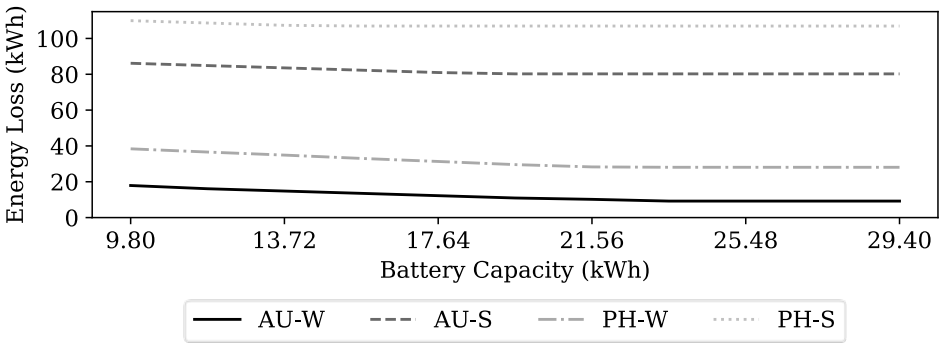

Figure 1.14 Impact of battery capacity on energy losses (kWh) when PV capacity = 16.8kW

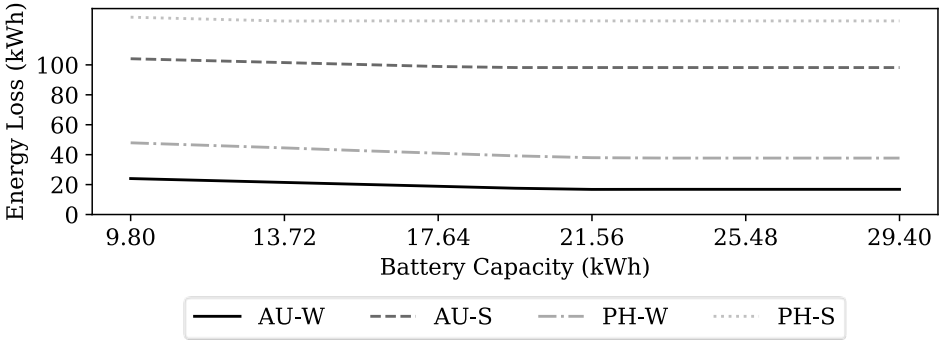

Figure 1.15 Impact of battery capacity on energy losses (kWh) when PV capacity = 19.6kW

The results demonstrate that the preferred capacities of the PV array and battery for this stand-alone PV energy system are affected by seasons and geographical location. Energy loss should also be taken into consideration so that the amount of unused energy can be minimized when we determine the most economical capacity of an off-grid PV energy system.

1.6 Non-Optimized Case Comparison

In this section, we compare the results of the optimized versus the non-optimized case. For the comparison, we use the AU-S scenario and energy system with a 11.2kW PV array and 9.8kWh battery. We assume that the preferred operation periods of appliances for the non-optimized case ($P_{a,t}^{non-opt.}$) are fixed and equal to the required operation time (T_a). Preferred operation periods for the optimized and non-optimized case are shown in Table 1.8.

Table 1.8 Energy consumption patterns under Non-opt. case and Opt. case of AU-S scenario

Appliance	$P_{a,t}^{non-opt.}$	$P_{a,t}^{opt.}$	Appliance	$P_{a,t}^{non-opt.}$	$P_{a,t}^{opt.}$
CLW	20 - 21	1 - 24	HAB (Evening)	20 - 23	20 - 23
CLD	22	1 - 24	INB (Evening)	20 - 23	20 - 23
DIW	23 - 24	1 - 24	REF	1 - 24	1 - 24
CFB (Morning)	7	7	EOR	19	19 - 20
CFB (Morning)	7	7	TOO	8	7 - 8
LEB (Morning)	7	7	COM (Morning)	8	7 - 8
LEB (Morning)	7	7	COM (Evening)	20	20 - 21
HAB (Morning)	7	7	DOL	8 or 19 - 23	7 - 8 or 19 - 23
HAB (Morning)	7	7	TVD (Morning)	8	7 - 8
INB (Morning)	7	7	TVD (Evening)	19 - 23	19 - 23
INB (Morning)	7	7	IMW (Morning)	7 - 8	7 - 8
CFB (Evening)	20 - 23	20 - 23	IMW (Evening)	19 - 23	19 - 23
LEB (Evening)	20 - 23	20 - 23	ENM	7 - 8 and 19 - 23	7 - 8 and 19 - 23

After running both cases, we obtain the results showing in Table 1.9. We observe that the optimized case satisfies the demand 36% more than the non-optimized case.

Table 1.9 Energy used by appliances (kWh) under the Opt. case and Non-opt. case of AU-S scenarios

	Total energy Demand	Energy used by appliances	Demand satisfaction
Opt. case of AU-S	26.41kWh	20.51kWh	77.66%
Non-opt. case of AU-S		11.01kWh	41.68%

Next, we increase the battery capacity in 20% increments to determine a battery capacity that can achieve a 100% demand satisfaction. The results are shown in Figure 16. We observe that for the optimized and non-optimized case, a 19.6kWh and 35.28kWh battery, respectively, suffices to fully meet the demand. As a result, using the optimization model, a 44% smaller battery can be used to meet the energy demand.

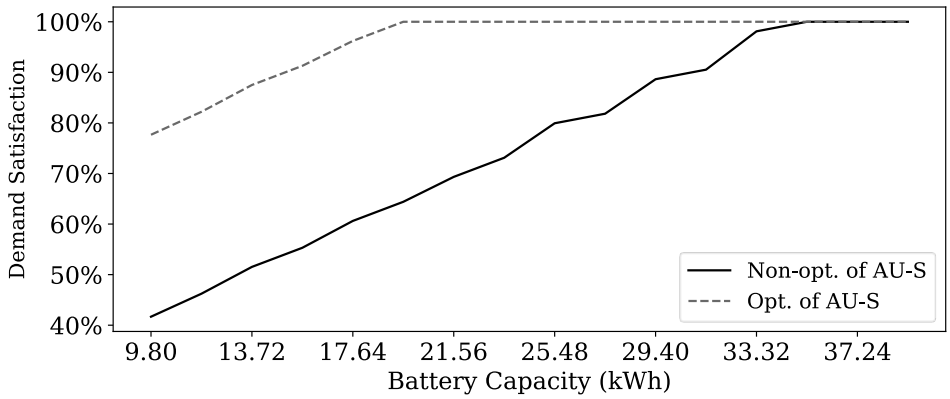

Figure 1.16 Impact of battery capacity on demand satisfaction (%) between the Opt. case and Non-opt. case of AU-S scenario when PV capacity = 11.2kW

1.7 Conclusion

We proposed an energy scheduling model of the stand-alone PV system and battery in an isolated residential house. We showed that is possible to optimize the use of direct solar energy and battery capacity for powering appliances in an off-grid situation. The model was tested under four scenarios based on the geographical location and season. The results showed that the battery capacity is more influential than the PV array capacity on meeting the demand. In addition, the Auburn-scenarios required a larger PV array and smaller battery capacity than the Phoenix-scenarios. The contribution of the proposed optimization was demonstrated by comparing the results to a non-optimized case. Under the same PV array capacity, the results showed that using

the optimization to schedule appliances, the energy demand can be fully met with a smaller battery capacity than the non-optimized case.

References

[1] Universal Achieving Universal Energy Access, United Nations Foundation, (2013) [Online], Available: http://www.unfoundation.org/what-we-do/issues/energy-and-climate/clean-energy-development.html

[2] E. S. Sreeraja, K. Chatterjeea, S. Bandyopadhyay, (2010). Design of isolated renewable hybrid power systems, Solar Energy 84, 1124-1136.

[3] H.R.Fallah Kohan, F.Lotfipour, M.Eslami, (2018). Numerical simulation of a photovoltaic thermoelectric hybrid power generation system, Solar Energy 174, 537-548.

[4] A. H. Habib, V. R. Disfani, J. Kleissl, R. A. de Callafon, (2017). Optimal Switchable Load Sizing and Scheduling for Standalone Renewable Energy Systems, Solar Energy 144, 707-720.

[5] A. H. Habib, V. R. Disfani, J. Kleissl, R. A. de Callafon, (2016). Quasi-dynamic load and battery sizing and scheduling for stand-alone solar system using mixed-integer linear programming, 2016 IEEE Conference on Control Applications (CCA).

[6] K. M. Tsui, S. C. Chan, (2012). Demand Response Optimization for Smart Home Scheduling Under Real-Time Pricing, IEEE Transactions on Smart Grid 3 (4), 1812-1821.

[7] A. Agnetis, G. de Pascale, P. Detti, A. Vicino, (2013). Load Scheduling for Household Energy Consumption Optimization, IEEE Transactions on Smart Grid 4 (4), 2364-2373.

[8] A. Molderink, V. Bakker, M. G. C. Bosman, J. L. Hurink, G. J. M. Smit, (2010). Management and Control of Domestic Smart Grid Technology, IEEE Transactions on Smart Grid 1 (2), pp.109-119.

[9] A. J. Conejo, J. M. Morales, L.Baringo, (2010). Real-Time Demand Response Model, IEEE Transactions on Smart Grid 1 (3), pp.236-242.

[10] M. Pedrasa, T. Spooner, I. MacGill, (2010). Coordinated Scheduling of Residential Distributed Energy Resources to Optimize Smart Home Energy Services, IEEE Transactions on Smart Grid 1 (2), 134-143.

[11] Z. Zhao, W. C. Lee, Y. Shin, K. B. Song, (2013). An Optimal Power Scheduling Method for Demand Response in Home Energy Management System, IEEE Transactions on Smart Grid 4 (3), 1391-1400.

[12] L. Guo, H. C. Wu, H. Zhang, T. Xia, S. Mehraeen, (2015). Robust Optimization for Home-Load Scheduling Under Price Uncertainty in Smart Grids, 2015 International Conference on Computing, Networking and Communications (ICNC).

[13] B. Moradzadeh, K. Tomsovic, (2013). Two-Stage Residential Energy Management Considering Network Operational Constraints, IEEE Transactions on Smart Grid 4 (4), 2339-2346.

[14] K. C. Sou, J. Weimer, H. Sandberg, K. H. Johansson, (2011). Scheduling smart home Appliances Using Mixed Integer Linear Programming, 50th IEEE Conference on Decision and Control and European Control Conference (CDC-ECC), 5144-5149.

[15] A. Mohsenian-Rad, V. Wong, J. Jatskevich, R. Schober, (2010). Optimal and Autonomous Incentive-Based Energy Consumption Scheduling Algorithm for Smart Grid, Innovative Smart Grid Technologies Conference (ISGT), 1-6.

[16] T. Markvart, (2000). Solar electricity, second ed. Wiley USA.

[17] National Centers for Environmental Information, (2012). National Solar Radiation Data Base: 1991- 2010 Update [Online], Available: ftp://ftp.ncdc.noaa.gov/pub/data/nsrdb-solar/solar-only/

[18] H. İzmitligil, H. A. Özkan, (2016). A Home Power Management System Using Mixed Integer Linear Programming for Scheduling Appliances and Power Resources, 2016 IEEE PES Innovative Smart Grid Technologies Conference Europe (ISGT-Europe), Ljubljana, 1-6.

Chapter 2 Designing a Residential Off-Grid Photovoltaic System

2.1 Abstract

Solar irradiance is abundant, eco-friendly, sustainable, and one of the most promising energy sources to address the shortage of energy in the future. In isolated areas where access to the grid is limited or restricted, a stand-alone photovoltaic (PV) system is particularly effective. In such a system, the available electrical energy mainly depends on the solar irradiance and the capacities of the PV array and battery. In this paper, we propose a Nelder-Mead algorithm for designing a residential off-grid PV system. The algorithm determines the capacities of the PV array and battery for cost-effectively operating the system. We use a mixed-integer programming model to day-ahead schedule the daily usage of appliances according to forecasted solar irradiance. The schedule is executed on a Monte Carlo simulation that considers the uncertainty of solar irradiance. The algorithm is tested using solar irradiance data at two locations in the USA. We perform a sensitivity analysis on the system by changing the penalty cost of non-served energy and the cost of the battery.

Keywords: Off-grid PV system, PV array capacity, Battery capacity, Residential PV system, Nelder-Mead algorithm

2.2 Introduction

According to a recent report from the U.S Energy Information Administration (EIA), the world electricity generation will grow by 69% from 21.6 trillion kWh (2012) to 36.5 trillion kWh (2040). The growth in electricity generation is forecasted to occur in non-Organization for Economic Co-operation and Development (non-OECD) countries where the infrastructures are still under development, and population size is growing rapidly. The rising living standard of emerging nations is increasing the energy demand in all sectors, including home, commercial service, and industry. The electricity generation is estimated to increase an average of 2.5% per year over the next 20 years and only an average of 1.2% per year in the OECD countries [1]. However, approximately 840 million people who live in rural areas in these countries still have no access to electricity [2]. Renewable sources such as solar, wind, and hydro are attractive solutions to the problem of providing access to energy. In addition, renewable energy plays a significant role in mitigating greenhouse gas (GHG) emissions as well as global warming issues caused by the increasing use of conventional fossil fuels [3]. Particularly, an off-grid renewable energy system is considered to meet energy demand in isolated areas where extending the grid network is unrealistic due to extreme cost and technical difficulties. Among various renewable energy systems, a stand-alone PV system is one of the most viable solutions since solar is an abundant, environmentally friendly, and sustainable energy source. However, when looking at off-grid PV systems, time-related factors, and geographical location should be considered since solar energy generation strongly depends on the availability of solar irradiance during a day [4]. To face the time and location dependency of solar energy, an off-grid PV system would require energy storage in a battery. The optimal design of an off-grid PV-battery system would also be necessary to use

the available solar energy efficiently and satisfy the user's energy demand in terms of optimal capacities of PV array and battery storage.

Many publications have proposed methods (i.e., an intuitive, numerical, analytical, artificial intelligence, commercial computer tools) for the optimal sizing of an off-grid PV system [5]. In [6], intuitive methods were studied to estimate the optimal capacity of an off-grid PV-battery system for providing the electrical loads in a residential house in Egypt according to energy demand. The author compared the life-cycle cost of the PV-battery system with a diesel generator. In [7], an intuitive method for determining the optimal capacity of the off-grid PV-battery system was proposed. The author estimated daily load demand, optimal tilt angle, and the capacity of PV array and battery using simple calculations. In [8], numerical methods for determining the PV module tilt angle and PV array size and battery capacity were implemented based on hourly meteorological data and energy demand using MATLAB. Loss of load probability (LLP) for the system designed by the proposed method was compared with the result of an intuitive method. In [9], a novel optimization method using the loss of power supply probability (LPSP) was presented to determine the size of an off-grid PV-battery system. The optimal design of the energy system was proposed based on the lowest levelized cost of energy. In [10], the authors represented a novel analytical model for optimal sizing of stand-alone PV systems. Algebraic equations for optimal PV array capacity, battery storage capacity, and the constant of integration were formulated. The optimal capacities of the PV array and battery are determined by various load demands and loss of load probability (LLP). In [11], the authors represented a new analytical method for determining the optimal capacity of an off-grid photovoltaic (PV) system. In order to derive mathematical formulations for optimal sizing of the energy system, MATLAB fitting tool was used to fit the resultant sizing curves after analyzing the energy flow of the energy system. In [12], an

optimization simulation model was developed to find an optimal PV array size to supply the lighting load using the renewable energy software HOMER. The authors compared the initial cost, the net present cost of the system, and energy cost with diesel generator operating cost. In [13], the authors proposed the method to find the optimal capacities of PV array and battery as a solution to supply the irrigation systems in six farming facilities of Spain. Photovoltaic-diesel hybrids and diesel systems were found to be the optimal energy generation solution by the software HOGA (Hybrid Optimization by Genetic Algorithms). In [14], the author represented fuzzy logic for the optimal sizing of a solar array and a battery in a stand-alone PV system. The fuzzy logic was developed using Matlab/Simulink in which the consumed energy and the monthly average of daily solar radiation of the region were used to determine the optimal capacity of the energy system. In [15], a hybrid method for optimal sizing of a stand-alone PV-battery system was proposed using analytical sizing equations with long-term performance. The authors used deterministic hourly load demand and solar irradiance. In [16], the authors proposed a new approach to determine the optimal capacity of an off-grid PV system using the combination of an analytical method and a machine learning approach for a generalized artificial neural network (GRNN). The GRNN helped to predict the optimal size of a PV system using the geographical coordinates of the targeted site instead of using mathematical formulas. In all of the studies, the primary objective was to determine the optimal capacity of the energy system without considering solar irradiance uncertainty and energy consumption patterns.

In this paper, we use the Nelder-Mead (N-M) optimization algorithm for the design of a residential stand-alone PV system. The objective of the optimization is to minimize the annual equivalent cost (AEC) of the capacities of the PV array and battery while satisfying the annual appliance-usage of a user. The non-served energy is included as a penalty cost in the objective cost

function. A mixed integer programming method is used to schedule the daily operation of appliances [17]. Since when the actual amount of solar irradiance is realized, the schedules may not be executed as planned, a Monte Carlo simulation that considers the uncertainty of the solar irradiance evaluates the actual operation.

The remainder of this paper is organized as follows: Section 2 presents the problem description. Section 3 proposes the energy system operation and simulation model. Section 4 details the solving algorithm, and Section 5 shows the case studies and simulation results. Finally, Section 6 ends with concluding remarks.

2.3 Problem description

A residential off-grid energy system is composed of energy generation units, energy storage, and energy demand by appliances. In an off-grid PV system, available solar irradiance mainly affects on satisfying energy demand. The daily energy scheduling model provides a day ahead of schedule for appliance operation based on forecasted solar irradiance. It pre-schedules to maximize the operation of higher priority appliances. However, when the amount of forecasted solar irradiance is less than actual solar irradiance, some appliances may not operate as it is pre-scheduled. An energy system manages a balance between available energy and energy demand by not operating low-priority appliances. The energy required by not operated appliances is considered as non-served energy. It is assumed that annual non-served energy becomes a penalty cost to increase the AEC of the energy system by multiplying it with the average electricity rate. The cost-efficient capacity of the energy system is determined by the AEC that minimizes the cost of PV array, battery, and non-served energy.

In Figure 2.1, the problem is solved with mixed-integer programming, Monte Carlo simulation, and the N-M algorithm. Under randomly generated capacities of PV array and battery, annual non-served energy is obtained by the energy scheduling model (step 1) and simulation (step 2) for actual energy system operation. The N-M algorithm (stet 3) provides the near-optimal capacities of the PV array and battery that minimizes the AEC of the energy system.

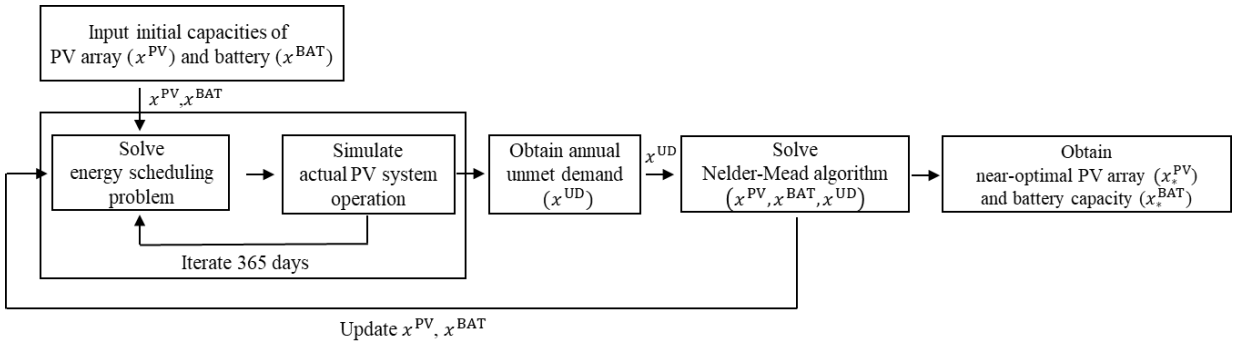

Figure 2.1 Problem-solving procedure

2.3.1 Residential off-grid energy system

It is assumed that the residential energy system consists of a PV array, a battery, a PV charging controller, and an inverter to supply power to all appliances in the residential home (Figure 2.2). The solar irradiance is converted into solar energy through the PV array. The generated solar energy is either used to operate appliances or stored in the battery. The battery supplies energy to operate appliances when the available solar energy is insufficient.

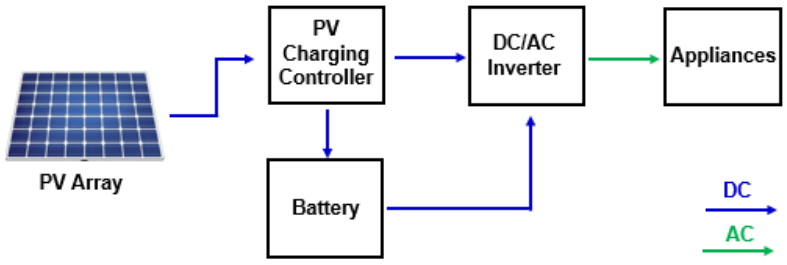

Figure 2.2 A residential off-grid energy system

The appliances at the residential home are classified as flexible/inflexible, uninterruptible, weekly-required operation, and dependent operation. Flexible appliances can operate anytime during a day, while inflexible appliances can only operate during fixed periods defined by the user. For example, a dishwasher is a flexible appliance, but a light bulb is an inflexible appliance. An uninterruptible appliance does not stop until it completes its operation cycle. A weekly-required appliance should operate once a week. Dependent operation implies that at least one other appliance precedes an appliance. A clothes washer is an example of an uninterruptible and weekly-required appliance. In addition, a clothes washer precedes a clothes dryer, exhibiting a dependent operation.

2.3.2 Daily energy scheduling model

To improve the efficiency of the solar energy system, the daily energy-scheduling model described in [17] is used. The model is a mixed-integer optimization problem and pre-schedules the daily operation of appliances a day ahead based on appliances priorities, energy consumption patterns, and solar irradiance forecasts. The optimization model is given in Eqs. (2.1) - (2.20).

$$\text{maximize} \sum_{t=1}^{\mathrm{T}} \sum_{a=1}^{\mathrm{A}} \mathrm{W_a} * x_{a,t}^{\text{app\_state}} \tag{2.1}$$

$$\mathrm{E}_t^{\mathrm{PV}} = \mathrm{S}_t^{\mathrm{PV}} * \mathrm{C}^{\mathrm{PV}} \tag{2.2}$$

$$\mathrm{E}_t^{\mathrm{PV}} = e_t^{\text{app\_pv}} + e_t^{\mathrm{chr}} + e_t^{\text{loss\_pv}} \tag{2.3}$$

$$\sum_{a=1}^{\mathrm{A}} \mathrm{E}_a * x_{a,t}^{\text{app\_state}} + \mathrm{E}_t^{\mathrm{R}} = (e_t^{\text{app\_pv}} + e_t^{\text{app\_bat}}) * \mathrm{INV}^{\mathrm{E}} \tag{2.4}$$

$$s_t^{\mathrm{bat}} = s_{(t-1)}^{\mathrm{bat}} * (1 - \mathrm{R}^{\mathrm{DCH}}) + \frac{\left(e_t^{\mathrm{chr}} * \mathrm{R}^{\mathrm{CHR}}\right)}{\mathrm{C}^{\mathrm{BAT}}} - \frac{e_t^{\text{app\_bat}}}{\mathrm{C}^{\mathrm{BAT}}} \tag{2.5}$$

$$s_{\mathrm{T}}^{\mathrm{bat}} \geq \mathrm{S}^{\mathrm{ESC}} \tag{2.6}$$

$$\mathrm{S}^{\mathrm{MIN}} \leq s_t^{\mathrm{bat}} \leq \mathrm{S}^{\mathrm{MAX}} \tag{2.7}$$

$$y_t^{\mathrm{chr}} + y_t^{\mathrm{dch}} \leq 1 \tag{2.8}$$

$$e_t^{\mathrm{app\_bat}} \leq y_t^{\mathrm{dch}} * \mathrm{R}^{\mathrm{MDC}} * \mathrm{C}^{\mathrm{BAT}} \tag{2.9}$$

$$e_t^{\mathrm{chr}} \leq y_t^{\mathrm{chr}} * \mathrm{R}^{\mathrm{MCH}} * \mathrm{C}^{\mathrm{BAT}} \tag{2.10}$$

$$\sum_{\mathrm{t}=1}^{\mathrm{T}} x_{a,t}^{\mathrm{app\_state}} \leq \mathrm{T}_a \tag{2.11}$$

$$\sum_{\mathrm{t}=1}^{\mathrm{T}} x_{a,t}^{\mathrm{app\_state}} = \mathrm{T}_a * z_a \qquad \forall\, a \in \mathrm{U}^{\mathrm{app}} \tag{2.12}$$

$$x_{a,t}^{\mathrm{app\_state}} \leq \mathrm{P}_{a,t} \tag{2.13}$$

$$\mathrm{T}_{a^*} - \sum_{n=1}^{\mathrm{N}} x_{a^*,n}^{\mathrm{app\_state}} \leq \mathrm{M} * \left(1 - x_{a,t+1}^{\mathrm{app\_state}}\right) \qquad \forall\, a \in \mathrm{S}, a^* \in \mathrm{S}_a, \text{and } \mathrm{N} = 1,2,..,t \tag{2.14}$$

$$x_{a,1}^{\mathrm{app\_state}} = 0 \qquad \forall\, a \in \mathrm{S} \tag{2.15}$$

$$x_{a,t}^{\mathrm{app\_state}} \leq 1 - x_{a,t}^{\mathrm{app\_end}} \qquad \forall\, a \in \mathrm{U}^{\mathrm{app}} \tag{2.16}$$

$$x_{a,t-1}^{\mathrm{app\_state}} - x_{a,t}^{\mathrm{app\_state}} \leq x_{a,t}^{\mathrm{app\_end}} \qquad \forall\, a \in \mathrm{U}^{\mathrm{app}} \tag{2.17}$$

$$x_{a,t-1}^{\mathrm{app\_end}} \leq x_{a,t}^{\mathrm{app\_end}} \qquad \forall\, a \in \mathrm{U}^{\mathrm{app}} \tag{2.18}$$

$$e_t^{\mathrm{app\_bat}}, e_t^{\mathrm{chr}}, e_t^{\mathrm{loss\_pv}}, e_t^{\mathrm{app\_pv}}, s_t^{\mathrm{bat}} \geq 0 \qquad \forall\, t \tag{2.19}$$

$$y_t^{\mathrm{chr}}, y_t^{\mathrm{dch}}, x_{a,t}^{\mathrm{app\_state}}, x_{a,t}^{\mathrm{app\_end}}, \mathrm{z}_a \in \{0,1\} \qquad \forall\, a, t \tag{2.20}$$

In Eq. (2.1), the objective of the model is to maximize the operation of higher priority appliances. The capacities of the PV array and battery, C^{PV} and $\mathrm{C}^{\mathrm{BAT}}$ respectively, are known parameters. Eq. (2.2) calculates the amount of forecasted solar energy. Eq. (2.3) ensures that the amount of forecasted solar energy is equal to the sum of the energy to operate appliances by the

PV array, the energy to charge the battery, and the energy loss. Eq. (2.4) enforces the fact that the sum of the total energy used by appliances and the reserved energy are equal to the sum of the energy from the PV array and the energy discharged from the battery. Eq. (2.5) represents the state of charge (SOC) of the battery during the current period. Eq. (2.6) sets a lower limit for the SOC during the last period. Eq. (2.7) constraints the SOC at all periods. Eq. (2.8) ensures that the battery cannot be charged and discharged during the same period. Eqs. (2.9) - (2.10) impose maximum limits on battery charging and discharging. Eq. (2.11) ensures that the appliances are scheduled to operate within the number of periods defined by the user. Eq. (2.12) represents uninterruptible appliances that either operate the entire required periods or do not operate at all. Eq. (2.13) enforces that the appliances are scheduled only during the user-defined preferred periods. Eqs. (2.14) - (2.15) describe the appliance operation sequencing. Eqs. (2.16) - (2.18) enforce the operation of uninterruptible appliances.

2.3.3 Energy system Monte Carlo simulation

A simulation model is developed to emulate the daily energy scheduling and the actual operation of the appliances. The simulation model emulates the operation of appliances by considering the uncertainties associated with the actual solar irradiance. In Figure 2.3, a pseudo-code of the simulation model is presented. The simulation model obtains the pre-schedules of the appliances from the energy-scheduling model and operates the energy-consumption system based on the actual amount of solar irradiance. The amount of generated solar energy is calculated every hour based on actual solar irradiance.

```
INPUT   Capacities of PV array and battery
FOR   Week 1 to 52
    FOR   Day 1 to 7
        # Pre-schedule appliances
        OBTAIN   24-hour forecasted solar irradiance data
        READ   Appliance parameters according to the type of the day: weekday, weekend, holiday
        COMPUTE   24-hour appliance schedule
        # System Operation
        FOR   Hour 1 to 24
            OBTAIN   Actual Solar irradiance for this hour
                CALCULATE   Amount of energy generated by PV based on the solar irradiance
            # Operate appliances
            IF   Available energy from the PV + battery   <   Total pre-scheduled energy
                Re-schedule operating appliances by switching off low-priority appliances
                Compute new amount of energy margin (if it is required)
            ENDIF
            COMPUTE   Total energy used by the appliance from the PV and battery,
                      energy charged to the battery, SOC level and energy loss
        ENDFOR   Hour
        # Weekly operation of appliances
        IF   Appliance has completed its weekly operation THEN
            Remove appliance for the rest of the week
        ELSE
            Increase priority of the appliance so it can operate the next day
        ENDIF
        Update   Initial SOC for the next day
    ENDFOR   Day
ENDFOR   Week
OUTPUT   Annual demand satisfaction (%), Annual unmet demand (kWh)
```

Figure 2.3 Simulation model pseudo-code

For simplicity, the actual solar irradiance is simulated by sampling from a normally distributed random variable where the mean equals the forecasted solar irradiance, and the standard deviation equals 5% of the mean. If the sum of actual solar energy generated by the PV array and available energy in the battery is less than the total amount of energy consumed by the pre-scheduled appliances during each period, the simulation model adjusts the operation of appliances by turning off lower priority appliances. Based on the actual operation of appliances, some variables that have an influence on the operation of appliances in the next period are recalculated and updated. If a weekly required appliance is operated on a day, the simulation model assigns a "0" value to its priority for the next day. It avoids operating the appliance for the rest of the week. Otherwise, it gradually increases its priority to ensure that it is more likely to operate the next day. The SOC during the last period becomes the initial SOC the next day. The priorities of appliances are initialized every first day of the week. The simulation model iterates the energy- scheduling model for 365 days to compute annual user demand satisfaction, which is the percentage of supplied energy to appliances compared to the total energy demanded. The simulation model also provides the annual non-served energy, total energy demanded minus the supplied energy.

2.4 Sizing the energy system

The Nelder-Mead algorithm described in [18] is used to determine a cost-efficient solution to the design of the PV system. The simplex method of linear programming is used to find a local minimum of an objective function of multiple variables. It has been proven successful in many applications [19]. In the design of the PV system, the objective is to minimize the annual equivalent cost (AEC) of the PV array and battery plus a penalty cost of non-served energy. The decision variables are the capacities of the PV array, $x^{\mathrm{PV}} = \mathrm{C}^{\mathrm{PV}}$ and battery, $x^{\mathrm{BAT}} = \mathrm{C}^{\mathrm{BAT}}$. The algorithm

starts by randomly generating three pairs ($x^{\mathrm{PV}}, x^{\mathrm{BAT}}$). For each pair, the Monte Carlo simulation in Figure 2.3 is executed. At each simulated day, the simulation calls the energy scheduling optimization model described in Eq. (2.1) - Eq. (2.20). The simulation outputs the annual non-served energy x^{NS}. The AEC of the energy system is computed by Eq. (21).

$$f(x^{\mathrm{PV}}, x^{\mathrm{BAT}}, x^{\mathrm{NS}}) = \mathrm{PV}^{\mathrm{COST}} * x^{\mathrm{PV}} + \mathrm{BAT}^{\mathrm{COST}} * x^{\mathrm{BAT}} + \mathrm{NS}^{\mathrm{COST}} * x^{\mathrm{NS}} \quad (2.21)$$

The parameter $\mathrm{NS}^{\mathrm{COST}}$ (\$/kWh) is the unit penalty cost of non-served energy. The parameters $\mathrm{PV}^{\mathrm{COST}}$ (\$/kW) and $\mathrm{BAT}^{\mathrm{COST}}$ (\$/kWh) are the AEC of the PV array and battery, respectively. The AEC is computed by Eq. (2.22).

$$AEC = NPV * \frac{i(1+i)^{\mathrm{N}}}{(1+i)^{\mathrm{N}} - 1} \quad (2.22)$$

Where *i* is the market interest rate, N the lifetime of the PV array (N^{PV}) and battery ($\mathrm{N}^{\mathrm{BAT}}$), NPV represents the net present value of the investment and operation costs. The pseudo-code of the N-M algorithm for solving the PV sizing problem is presented in Figure 2.4.

Randomly generate 3 initial solutions: $v_1(x_1^{\mathrm{PV}}, x_1^{\mathrm{BAT}}), v_2(x_2^{\mathrm{PV}}, x_2^{\mathrm{BAT}}), v_3(x_3^{\mathrm{PV}}, x_3^{\mathrm{BAT}})$
Evaluate demand loss and objective function value for each solution: f(v_1), f(v_2), f(v_3)
REPEAT
    Identify the highest (W: worst), second highest (G: good) and lowest (B: best) solutions based on objective function values f(W), f(G), f(B), respectively
    Obtain a solution M = (G + B)/2, Evaluate demand loss(M), f(M)
    Perform **reflection**:
        Obtain a solution R = 2*M- W, Evaluate demand loss(R), f(R)
    IF f(R) < f(G):
        IF f(B) < f(R):
            Replace W ← R, f(W) ← f(R)
        ELSE:
            Perform **expansion**:
                Obtain a solution E= 2*R – M
                Evaluate demand loss(E), f(E)
            IF f(E) < f(R):
                Replace W ← E, f(W) ← f(E)
            ELSE:
                Replace W ← R, f(W) ← f(R)
    ELSE:
        IF f(R) < f(W):
            Replace W ← R, f(W) ← f(R)
        Perform **contraction**:
            Obtain a solution C1= (W + M)/2, solution C2= (M + R)/2
            Evaluate demand loss(C1), demand loss(C2), f(C1), f(C2)
            Obtain a solution C ← min(f(C1), f(C2))
        IF f(C) = f(C1):
            Replace C ← C1, f(C) ← f(C1),
        ELSE:
            Replace C ← C2, f(C) ← f(C2)
        IF f(C) < f(W):
            Replace W ← C, f(W) ← f(C)
        ELSE:
            Perform **shrink** toward a solution B:
                Obtain a solution S = (B + W)/2
                Evaluate demand loss(s), f(s)
                Replace W ← S, G ← M, f(W) ← f(S), f(G) ← f(M)
UNTIL $\left|1 - \frac{f(B)}{f(W)}\right| \times 100 < 0.1\%$

Figure 2.4 Nelder-Mead algorithm pseudo-code for sizing the PV system

2.5 Case studies and results

To verify the model under different annual solar irradiance profiles, we create two case studies given in Table 2.1. All models are solved on a 3.2GHz Core i5 processor with 8GB of memory. It takes 7.2 minutes in each case to obtain the solutions.

Table 2.1 Case studies

Name	City	State
AU	Auburn	Alabama
PH	Phoenix	Arizona

2.5.1 System Data

In these case studies, we consider 364 days (7 days/week*52 weeks). The numbers of days per day type are given in Table 2.2.

Table 2.2 Number of days per day types

Type	Days	Description
Weekday	245	Monday - Friday
Weekend	97	Saturday, Sunday
Holiday	22	National holidays in the U.S. (7) Summer vacation (7) Thanksgiving break (4) Christmas break (4)

We consider a 3-bedroom and 2-bathroom house with a 4-person household. We divide a typical day into 24 equal periods of 1-hour length. During the weekday, we assume that the family wakes up at 6 AM, leaves for school and work at 8 AM, returns home at 6 PM and goes to bed at 11 PM. During the weekend, they wake up and go to bed at the same time as the weekdays, but they stay at home all day. We also assume that the family leaves home on holidays. The energy consumptions (kWh) of 15 appliances in the house are given in Table 2.3.

Table 2.3 Appliance energy consumption

Short Name	Full name	Energy Consumption (kWh)
CLW	Clothes Washer (Warm wash, Cold rinse)	2.300
CLD	Clothes Dryer (Light Load)	2.500
DIW	Dish Washer	1.200
CFB	CFL Bulb (11W)	0.011
LEB	LED Bulb (10W)	0.010
HAB	Halogen Bulb (40W)	0.040
INB	Incandescent Bulb (40W)	0.040
REF	Refrigerator (17 cu. ft., frost-free)	0.049
TOO	Toaster Oven	0.750
EOS	Electric Oven/Range (Surface)	1.000
EOR	Electric Oven/Range (Oven)	2.300
COM	Coffee Machine (Brew, Warmer on)	0.400
DOL	Desktop or Laptop	0.020
TVD	LED TV (40"-49") / Satellite Dish	0.056
IMW	Internet Modem / Wireless Router	0.014
REN	Reserved Energy	0.500

We consider the washer, dryer, and dishwasher flexible appliances and the washer and dishwasher uninterruptible appliances. The washer and dryer are required once a week, and the electric oven/range is required at noon only on weekends. During a holiday, only the refrigerator operates. 0.5kWh of energy (REN) is reserved for unexpected usage of appliances such as charging a cell phone or operating a hairdryer. The requested operations of the appliances are shown in Tables 2.4-2.5. We create twenty-one additional appliances to represent appliances that are requested to operate more than once during a day. For example, during the weekdays, we represent the TVD by two different appliances. One appliance operates in the morning (TVD-Morning), and another appliance operates in the evening (TVD-Evening). We arbitrarily create preferred operation periods and priorities. We give the specifications of the PV-battery system in Tables 2.6-2.7. The life expectancy of the Lithium-ion battery is normally 5 to 15 years; however, we assumed that it is five years since the battery would be highly used under the off-grid situation. Additionally,

it is assumed that the degradation of PV array and battery are considered in the annual equivalent cost.

Table 2.4 Requested operation periods (weekday)

Appliance	Qty	T_a (H)	$P_{a,t}$	W_a	Appliance	Qty	T_a (H)	$P_{a,t}$	W_a
		Summer (Winter)	Summer (Winter)				Summer (Winter)	Summer (Winter)	
CLW	1	2(2)	1(1) - 24(24)	8	HAB (Evening)	10	4(5)	20(19) - 23(23)	6
CLD	1	1(1)	1(1) - 24(24)	6	INB (Evening)	10	4(5)	20(19) - 23(23)	4
DIW	1	2(2)	1(1) - 24(24)	7	REF	1	24(24)	1(1) - 24(24)	10
CFB1 (Morning)	6	1(2)	7(7) - (8)	10	TOO	1	1(1)	7(7) - 8(8)	9
CFB2 (Morning)	6	1(2)	7(7) - (8)	3	EOR	1	1(1)	19(19) - 20(20)	9
LEB1 (Morning)	6	1(2)	7(7) - (8)	6	COM (Morning)	1	1(1)	7(7) - 8(8)	6
LEB2 (Morning)	6	1(2)	7(7) - (8)	3	COM (Evening)	1	1(1)	20(20) - 21(21)	5
HAB1 (Morning)	5	1(2)	7(7) - (8)	5	DOL	1	7(7)	7(7) - 8(8) or 19(19) - 23(23)	7
HAB2 (Morning)	5	1(2)	7(7) - (8)	3	TVD (Morning)	1	2(2)	7(7) - 8(8)	6
INB1 (Morning)	5	1(2)	7(7) - (8)	4	TVD (Evening)	1	5(5)	19(19) - 23(23)	8
INB2 (Morning)	5	1(2)	7(7) - (8)	3	IMW (Morning)	1	2(2)	7(7) - 8(8)	7
CFB (Evening)	12	4(5)	20(19) - 23(23)	10	IMW (Evening)	1	5(5)	19(19) - 23(23)	7
LEB (Evening)	12	4(5)	20(19) - 23(23)	8	REN	1	7(7)	7(7) - 8(8) and 19(19) - 23(23)	-

Table 2.5 Requested operation periods (weekend)

Appliance	Qty	T_a (H)	$P_{a,t}$	W_a	Appliance	Qty	T_a (H)	$P_{a,t}$	W_a
		Summer (Winter)	Summer (Winter)				Summer (Winter)	Summer (Winter)	
CLW	1	2(2)	1(1) - 24(24)	8	HAB (Evening)	10	4(5)	20(19) - 23(23)	8
CLD	1	1(1)	1(1) - 24(24)	6	INB (Evening)	10	4(5)	20(19) - 23(23)	4
DIW	1	2(2)	1(1) - 24(24)	7	REF	1	24(24)	1(1) - 24(24)	10
CFB1 (Morning)	6	1(2)	7(7) - (8)	5	TOO	1	1(1)	7(7) - 8(8)	9
CFB2 (Morning)	6	1(2)	7(7) - (8)	3	EOS	1	1(1)	12(12) - 13(13)	9
LEB1 (Morning)	6	1(2)	7(7) - (8)	10	EOR	1	1(1)	19(19) - 20(20)	9
LEB2 (Morning)	6	1(2)	7(7) - (8)	3	COM (Morning)	1	1(1)	7(7) - 8(8)	8
HAB1 (Morning)	5	1(2)	7(7) - (8)	6	COM (Noon)	1	1(1)	12(12) - 13(13)	6
HAB2 (Morning)	5	1(2)	7(7) - (8)	3	COM (Evening)	1	1(1)	20(20) - 21(21)	5
INB1 (Morning)	5	1(2)	7(7) - (8)	4	DOL (All day)	1	17(17)	7(7) - 23(23)	7
INB2 (Morning)	5	1(2)	7(7) - (8)	3	TVD (All day)	1	17(17)	7(7) - 23(23)	8
CFB (Evening)	12	4(5)	20(19) - 23(23)	6	IMW (All day)	1	17(17)	7(7) - 23(23)	7
LEB (Evening)	12	4(5)	20(19) - 23(23)	10	REN	1	17(17)	7(7) - 23(23)	-

Table 2.6 PV array specifications

Parameter	Value	Description
PV^{COST}	102.78($/kW)	AEC of PV electricity per kW
PV^{CF}	0.0736	Capital recovery factor of PV array
N^{PV}	20(years)	Life expectancy of PV array
i	4%	Market interest rate
INV^{E}	99%	Inverter efficiency

Table 2.7 Battery specifications

Parameter	Value	Description
BAT^{COST}	163.37($/kWh)	AEC of battery energy per kWh
BAT^{CF}	0.2246	Capital recovery factor of battery
N^{BAT}	5(years)	Life expectancy of battery (Lithium Ion)
i	4%	Market interest rate
S^{ISC}	30%	Initial amount of energy in the battery
S^{ESC}	30%	End amount of energy in the battery
S^{MIN}	5%	Minimum SOC
S^{MAX}	95%	Maximum SOC
R^{CHR}	99%	Charging efficiency
R^{DCH}	0.139%	Self-discharging efficiency
R^{MCH}	51%	Maximum charging power
R^{MDC}	51%	Maximum discharging power

2.5.2 Forecasted and actual solar irradiance

For daily forecasts of solar irradiance, we use historical solar irradiance from the National Solar Radiation Database [20]. To represent variability and uncertainty in the actual solar irradiance, we use Monte Carlo random sampling. In Figures 2.5-2.6, we plot the forecasted and actual (Monte Carlos sampled) hourly solar irradiances corresponding to January 1 in AU and PH.

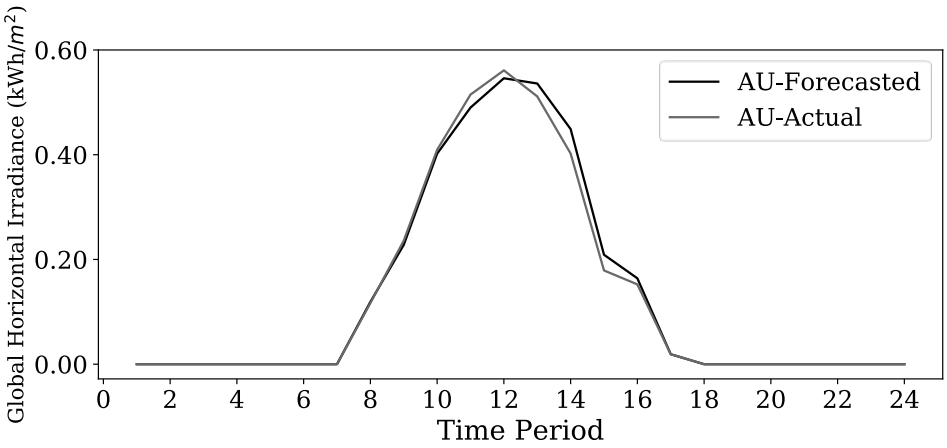

Figure 2.5 Forecasted and actual solar irradiance on January 1 in AU

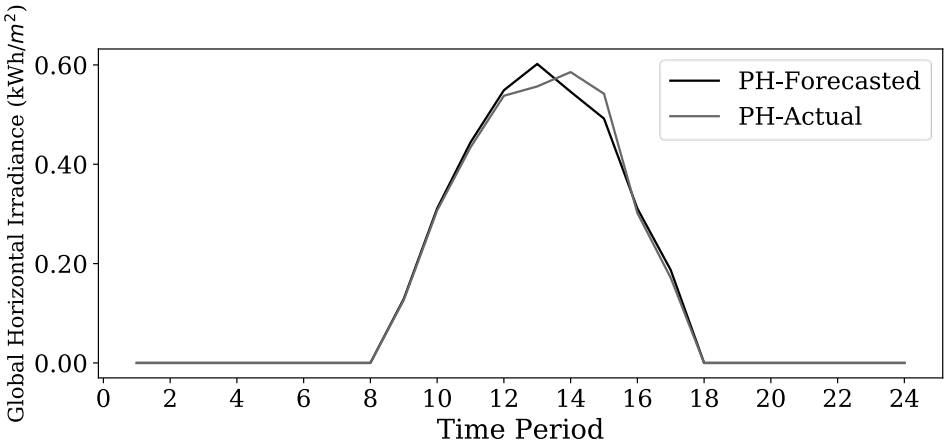

Figure 2.6 Forecasted and actual solar irradiance on January 1 in PH

In Figure 2.7, we show the annual amount of forecasted and actual electrical energy generated by a PV array of capacity 11.2kW. In AU, 0.01% more solar energy was forecasted than actually generated. In contrast, in PH, 0.07% less solar energy was forecasted than actually generated. The plot also shows the annual energy requested by the appliances (7,389.28kWh).

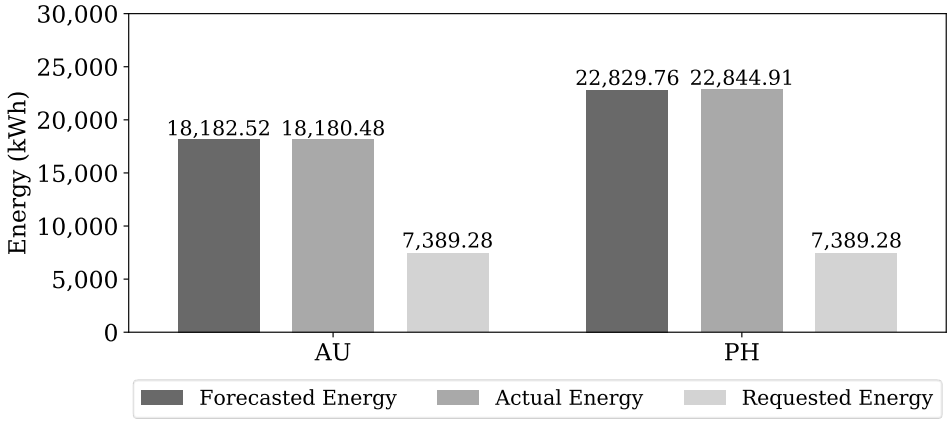

Figure 2.7 PV solar forecasted, generated and requested energy by location

2.5.3 Sizing the PV array and battery capacity

We use the Nelder-Mead algorithm to find cost-efficient capacities for the PV array and battery. For the penalty cost of non-served energy, we use 0.13 ($/kWh) from the U.S. Energy Information Administration [21]. We do not consider incidental costs such as operation and maintenance. Thus, Eq. (2.23) becomes:

$$f(x^{\mathrm{PV}}, x^{\mathrm{BAT}}, x^{\mathrm{NS}}) = 102.78x^{\mathrm{PV}} + 163.37x^{\mathrm{BAT}} + 0.13x^{\mathrm{NS}} \tag{2.23}$$

The Nelder-Mead algorithm starts by randomly generating three solutions. After executing the simulation model for the three solutions, the values of annual non-served energy x^{NS} are obtained. Then, Eq. (2.23) is computed for each solution. Table 2.8 shows the values for the first iteration of the algorithm. The solution v_1 is infeasible and therefore it is not considered in the next iteration.

Table 2.8 First iteration of the Nelder-Mead algorithm

Solutions	x^{PV}	x^{BAT}	x^{NS}		$f(x^{\mathrm{PV}}, x^{\mathrm{BAT}}, x^{\mathrm{NS}})$	
			AU	PH	AU	PH
v_1	1.59kW	37.12kWh	-	-	-	-
v_2	14.08kW	43.81kWh	39.29kWh	14.70kWh	$8,606.09	$8,606.14
v_3	23.99kW	31.31kWh	5.43kWh	2.50kWh	$7,581.38	$7,581.00

In Figures 2.8-2.9, we show the iterations of the Nelder-Mead algorithm. Figure 2.10 shows the convergence of the Nelder-Mead algorithm. The algorithm converges after 42 iterations for the AU case and 35 iterations for the PH case.

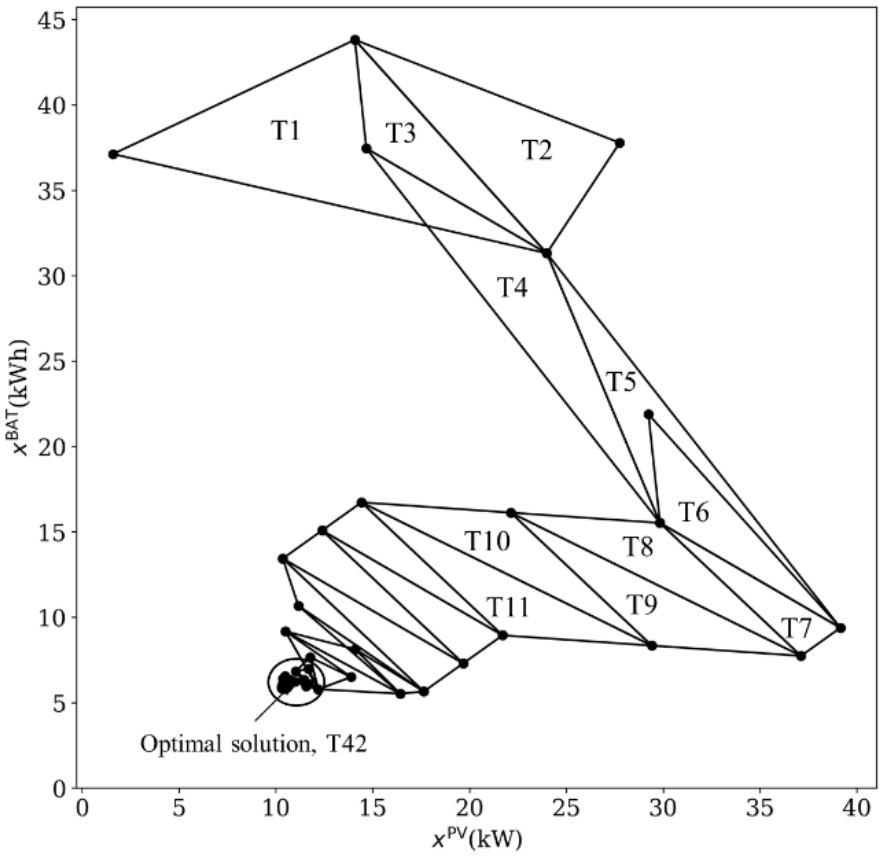

Figure 2.8 Nelder-Mead algorithm iterations for AU case

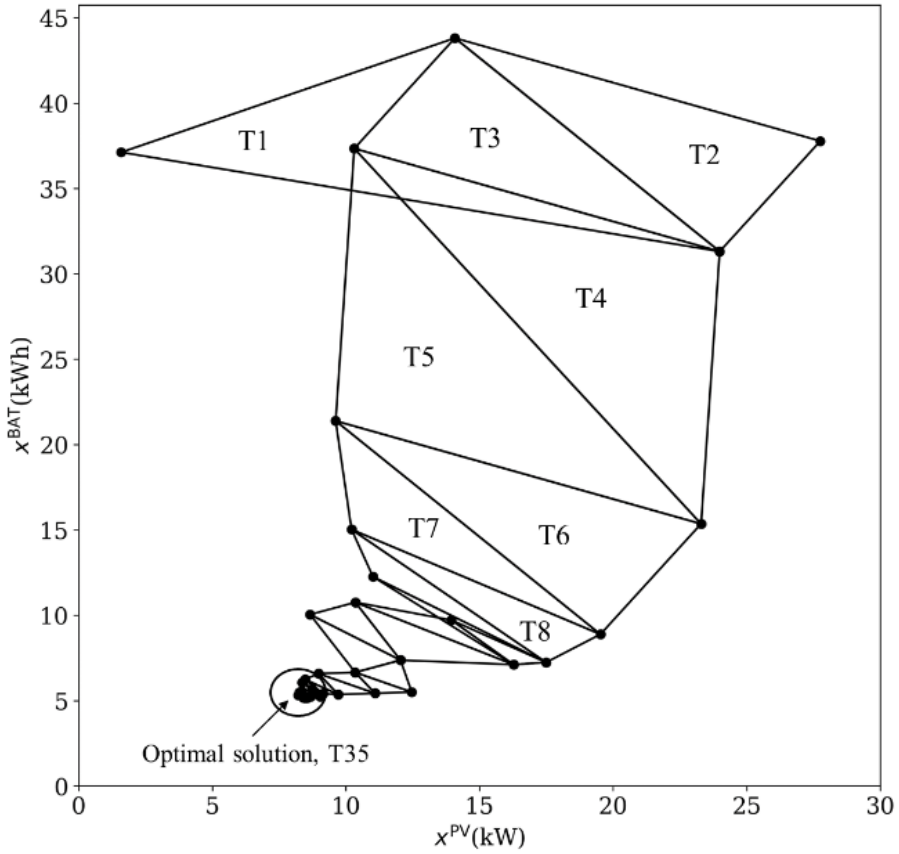

Figure 2.9 Nelder-Mead algorithm iterations for PH case

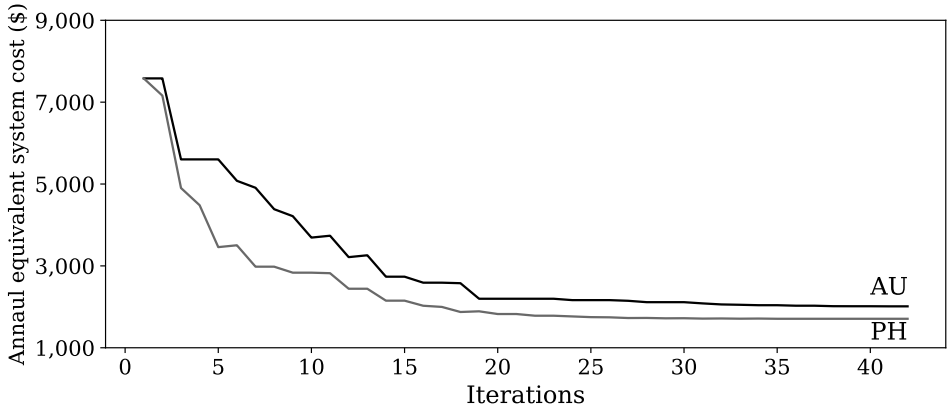

Figure 2.10 Convergence of the Nelder-Mead algorithm

In Table 2.9, we present the results. In AU, the energy system consists of a 10.31kW PV array and 5.83kWh battery with the AEC of $2,011.87. In PH, the energy system consists of an 8.39kW PV array and 5.18kWh battery with the AEC of $1,708.02.

Table 2.9 Nelder-Mead algorithm results

Case	# of iterations	PV capacity	Battery capacity	Non-served energy	Annualized system cost
AU	42	10.31kW	5.83kWh	2,961.15kWh	$2,011.87
PH	35	8.39kW	5.18kWh	3,294.21kWh	$1,708.02

2.6 Nelder-Mead results simulation

We execute the simulation model for the solutions provided by the Nelder-Mead algorithm (Table 2.9). We assume that the energy-scheduling model is solved every midnight at 12:00 a.m. The operation of the appliances for the next twenty-four hours is simulated using actual solar irradiance (Monte Carlo samples) and the pre-schedules from the scheduling optimization model. The model simulates the operation of the appliances during one year. In Figure 2.11, we show the number of days in which appliances operated as pre-scheduled. In AU, the appliances operated as pre-scheduled for 319 days while in PH the appliances operated as pre-scheduled for 318 days.

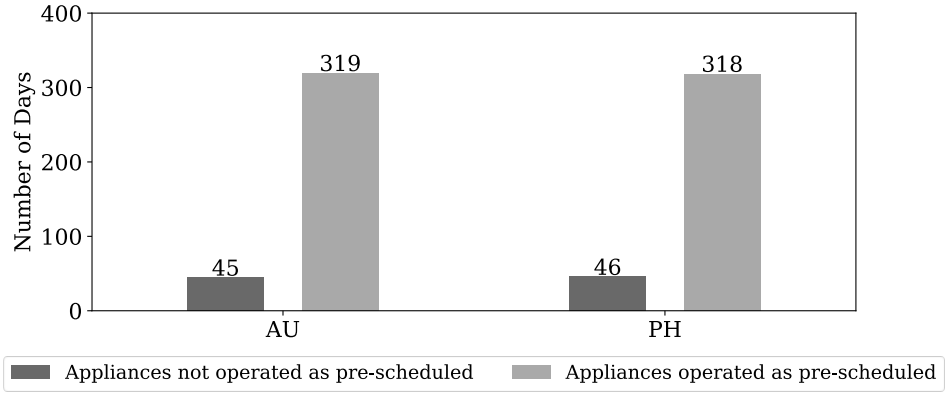

Figure 2.11 Days that appliances operated as pre-scheduled

Table 2.10 illustrates a pre-schedule and actual operation of appliances during the fifth day of week 2 in AU.

Table 2.10 Pre-schedule and actual operation of appliances in AU

Appliance	Results		Appliance	Results	
	Pre-schedule	Actual operation		Pre-schedule	Actual operation
CLW	-	-	HAB (Evening)	19 - 22	19 - 22
CLD	-	-	INB (Evening)	-	-
DIW	12 - 13	12 - 13	REF	1 - 24	1 - 24
CFB1 (Morning)	7 - 8	7 - 8	TOO	-	-
CFB2 (Morning)	7 - 8	7 - 8	EOR	-	-
LEB1 (Morning)	7 - 8	7 - 8	COM (Morning)	7	7
LEB2 (Morning)	7 - 8	7	COM (Evening)	-	-
HAB1 (Morning)	7 - 8	7 - 8	DOL	7 - 8, 19 - 23	7 - 8, 19 - 23
HAB2 (Morning)	7	7	TVD (Morning)	7 - 8	7 - 8
INB1 (Morning)	7 - 8	7 - 8	TVD (Evening)	19 - 23	19 - 23
INB2 (Morning)	-	-	IMW (Morning)	7 - 8	7 - 8
CFB (Evening)	19 - 23	19 - 23	IMW (Evening)	19 - 23	19 - 23
LEB (Evening)	19 - 23	19 - 23	ENM	7 - 8, 19 - 23	7 - 8, 19 - 23

The LEB2 (morning) appliance was pre-scheduled to operate during periods 7 and 8. However, the appliance did not operate during period 8 because the amount of actual available energy was less than the forecasted available energy. Table 11 shows similar data for PH on the second day of week 41. The LEB2 (morning) and CFB2 (morning) appliances were pre-scheduled to operate during periods 7 and 8. However, they only operated during period 7.

Table 2.11 Pre-schedule and actual operation of appliances in PH

Appliance	Results		Appliance	Results	
	Pre-schedule	Actual operation		Pre-schedule	Actual operation
CLW	-	-	HAB (Evening)	19 - 20	19 - 22
CLD	-	-	INB (Evening)	-	-
DIW	12 - 13	12 - 13	REF	1 - 24	1 - 24
CFB1 (Morning)	7 - 8	7 - 8	TOO	-	-
CFB2 (Morning)	7 - 8	7	EOS	12	12
LEB1 (Morning)	7 - 8	7 - 8	EOR	-	-
LEB2 (Morning)	7 - 8	7	COM (Morning)	7	7
HAB1 (Morning)	7 - 8	7 - 8	COM (Noon)	12	12
HAB2 (Morning)	7 - 8	7 - 8	COM (Evening)	-	-
INB1 (Morning)	7 - 8	7 - 8	DOL (All day)	7 - 8, 19 - 23	7 - 8, 19 - 23
INB2 (Morning)	7 - 8	7 - 8	TVD (All day)	7 - 8, 19 - 23	7 - 8, 19 - 23
CFB (Evening)	19 - 23	19 - 23	IMW (All day)	7 - 8, 19 - 23	7 - 8, 19 - 23
LEB (Evening)	19 - 23	19 - 23	ENM	7 - 8, 19 - 23	7 - 8, 19 - 23

Table 2.12 shows the annual operation rate of the appliances. It is defined as the percentage of annual operating hours of an appliance divided by its annual required operation hours.

Table 2.12 Appliances annual operation rate

Appliance	Annual required hour (H)	Annual operated hour (H)		Annual operation rate (%)	
		AU	PH	AU	PH
CLW	102	101	102	99.02%	100.00%
CLD	51	47	49	92.16%	96.08%
DIW	684	648	667	94.74%	97.51%
CFB	2,559	964	637	37.67%	24.89%
LEB	2,559	1,960	1,030	76.59%	40.25%
HAB	2,559	742	351	29.00%	13.72%
INB	2,559	556	219	21.73%	8.56%
REF	8,736	8,554	8,304	97.92%	95.05%
TOO	342	215	158	62.87%	46.20%
EOS	97	88	94	90.72%	96.91%
EOR	342	0	0	0.00%	0.00%
COM	781	348	263	44.56%	33.67%
DOL	3,364	3,183	3,272	94.62%	97.27%
TVD	3,364	3,061	2,890	90.99%	85.91%
IMW	3,364	3,322	3,327	98.75%	98.90%

The average operation rate of all appliances is 69.57% in AU and 68.76% in PH. When there is not enough energy, the lower priority appliances requiring less energy and longer operation periods such as TVD and IMW are more likely to be selected than higher priority appliances that need more energy for shorter operation periods. This is the reason why the operation rate of the appliance EOR is 0% in AU and PH even though its priority (9) is higher than the other appliances.

Figure 2.12 shows the average hourly SOC over the year. The charging/discharging periods are different in AU and PH. However, the battery always maintained its maximum SOC (95%) during period 17 and 18, to operate appliances during the evening.

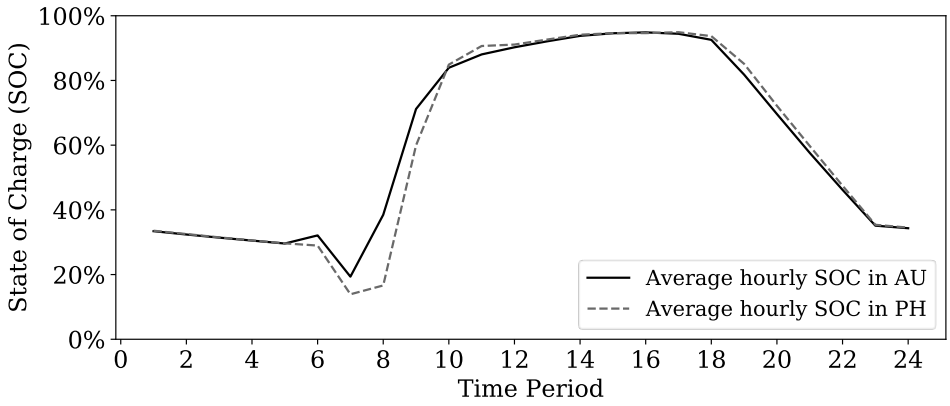

Figure 2.12 Annual average SOC of the battery

Table 2.13 shows the annual demand satisfaction calculated as the percentage of actual PV energy used by the appliances compared to the energy demanded. The annual demand satisfaction in AU is 1.05 times more than in PH even though the total generated solar energy in PH is 1.0009 times more than in AU. This discrepancy is because the amount of solar irradiance in AU is 1.79 times more than in PH during periods 7 and 8. In these periods, several appliances such as the toaster oven and coffee machine are requested to operate. Although sufficient solar energy was generated in AU and PH, annual energy demanded was not fully satisfied, mainly because the penalty cost of non-served energy is more cost-efficient than increasing the capacity of the battery needed for running appliances during the evening.

Table 2.13 Annual energy and demand satisfaction

Case	Energy demanded	PV energy used	Non-served energy	Demand satisfaction
AU	7,389.08kWh	4,427.49kWh	2,961.15kWh	59.92%
PH	7,389.08kWh	4,094.82kWh	3,294.21kWh	55.42%

Table 2.14 summarizes the annual energy usage from the PV-battery system. In AU, 1.08 times more energy is consumed than in PH. Moreover, 1.06 times more unused energy occurred in PH than in AU due to the higher solar irradiance in PH. Notice a large amount of unused energy

occurring in AU and PH even though the demand satisfaction is 59.92% and 55.42%, respectively. It is more cost-efficient to curtail the energy demand for evening appliances than to increase the capacity of the battery. Therefore, we perform a sensibility analysis of the penalty cost for non-served energy.

Table 2.14 Total energy usage

Case	Appliances from PV	Appliances from battery	Conversion losses	Unused energy
AU	2,729.27kWh	1,698.22kWh	90.36kWh	12,186.34kWh
PH	2,508.25kWh	1,586.57kWh	83.57kWh	12,915.80kWh

2.7 Sensitivity Analysis

To evaluate the effect of the penalty cost of non-served energy, we change the value $\mathrm{NS}^{\mathrm{COST}}$ from 0.13($/kWh) to 20.13($/kWh) in increments of 0.5($/kWh). Table 2.15 gives the system characteristics in AU for different penalty costs of non-served energy. The table shows that the AEC of energy system increases as the penalty cost of non-served energy increases.

Table 2.15 PV array and battery capacities versus Non-served energy cost (AU)

Penalty cost of non-served energy ($/kWh)	PV capacity (kW)	Battery capacity (kWh)	Non-served energy (kWh)	Annualized cost ($)
0.13	10.31	5.83	2,961.15	2,012.09
0.63	10.31	9.84	2,022.35	2,667.18
1.13	10.38	17.49	566.80	3,924.12
1.63	10.68	17.73	503.16	3,994.16
2.13	11.52	18.54	372.01	4,212.83
⋮	⋮	⋮	⋮	⋮
5.13	17.86	18.78	148.20	4,903.66
7.13	19.84	19.67	97.77	5,252.57
10.13	24.16	19.57	45.65	5,680.24
⋮	⋮	⋮	⋮	⋮
14.13	28.30	20.27	14.30	6,220.11
⋮	⋮	⋮	⋮	⋮
20.13	28.35	20.32	9.40	6,233.40

When the penalty cost of non-served energy equals 1.13($/kWh), non-served energy sharply decreases from 2,022.35kWh to 566.80kWh. When the penalty cost of non-served energy reaches 20.13($/kWh), almost all energy requested is fulfilled.

To evaluate the effect of the cost of the battery, we change $\mathrm{BAT}^{\mathrm{COST}}$ from 163.37($/kWh) to 32.67($/kWh) in decrements of 32.67($/kWh) (20% of 163.37). We set the cost of non-served energy to 0.13($/kWh). Table 2.16 gives the system characteristics for different values of the parameter $\mathrm{BAT}^{\mathrm{COST}}$. The table shows that non-served energy is not significantly affected by the cost of the battery when the penalty cost of non-served energy is 0.13(S/kWh).

Table 2.16 PV array and battery capacities versus Annualized battery cost (AU)

AEC of the battery ($/kWh)	PV capacity (kW)	Battery capacity (kWh)	Non-served energy (kWh)	Annualized cost ($)
32.67	10.30	9.03	2,207.41	1,353.65
65.35	12.15	5.71	2,920.23	1,621.94
98.02	10.30	6.27	2,853.47	1,673.23
130.70	10.41	5.91	2,938.28	1,842.39
163.37	10.31	5.83	2,961.15	2,012.12

To study how the cost of the battery and penalty cost of non-served energy relate to non-served energy, we change simultaneously the parameters $\mathrm{BAT}^{\mathrm{COST}}$ and $\mathrm{NS}^{\mathrm{COST}}$. Figure 2.13 shows that at the higher and lower costs of non-served energy, the cost of the battery does not significantly affect non-served energy. We do not perform a sensitivity study on the price of the PV arrays because most of the demand occurs at the evening hours where the capacity of the battery is more relevant.

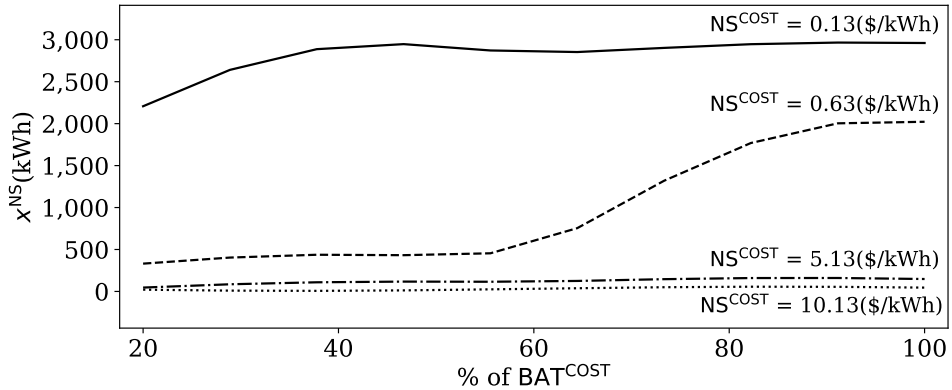

Figure 2.13 Effect of UD^{COST} and BAT^{COST} on x^{NS}

2.8 Conclusion

We proposed an off-grid PV system design approach that considers energy consumption scheduling and system operation under solar irradiance uncertainty. The solution method combined the Nelder-Mead algorithm, mixed-integer programming, and Monte Carlo simulation. We determined a cost-efficient solution for the PV array and battery capacities at two geographical locations, AU and PH. Because AU had less solar irradiance than PH, a more costly system was required in AU. To meet the demand, the capacity of the battery was more influential than the PV array capacity in both locations. The sensitivity analysis showed that the opportunity cost of the non-served energy is a key factor in order to meet the demand with solar energy.

References

[1] U.S. Energy Information Administration (EIA). International Energy Outlook 2016, DOE/EIA-0484(2016) 82. Washington, DC. https://www.eia.gov/outlooks/ieo/pdf/0484(2016).pdf (accessed 3 February 2019)

[2] Energy Sector Management Assistance Program (ESMAP) of World Bank, The Energy Progress Report, (2019). https://trackingsdg7.esmap.org/data/files/download-documents/2019-tracking_sdg7-complete-rev030320.pdf (accessed 30 March 2020)

[3] S. Rohit, S. C. Bhattacharyya, (2014). Off-grid electricity generation with renewable energy technologies in India: an application of HOMER, Renewable Energy 62, 388-398.

[4] D. Thevenard, S. Pelland, (2013). Estimating the uncertainty in long-term photovoltaic yield predictions, Solar Energy 91, 432-445.

[5] T. Khatib, Ibrahim A. Ibrahim, A. Mohamed, (2016). A review on sizing methodologies of photovoltaic array and storage battery in a standalone photovoltaic system, Energy Conversion and Management 120, 430-448

[6] G. E. Ahmad, (2002). Photovoltaic-powered rural zone family house in Egypt, Renewable Energy 26(3), 379-390

[7] M. M. H. Bhuiyan, M. Ali Asgar, (2003). Sizing of a stand-alone photovoltaic power system at Dhaka, Renewable Energy 28(6), 929-938

[8] H. A. Kazem, T. Khatib, K. Sopianb, (2013). Sizing of a standalone photovoltaic/battery system at minimum cost for remote housing electrification in Sohar, Oman, Energy and Buildings 61, 108-115

[9] N. D. Nordin, H. A. Rahman, (2016). A novel optimization method for designing stand alone photovoltaic system, Renewable Energy 89, 706-715

[10] A Q. Jakhrani, A. Othman, A. R. H. Rigit, S. R. Samo, S. A. Kamboh, (2012). A novel analytical model for optimal sizing of standalone photovoltaic systems, Energy 46(1), 675-682

[11] T. Khatib, A. Mohamed, K. Sopian, M. Mahmoud, (2012). A New Approach for Optimal Sizing of Standalone Photovoltaic Systems, International Journal of Photoenergy 2012

[12] A. Al-Waeli, A. Aziz, A. H. A. Alwaeli, A. K. Hussein, (2013). Optimal sizing of photovoltaic systems using HOMER for Sohar, Oman, International Journal of Renewable Energy Research 3(2), 301-307

[13] J. Carroquino, R. Dufo-López, J. L. Bernal-Agustínb, (2015). Sizing of off-grid renewable energy systems for drip irrigation in Mediterranean crops, Renewable Energy 76, 566-574

[14] C. B. Salah, K.Lamamra, A. Fatnassi, (2015). New optimally technical sizing procedure of domestic photovoltaic panel/battery system, Journal of Renewable and Sustainable Energy 7

[15] P. G. Nikhil, D. Subhakar, (2013). Sizing and Parametric Analysis of a Stand-Alone Photovoltaic Power Plant, IEEE Journal of Photovoltaics 3(2), 776-784

[16] T. Khatib, W. Elmenreich, (2014). An Improved Method for Sizing Standalone Photovoltaic Systems Using Generalized Regression Neural Network, International Journal of Photoenergy 2014

[17] D. Cho, J. Valenzuela, (2019). Scheduling energy consumption for residential stand-alone photovoltaic systems, Solar Energy 187, 393-403.

[18] John H. M., Kurtis K. F, (2004). Numerical Methods Using Matlab, fourth ed. Prentice-Hall Inc., New Jersey, pp.430-436

[19] P. Piela, J. Mitzel, E. Gu¨lzow, J. Hunger, A. Kabza, L. J€orissen, F. Valle, A. Pilenga, T. Malkow, G. Tsotridis, (2017). Performance optimization of polymer electrolyte membrane fuel cells using the Nelder-Mead algorithm, Hydrogen energy 42, 20187-20200

[20] National Centers for Environmental Information, National Solar Radiation Data Base: 1991-2010. ftp://ftp.ncdc.noaa.gov/pub/data/nsrdb-solar/solar-only/(accessed 3 February 2019)

[21] U.S. Energy Information Administration (EIA). Electric Power Monthly with Data for August 2019. Washington, DC. https://www.eia.gov/electricity/monthly/current_month/epm.pdf (accessed 1 November 2019)

Chapter 3 A Stochastic Optimization Model for Determining the Capacity of a Residential Off-grid PV-Battery System

3.1 Abstract

Electricity generation by renewable energy sources represents a promising solution to most isolated areas. Renewable energy is an environmentally friendly, sufficient and sustainable energy resource that can solve the energy deficit of the present and future. Among various renewable energy sources, solar power is applicable everywhere as long as there is solar irradiance. It is particularly useful for isolated areas where there is no access to any other source of electricity. However, the inherent uncertainty of solar irradiance and climate changes may result in a high initial investment cost that could make this energy system uneconomical. In this paper, we propose a stochastic optimization model for determining the capacity of a residential off-grid energy system that considers solar irradiance uncertainty and hourly energy consumption patterns. The energy system consists of a PV array, battery, and a diesel generator. We use a mixed-integer programming method that uses scenarios to represent the uncertainty of solar irradiance. The optimization model determines the system capacity to supply the energy demanded at each period by minimizing the AEC of investment and the fuel cost of using a diesel generator. We compare the optimized case with the non-optimized case to assess the effect of scheduling. The effect of number of scenarios on the solutions is evaluated by changing the number of scenarios considered.

Keywords: Off-grid PV system, PV array capacity, Battery capacity, Solar irradiance uncertainty, Energy consumption scheduling, Mixed integer programming, Stochastic optimization

3.2 Introduction

As the technology of PV array and battery is becoming more affordable, the propagation of stand-alone PV systems is rapidly growing across the world. It is expected that world solar energy generation will rise by 641.71% from 1,298.26 billion kWh (2020) to 8,331.10 billion kWh (2050) according to a recent report from the U.S Energy Information Administration (EIA) [1]. Nevertheless, a major challenge in PV applications is the determination of the optimal relationship between PV array and battery capacity to supply energy when it is needed. Determining an optimal configuration of an off-grid PV energy system can ensure efficient utilization of the solar energy in terms of economic and environmental factors. In addition, the amount of solar irradiance is unpredictable and largely affected by weather and climates changes. For over several decades, various approaches and methodologies have been developed to study the sizing of an off-grid PV system. In [3], the author used simple calculations to estimate the size of a PV array and the battery combination in a residential house in Egypt. The author compared the life cost of 1kWh generated energy from the designed PV system with a diesel generator. In [4], the size of a PV array and battery was calculated based on a mathematical model that takes into account factors such as estimated load demand, the tilt angle of the PV array. In [5], a time-series energy balance algorithm was used to create a cost versus reliability curve to find the optimal combination of a PV array size and the battery capacity that minimized system cost while maintaining user comfort. In [6], the Firefly Algorithm was used for sizing an off-grid PV system by minimizing the loss of power supply probability. The algorithm was tested under two different charge-controller cases. In [7],

the amp-hour method was used to determine PV array and battery capacities based on the loss of power supply probability (LPSP). An economic analysis was done to determine the levelized cost of energy for the proposed system. In [8], Borowy's method was used to investigate the optimal size of an off-grid PV-battery system under the conditions of a fixed tilt angle and various configurations of the PV array and battery. The optimal size combination at the minimum system cost was obtained given the LPSP. In addition to these studies, in [9], an artificial neural network-based genetic algorithm model was developed for creating the sizing curve for off-grid PV systems given the LPSP. The effectiveness of the proposed approach was tested by comparing with the results of numerical methods. In these studies, the primary objective was to determine the optimal size of the energy system without considering solar irradiance uncertainty and energy consumption patterns.

Several studies have examined the optimal sizing of an off-grid PV system under solar irradiance uncertainty. In [10], a techno-economic sizing methodology of a stand-alone PV system was implemented to optimize the system size given solar radiation generated by a Markov transition matrix. In [11], a design space approach was used for the optimal sizing of PV-battery system using the chance constrained programming method. The author compared the result of the deterministic case with the stochastic case. In [12], the authors developed stochastic analysis methods including the Markov chain and beta probability density function in order to optimize the size of the PV array and energy storage. In [13], a fast sizing approach was proposed to optimize the size of a PV system. This method created climate cycles including the extreme climate condition, calculated the size of the PV array and the battery for a given climate cycle. The optimal configuration of the PV array and battery was determined based on the minimum total annual cost of the system. In [14], the author optimized the capacity of energy storage given the PV array size

in three different locations in the U.S. and found the optimal combination of PV size and battery capacity by limiting the battery size and sunlight availability. In all of these studies, the authors considered the uncertainty of solar irradiance, but energy consumption pattern was not considered.

In this paper, we propose a stochastic optimization model for determining the capacity of an off-grid PV-battery system to ensure a minimum annual equivalent cost (AEC). Since the energy supplied by an off-grid PV-battery system depends on the daily solar irradiance, we add a home-backup diesel generator to supply energy when the PV-battery system is insufficient. We use scenarios to represent the uncertainty of solar irradiance. The objective of the model is to determine the cost-efficient capacity of an off-grid PV-battery system to satisfy the energy consumption schedule of home appliances over a time horizon of one year. The contributions of this paper are:

- A mathematical model to determine an optimal capacity of an off-grid PV-battery system at minimum AEC with expected diesel fuel usage
- A model that considers uncertainties of solar irradiance and user energy consumption patterns
- An extensive analysis to evaluate the effect of scheduling and number of scenarios

The remainder of this paper is organized as follows: Section 2 presents the problem description. Section 3 discusses problem formulation. Section 4 presents the experimental results. Finally, Section 5 ends with concluding remarks.

3.3 Problem description

PV array and battery capacities depend on available solar irradiance, ambient temperature, and energy demand during the day. It is especially important to consider various solar irradiance occasions to better estimate the PV-battery system capacity because of inherent solar irradiance

uncertainty. The well-optimized capacity of a PV-battery system provides energy efficiently to satisfy energy demand by operating required appliances. However, the worst solar irradiance day of the year can primarily affect the determination of an energy system capacity since solar energy is the only energy source. It leads to having larger PV array and battery capacities compared to those required during ordinary daily energy consumptions. An oversized energy system causes high AEC to invest and makes an energy system uneconomical since it generates an unnecessary amount of energy on most days. Meanwhile, a small-sized energy system can save the investment cost but does not assure generating enough amount of energy to satisfy energy demand when there are sudden weather changes during the day. A home-backup diesel generator allows for a balance between a stable supply of energy and having a cost-efficient energy system capacity. It also ensures that the diesel generator mitigates an oversizing problem of an energy system by supplying the required amount of energy when there is not enough energy from the PV array and battery. Thus, the optimal use of a diesel generator can contribute to determining a cost-efficient capacity of an energy system. Energy consumption management is also indispensable in achieving higher system efficiency and user comfort.

3.3.1 Residential off-grid energy system with a diesel generator

In Figure 3.1, a residential off-grid PV-battery system consists of PV arrays, a PV charge controller, an inverter, a battery, a home-backup diesel generator, and energy demand required by using appliances at home. PV arrays convert solar irradiance into available electrical energy. A PV charging controller prevents the battery from being overcharged and an inverter changes DC power into AC power. A battery stores the remaining energy and enables appliances to be operated when there is not enough solar irradiance. A diesel generator is scheduled to provide energy to

appliances when energy from PV arrays and the battery are limited. It is assumed that all appliances including a diesel generator operate in a binary manner “on (=1)” or “off (=0)”.

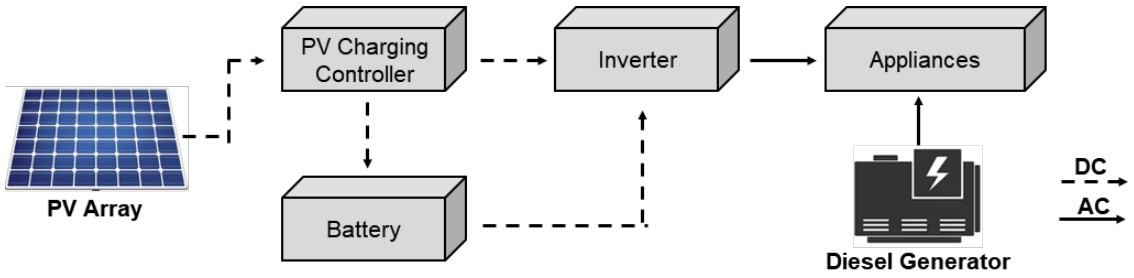

Figure 3.1 A residential off-grid energy system with a diesel generator

3.3.2 Creating solar irradiance scenario

To represent various occasions of solar irradiance uncertainty and variability, *s*-scenario of annual hourly forecasted solar irradiance profiles are created. We use the 12-year of typical metrological year (TYP) data between the year 1994 and the year 2005 from the National Solar Radiation Database [15]. In Figure 3.2, we divide all annual hourly solar irradiance data into four categories based on seasons - Winter (Dec.-Feb.), Spring (Mar.-May), Summer (Jun.-Aug.), Fall (Sep.-Nov.) -.

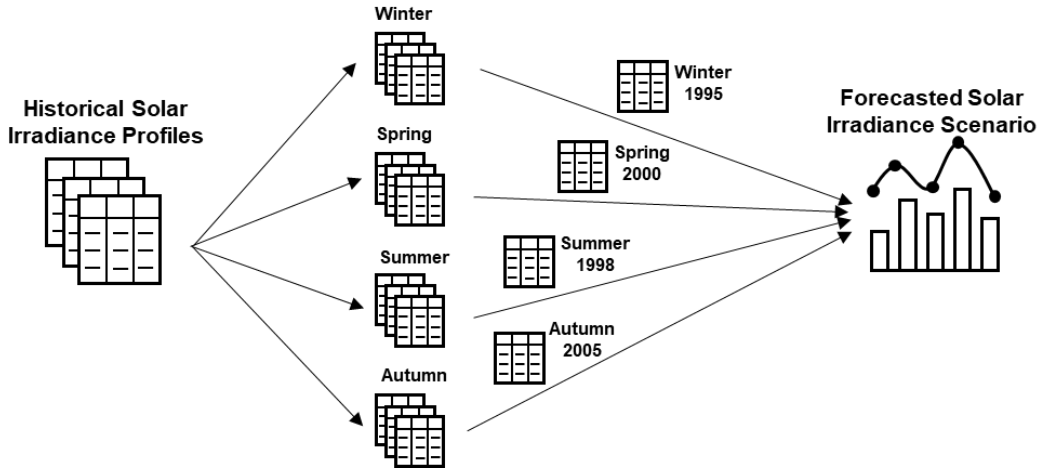

Figure 3.2 Create forecasted solar irradiance scenario

We combine seasonal hourly solar irradiance profiles from randomly chosen years to create a yearly solar irradiance scenario. Among a total 12^4 possible profile configurations, *s*-profile are randomly chosen and considered as forecasted solar irradiance scenarios. It is assumed that the probability of solar irradiance scenario occurrence (P_s) is equal to $\frac{1}{s}$.

3.3.3 Modeling energy consumption scheduling

Daily energy demand is determined by the energy consumption rate and required operation periods of appliances. Energy consumption scheduling contributes to estimating the cost-efficient capacity of an energy system by shifting operation periods of some appliances anytime based on user preferred operation periods during the day. The proposed optimization model considers the operation schedule of appliances determine the optimal capacities of the PV array, battery and the usage of diesel fuel at the minimum AEC.

3.3.3.1 Appliance operation period

A day is divided into L equal periods of $T = \frac{24}{L}$ hours. It is assumed that period t represents a timeframe between period $t-1$ and period t. For instance, when T equals 1-hour, period 6 represents a timeframe from period 5 to period 6. Required operation periods of appliance a during day d are determined by the number of $T_{d,a}$. If $T_{d,a}$ of appliance a equals 1 and the user preferred operation period of appliance a is period 6, appliance a starts operation at period 5 and completes at period 6.

3.3.3.2 Appliance operation type

It is assumed that there are two types of appliances, schedulable and non-schedulable. A schedulable appliance can be operated at a time based on the user preferred operation period of the appliance. A washing machine and a dishwasher are examples of a schedulable appliance. In contrast, a non-schedulable appliance cannot change its operation periods. A light bulb and refrigerator are examples of a non-schedulable appliance. We define the set $\mathrm{S}^{\mathrm{app}}$, $\mathrm{NS}^{\mathrm{app}}$ to group the schedulable and non-schedulable appliances.

$$\mathrm{S}^{\mathrm{app}} = \{a_1, a_2, \dots a_{\mathrm{s}}\} \text{ where } s \in \{1,2, \dots, \mathrm{A}\}$$

$$\mathrm{NS}^{\mathrm{app}} = \{a_1^*, a_2^*, \dots a_{\mathrm{s}}^*\} \text{ where } s \in \{1,2, \dots, \mathrm{A}\}$$

3.3.3.3 Uninterruptible appliance

An uninterruptible appliance can stop operation when it completes the required operation period. For instance, a dishwasher cannot stop once it starts operation. We define the set $\mathrm{U}^{\mathrm{app}}$ to group the uninterruptible appliances.

$$\mathrm{U}^{\mathrm{app}} = \{a_1, a_2, \dots a_s\} \text{ where } s \in \{1,2, \dots, A\}$$

3.3.3.4 Appliance operation sequencing

Some appliances cannot start operation before completing the operation of a particular appliance. For example, a dryer cannot start before finishing the operation of a washing machine. We define the set $\mathrm{SQ}^{\mathrm{app}}$ to include all appliances that are preceded by at least one appliance and the set $\mathrm{SQ}_a^{\mathrm{app}}$ to describes the appliances that precede a.

$$\mathrm{SQ}_a^{\mathrm{app}} = \{a_1, a_2, \dots a_s\} \text{ where } s \in \{1,2, \dots, A\} \text{ and } a \in \mathrm{SQ}^{\mathrm{app}}$$

3.3.3.5 Operation period preference

User preferred operation period of appliances are represented by a binary matrix P. The entry $P_{d,a,t}$ of the matrix is equal to "1" if the user prefers to operate the appliance a during period t of day d. Each column represents an operation period t from 1 to L and each row describes preferred operation periods of an appliance. For example, $P_{1,1,1} = 1$ represents that the user prefers to turn on appliance 1 during period 1 of day 1. If an appliance requires to operate twice during different periods of a day, it is represented by two appliances in each row, respectively. Figure. 3.3, represents examples of preferred operation periods of three appliances on day 1 when L equals 24 (1 period = 1-hour). If it is assumed that all $T_{1,a}$ equals 2, Appliance 1 requires an uninterruptible operation and is a schedulable appliance that can be operated at any two consecutive periods during a day. Appliance 4 is schedulable and operates two periods during period 6 and 7 or during period 20 and 21. Appliance 20 is non-schedulable and should operate during periods 6 and 7, as well as periods 20 and 21.

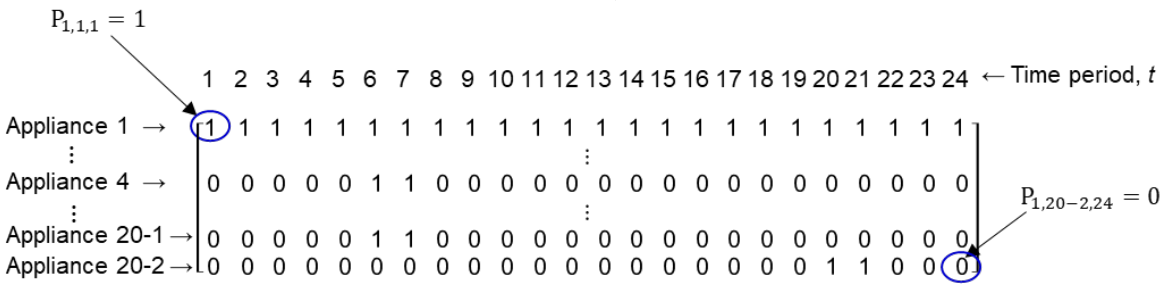

Figure 3.3 Operation period preference matrix $P_{1,a,t}$

3.3.3.6 Diesel generator operation

A diesel generator provides electrical energy to appliances when energy supply of the PV array and battery is limited. It also deals with unexpected climate change in isolated areas. In order to maximize the lifespan of a diesel generator, we limit maximum daily operation time and assume

that it receives preventative maintenance on a regular basis. Operation of a diesel generator during period t of day d under scenario s is described by a binary variable $z_{s,d,t}^{\mathrm{DG}}$(1 = "on" or 0 = "off"). When the required energy is supplied by diesel fuel during period t of day d under scenario s ($e_{s,d,t}^{\mathrm{F}} > 0$), it is considered that the diesel generator operates during period t of day d under scenario s ($z_{s,d,t}^{\mathrm{DG}} = 1$). It is scheduled to operate within the maximum daily operation time (T^{DG}) during a day. If a diesel generator operates at least once under scenario s ($x_s^{\mathrm{F}} > 0$), AEC of a diesel generator occurs ($z_s^{\mathrm{DG}} = 1$).

3.4 Optimization model

The proposed optimization model is given in Eq. (3.1) to Eq. (3.22). It can be solved by a mixed integer programming method. The formulation of the problem includes the objective function and all of the energy system constraints. Considering the number of randomly selected scenarios, the solution of the problem provides the optimal capacities of the PV array, battery and the expected diesel fuel cost at the minimum AEC of an energy system.

$$\text{minimize } \mathrm{C}^{\mathrm{PV}} * x^{\mathrm{PV}} + \mathrm{C}^{\mathrm{BAT}} * x^{\mathrm{BAT}} + \sum_{s=1}^{\mathrm{S}} \mathrm{P_s} * (\mathrm{C}^{\mathrm{DG}} * z_s^{\mathrm{DG}} + \mathrm{C}^{\mathrm{F}} * x_s^{\mathrm{F}}) \tag{3.1}$$

$$\mathrm{E}_{s,d,t}^{\mathrm{PV}} = \mathrm{S}_{s,d,t} * \mathrm{B}^{\mathrm{PV}} * x^{\mathrm{PV}} \tag{3.2}$$

$$\mathrm{E}_{s,d,t}^{\mathrm{PV}} = e_{s,d,t}^{\mathrm{app\_pv}} + e_{s,d,t}^{\mathrm{chr}} + e_{s,d,t}^{\mathrm{loss\_pv}} \tag{3.3}$$

$$x_s^{\mathrm{F}} = \sum_{d=1}^{\mathrm{D}} \sum_{t=1}^{\mathrm{T}} e_{s,d,t}^{\mathrm{F}} \tag{3.4}$$

$$x_s^{\mathrm{F}} \leq \mathrm{M} * z_s^{\mathrm{DG}} \tag{3.5}$$

$$e_{s,d,t}^{\mathrm{F}} \leq \mathrm{M} * z_{s,d,t}^{\mathrm{DG}} \tag{3.6}$$

$$\sum_{t=1}^{T} z_{s,d,t}^{\mathrm{DG}} \leq \mathrm{T}^{\mathrm{DG}} \tag{3.7}$$

$$\sum_{a} \mathrm{E}_{d,a} * x_{s,d,a,t}^{\mathrm{app\_state}} + \sum_{a^*} \mathrm{E}_{d,a^*} * \mathrm{P}_{\mathrm{d},a^*,\mathrm{t}} + \mathrm{E}_{d,t}^{\mathrm{R}} = \left(e_{s,d,t}^{\mathrm{app\_pv}} + e_{s,d,t}^{\mathrm{app\_bat}}\right) * \mathrm{R}^{\mathrm{INV}} + \ e_{s,d,t}^{\mathrm{F}}$$

$$\forall\ a\ \in \mathrm{S}^{\mathrm{app}}, a^* \in \mathrm{NS}^{\mathrm{app}} \tag{3.8}$$

$$e_{s,d,t}^{\mathrm{bat}} = e_{(s,d,t-1)}^{\mathrm{bat}} * (1 - \mathrm{R}^{\mathrm{DCH}}) + e_{s,d,t}^{\mathrm{chr}} * \mathrm{R}^{\mathrm{CHR}} - e_{s,d,t}^{\mathrm{app\_bat}} \tag{3.9}$$

$$\mathrm{S}^{\mathrm{MIN}} * \mathrm{B}^{\mathrm{BAT}} * x^{\mathrm{BAT}} \leq\ e_{s,d,t}^{\mathrm{bat}} \leq\ \mathrm{S}^{\mathrm{MAX}} * \mathrm{B}^{\mathrm{BAT}} * x^{\mathrm{BAT}} \tag{3.10}$$

$$y_{s,d,t}^{\mathrm{chr}} +\ y_{s,d,t}^{\mathrm{dch}} \leq 1 \tag{3.11}$$

$$e_{s,d,t}^{\mathrm{chr}} \leq\ \mathrm{R}^{\mathrm{MCH}} \tag{3.12}$$

$$e_{s,d,t}^{\mathrm{app\_bat}} \leq\ \mathrm{R}^{\mathrm{MDC}} \tag{3.13}$$

$$e_{s,d,T}^{\mathrm{bat}} \geq \mathrm{S}^{\mathrm{ESC}} * \mathrm{B}^{\mathrm{BAT}} * x^{\mathrm{BAT}} \tag{3.14}$$

$$e_{s,d,T}^{\mathrm{bat}} = e_{s,d+1,1}^{\mathrm{bat}} \tag{3.15}$$

$$\sum_{\mathrm{t}=1}^{\mathrm{T}} x_{s,d,a,t}^{\mathrm{app\_state}} =\ \mathrm{T}_{d,a} \qquad \forall\ a\ \in \mathrm{S}^{\mathrm{app}} \tag{3.16}$$

$$x_{s,d,a,t}^{\mathrm{app\_state}} \leq\ \mathrm{P}_{d,a,t} \qquad \forall\ a\ \in \mathrm{S}^{\mathrm{app}} \tag{3.17}$$

$$x_{s,d,a,1}^{\mathrm{app\_state}} = 0 \qquad \forall\ a \in \mathrm{SQ}^{\mathrm{app}} \tag{3.18}$$

$$\mathrm{T}_{d,a^*} - \sum_{n=1}^{\mathrm{N}} x_{s,d,a^*,n}^{\mathrm{app\_state}} \leq \mathrm{M} * \left(1 - x_{s,d,a,t+1}^{\mathrm{app\_state}}\right)$$

$$\forall\ a \in \mathrm{SQ}^{\mathrm{app}}, a^* \in \mathrm{SQ}_a^{\mathrm{app}}, \text{and } \mathrm{N} = 1,2,..,t \tag{3.19}$$

$$x_{s,d,a,t}^{\mathrm{app\_state}} \leq 1 - x_{s,d,a,t}^{\mathrm{app\_end}} \qquad \forall\ a \in \mathrm{U}^{\mathrm{app}} \tag{3.20}$$

$$x_{s,d,a,t}^{\mathrm{app\_state}} - x_{s,d,a,t+1}^{\mathrm{app\_state}} \leq x_{s,d,a,t+1}^{\mathrm{app\_end}} \qquad \forall\ a \in \mathrm{U}^{\mathrm{app}} \tag{3.21}$$

$$x_{s,d,a,t}^{\mathrm{app\_end}} \leq\ x_{s,d,a,t+1}^{\mathrm{app\_end}} \qquad \forall\ a \in \mathrm{U}^{\mathrm{app}} \tag{3.22}$$

The objective function in Eq. (3.1) minimizes the AEC of the energy system. The parameters C^{PV} and $\mathrm{C}^{\mathrm{BAT}}$ are the AEC of a single PV array and battery. The integer decision variables x^{PV} and x^{BAT} represent the numbers of PV arrays and battery modules, respectively. The parameter C^{DG} represents the AEC of a diesel generator and C^{F} is the diesel fuel cost per kWh. Based on the occurrence probability of scenario s (P_s), a binary variable z_s^{DG} represents the operation status of the diesel generator and the decision variable x_s^{F} its annual amount of electrical energy generated by using diesel fuel. All other costs are excluded.

The constraint in Eq. (3.2) ensures that the forecasted solar irradiance is converted into available electrical energy as PV arrays where B^{PV} is the capacity of a basic single PV array. The constraint given in Eq. (3.3) shows that the PV output ($\mathrm{E}_{s,d,t}^{\mathrm{PV}}$) equals, at any period t of day d under scenario s, the sum of energy to operate the appliances ($e_{s,d,t}^{\mathrm{app\_pv}}$), the energy to charge a battery ($e_{s,d,t}^{\mathrm{chr}}$) and energy loss ($e_{s,d,t}^{\mathrm{loss\_pv}}$). In Eq. (3.4) states that annual electrical energy generated by a diesel generator is derived from the sum of generated energy at period t of day d under scenario s. Eq. (3.5) ensures that AEC of a diesel generator occurs ($z_s^{\mathrm{DG}} = 1$) only if diesel fuel is used at least once under scenario *s* where variable z_s^{DG} is a binary variable and M is a big number. Eq. (3.6) enforces that a diesel generator is operated ($z_{s,d,t}^{\mathrm{DG}} = 1$) only if a diesel fuel is consumed during any period t of day d under scenario s where variable $z_{s,d,t}^{\mathrm{DG}}$ is a binary variable and M is a big number. To guarantee a durable life of a diesel generator, Eq. (3.7) ensures that it only operates within the daily maximum operation time defined by the user (T^{DG}). Energy demand consists of required energy by schedulable and, non-schedulable appliances and reserved energy during period t of day d under scenario s. The constraint given in Eq. (3.8) represents the energy consumed by all appliances and that reserved energy are derived from the PV array ($e_{s,d,t}^{\mathrm{app\_pv}}$)

and/or a battery ($e_{s,d,t}^{\text{app\_bat}}$) and/or a diesel fuel ($e_{s,d,t}^{\text{F}}$) during each period t of day d under scenario s. The parameter $\text{E}_{d,a(a^*)}$ is the energy required by schedulable ($a \in \text{S}^{\text{app}}$) or non-schedulable appliances ($a^* \in \text{NS}^{\text{app}}$) of day d. $\text{E}_{d,t}^{\text{R}}$ is reserved energy for the occasional operation of small appliances such as a cell phone charger. The available energy in a battery is calculated by Eq. (3.9). We assume that energy starts with 30% of battery capacity. In order to guarantee a desirable lifespan of a battery, the available energy in a battery should be between S^{MIN} and S^{MAX} of battery capacity at all periods in Eq. (3.10). The Eq. (3.11) enforces that a battery cannot charge and discharge at the same period where the variables $y_{s,d,t}^{\text{chr}}$ and $y_{s,d,t}^{\text{dch}}$ are binary and represent charging ($y_{s,d,t}^{\text{chr}} = 1$) or discharging ($y_{s,d,t}^{\text{dch}} = 1$) of a battery, respectively. Eq. (3.12) ensures that the energy charged to a battery must be less than or equal to the maximum charging rate (R^{MCH}) of the battery capacity at all periods. Similarly, in Eq. (3.13), the energy discharged from the battery must be less than or equal to the maximum discharging rate (R^{MCH}) of battery capacity at all periods. To ensure enough amount of energy in a battery for the next day, in Eq. (3.14), the available energy in a battery at the last period ($e_{s,d,T}^{\text{bat}}$) should be greater than or equal to battery end SOC (S^{ESC}) of battery capacity. Eq. (3.15) states that the available energy in a battery during the last period ($e_{s,d,T}^{\text{bat}}$) should be the available energy in a battery during the first period of the next day ($e_{s,d+1,1}^{\text{bat}}$). In Eq. (3.16), all schedulable appliances should satisfy daily required operation periods ($\text{T}_{d,a}$) where the binary variable $x_{s,d,a,t}^{\text{app\_state}}$ represents the operation state of the appliances. Eq. (3.17) ensures that all schedulable appliances will only operate within user-defined preferred operation periods ($\text{P}_{d,a,t} = 1$). For appliances in the set SQ^{app}, the sequential operation of an appliance is defined by Eq. (3.18) - (3.19) where M is a big number. In Eq. (18), appliance a in the set SQ^{app} cannot operate during any of the first periods since it can be "on" only after the

completion of at least one appliance in the set $\mathrm{SQ}_a^{\mathrm{app}}$. Eq. (3.19) ensures that appliance a cannot operate until the operation of appliance a^* is completed ($\mathrm{T}_{d,a^*} - \sum_{n=1}^{\mathrm{N}} x_{s,d,a^*,n}^{\mathrm{app\_state}} > 0$) at each period. If appliance a^* has finished the operation until period t ($\mathrm{T}_{d,a^*} - \sum_{n=1}^{\mathrm{N}} x_{s,d,a^*,n}^{\mathrm{app\_state}} = 0$), appliance a can be "on" or "off" after period t. For appliances in the set $\mathrm{U}^{\mathrm{app}}$, Eq. (20)-(22) ensure that an appliance will not stop after it starts operations [16]. In Eq. (3.20)-(3.21), appliance a finishes operation at period t ($x_{s,d,a,t}^{\mathrm{app\_state}} = 1$ and $x_{s,d,a,t}^{\mathrm{app\_end}} = 0$), the status of appliance a is changed from "on" to "off" at period $t+1$ ($x_{s,d,a,t+1}^{\mathrm{app\_state}} = 0$ and $x_{s,d,a,t+1}^{\mathrm{app\_end}} = 1$). Eq. (3.22) ensures that the operation of appliance a cannot resume after period t if it completes the operation at period t.

3.5 Experimental results

To verify the proposed optimization model under the considered number of solar irradiance scenarios, we use 12-year historical solar irradiance data of Auburn, AL, U.S.A. We assume that L equals 24, with one day divided into 24 periods. We solve all models with Gurobi version 9.0 of Python Pyomo on a workstation with AMD Ryzen 3900X processor and 32GB of RAM [17]. It takes up to 96 hours to obtain the solutions.

3.5.1 Solar irradiance scenario

We randomly choose 20 solar irradiance scenarios in Auburn, AL from 12^4 of all possible solar irradiance profile configurations. In Table 3.1, we sort 20 scenarios in descending order by the amount of annual solar irradiance. We assume scenario 1 is the best scenario and scenario 20 is the worst scenario. The average scenario is obtained by averaging hourly solar irradiance data

of 20 scenarios. The average annual solar irradiance of 20 scenarios equals to 1,615.69 (kW/m^2). In the best scenario, there is 92% less solar irradiance on the worst day than the best day. Similarly, in the worst scenario, there is 95% less solar irradiance on the worst day than the best day.

Table 3.1 Solar irradiance of 20 scenarios and average scenario

Scenario	Yearly total (kW/m^2)	Daily avg. (kW/m^2)	Best day (kW/m^2)	Worst day (kW/m^2)
1	1,795.96	4.92	7.97	0.65
2	1,759.64	4.82	7.96	0.77
3	1,752.91	4.80	7.96	0.58
4	1,718.43	4.71	7.96	0.66
5	1,689.44	4.63	8.01	0.63
6	1,666.51	4.57	8.12	0.63
7	1,661.85	4.55	7.87	0.65
8	1,643.18	4.50	7.99	0.58
9	1,638.17	4.49	7.83	0.65
10	1,632.73	4.47	7.91	0.65
11	1,620.94	4.44	7.99	0.63
12	1,620.87	4.44	7.94	0.77
13	1,595.78	4.37	7.91	0.56
14	1,571.36	4.31	7.88	0.61
15	1,567.23	4.29	7.95	0.68
16	1,551.71	4.25	8.00	0.68
17	1,505.15	4.12	7.94	0.58
18	1,488.10	4.08	7.94	0.69
19	1,427.59	3.91	7.75	0.65
20	1,406.26	3.85	7.69	0.42
Average scenario	1,615.69	4.43	6.99	1.79

In Figures 3.4-3.7, we represent seasonal hourly solar irradiance profiles of the best, worst and average scenario.

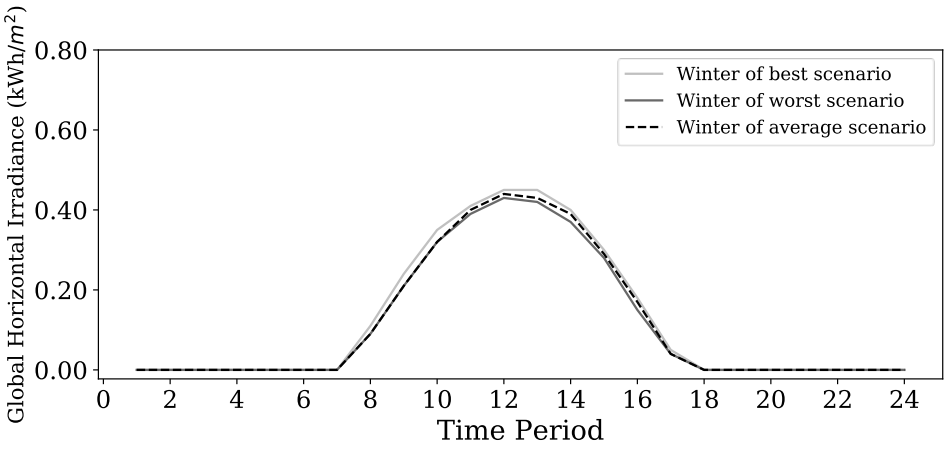

Figure 3.4 Seasonal hourly solar irradiance profiles of best, worst and average scenario in winter

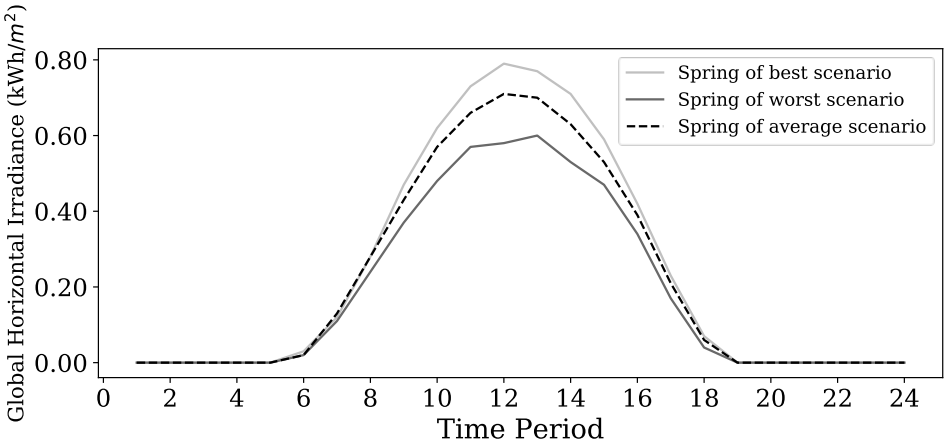

Figure 3.5 Seasonal hourly solar irradiance profiles of best, worst and average scenario in spring

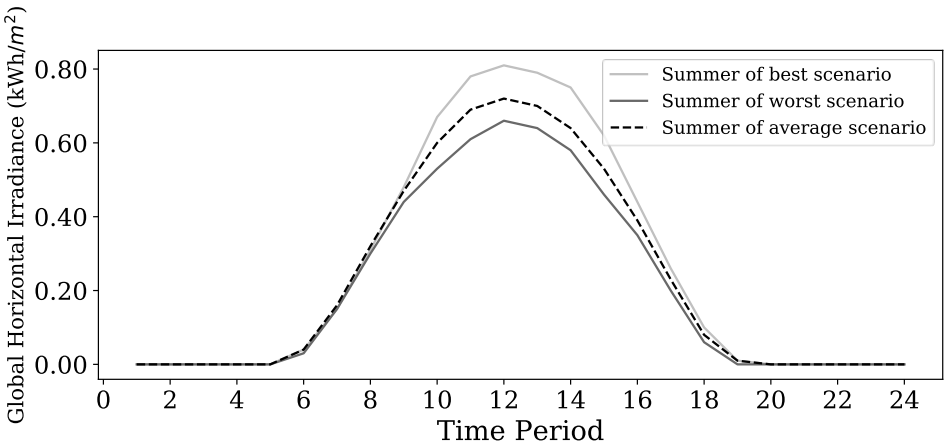

Figure 3.6 Seasonal hourly solar irradiance profiles of best, worst and average scenario in summer

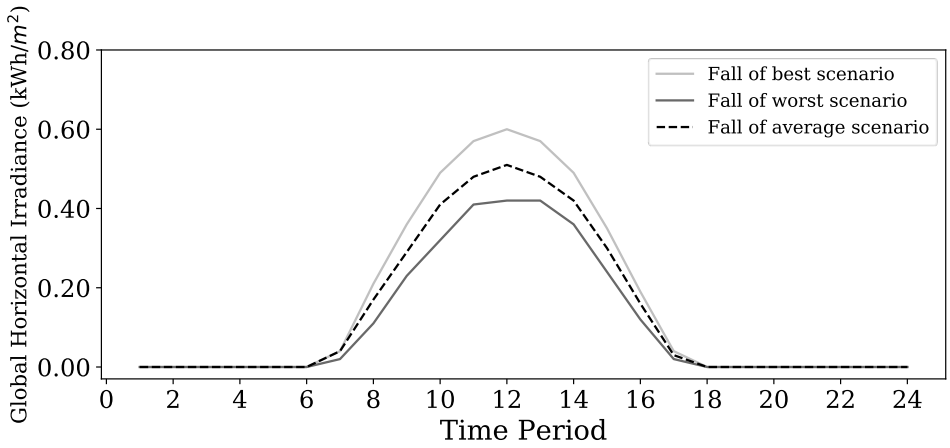

Figure 3.7 Seasonal hourly solar irradiance profiles of best, worst and average scenario in fall

In Figures 3.8-3.9, we represent hourly solar irradiance profiles of the best (worst) day under the best, worst and average scenario. On average, hourly solar irradiance reaches the peak during period 12 and, no solar irradiance exists after period 20 under all scenarios.

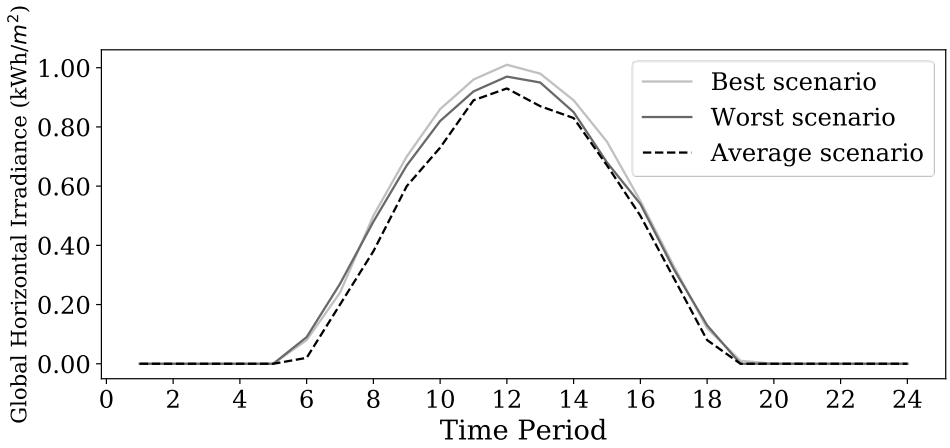

Figure 3.8 Hourly solar irradiance of best day under best, worst and average scenario

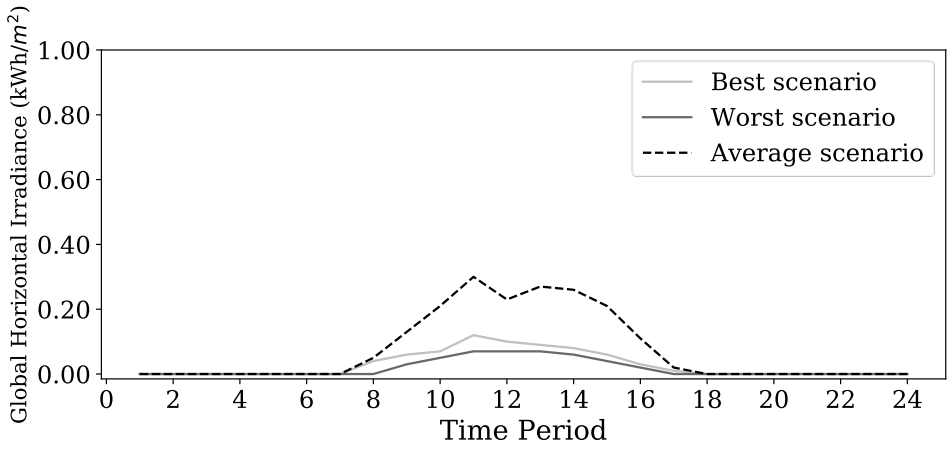

Figure 3.9 Hourly solar irradiance of worst day under best, worst and average scenario

3.5.2 System data

In the experiment, we consider 365 days of one year to determine the optimal capacity of the energy system at the minimum AEC. We represent the number of days based on the types of the day. In Table 3.2, weekdays (Mon.-Fri.) and weekends (Sat., Sun.) are dived into "season name-weekday" and "season name-weekend", respectively.

Table 3.2 Number of days based on day types

Day type	Days	Description
Spring & Summer- Weekday	123	March, April, May, June, July, August
Spring & Summer - Weekend	50	
Fall & Winter - Weekday	122	September, October, November, December, January, February
Fall & Winter - Weekend	47	
Holiday	23	National holidays in the U.S. (7), Summer vacation (7), Thanksgiving break (4), Christmas break (5)

We assumed a residential house with 3-bedrooms and 2-bathrooms. 4-family members leave home at 8 AM and return home at 6 PM during the weekdays but stays at home during the weekends. Family members wake up at 6AM and go to bed at 11PM every day. They leave home during the holidays. Home appliance information is represented in Table 3.3. There are 15 physical

appliances and we add 2 appliances for weekdays (COM, TVD) and weekends (COM) that require to operate at least once during a day, respectively. For example, one TVD is represented TVD - 1and TVD - 2. We have 9 schedulable appliances - CLW, CLD, DIW, TOO, EOS, EOR, COM, DOL, TVD - that can be scheduled to operate at any period during the day based on user preferred operation period. CLW and DIW require uninterruptible operation. Additionally, CLW and CLD operate sequentially every Sunday, DIW operates every two days. 0.5kWh of reserved energy is assigned to operate occasionally required appliances such as a cell phone charger or a hairdryer. Only the refrigerator operated for 24 hours during the holidays.

Table 3.3 Appliances

Label	Full name	Characteristics	Energy consumption (kWh)
CFB	CFL Bulb (11W)	Non-schedulable	0.011
LEB	LED Bulb (10W)	Non-schedulable	0.010
HAB	Halogen Bulb (40W)	Non-schedulable	0.040
INB	Incandescent Bulb (40W)	Non-schedulable	0.040
REF	Refrigerator (17 cu. ft., frost-free)	Non-schedulable	0.049
IMW	Internet Modem / Wireless Router	Non-schedulable	0.014
CLW	Clothes Washer (Warm wash, Cold rinse)	Schedulable / Uninterruptible	2.300
CLD	Clothes Dryer (Light Load)	Schedulable / Sequencing	2.500
DIW	Dish Washer	Schedulable / Uninterruptible	1.200
TOO	Toaster Oven	Schedulable	0.750
EOS	Electric Oven/Range (Surface)	Schedulable	1.000
EOR	Electric Oven/Range (Oven)	Schedulable	2.300
COM	Coffee Machine (Brew, Warmer on)	Schedulable	0.400
DOL	Desktop or Laptop	Schedulable / Interruptible	0.020
TVD	LED TV (40"-49") / Satellite Dish	Schedulable / Interruptible	0.056
REN	Reserved Energy	Non-schedulable	0.500

In Tables 3.4-3.5, we arbitrarily define the required operation period and user preferred operation period of appliances based on types of days. Based on user energy consumption patterns in Tables 4-5, total yearly energy demand by all appliances and reserved energy equals 6,719.69kWh. Specifications of a PV array, battery, and a diesel generator are represented in Tables 3.6-3.8.

Table 3.4 Operation period preference (weekday)

Preferred period (Fall and Winter only) Preferred period (All seasons)

Appliance	Qty	$T_{d,a}$		$P_{d,a,t}$: weekdays																							
		Spring-Summer	Fall-Winter	1	2	3	4	5	6	7	8	9	10	11	12	13	14	15	16	17	18	19	20	21	22	23	24
CFB	12	5	7																								
LEB	12	5	7																								
HAB	10	5	7																								
INB	10	5	7																								
REF	1	24	24																								
IMW	1	8	8																								
CLW	1	2	2																								
CLD	1	1	1																								
DIW	1	2	2																								
TOO	1	1	1																								
EOR	1	1	1																								
COM - 1	1	1	1																								
COM - 2	1	1	1																								
DOL	1	6	6																								
TVD - 1	1	1	1																								
TVD - 2	1	4	4																								
RSE	1	7	7																								

Table 3.5 Operation period preference (weekend)

Preferred period (Fall and Winter only) Preferred period (All seasons)

Appliance	Qty	$T_{d,a}$		$P_{d,a,t}$: weekend																							
		Spring-Summer	Fall-Winter	1	2	3	4	5	6	7	8	9	10	11	12	13	14	15	16	17	18	19	20	21	22	23	24
CFB	12	5	7																								
LEB	12	5	7																								
HAB	10	5	7																								
INB	10	5	7																								
REF	1	24	24																								
IMW	1	17	17																								
CLW	1	2	2																								
CLD	1	1	1																								
DIW	1	2	2																								
TOO	1	1	1																								
EOS	1	1	1																								
EOR	1	1	1																								
COM - 1	1	1	1																								
COM - 2	1	1	1																								
COM - 3	1	1	1																								
DOL	1	12	12																								
TVD - 1	1	4	4																								
TVD - 2	1	10	10																								
RSE	1	17	17																								

Table 3.6 PV array specifications

Parameter	Value	Description
B^{PV}	0.315(kW)	Basic PV array capacity
C^{PV}	32.38($)	AEC of basic PV array capacity
F^{PV}	0.0736	Capital recovery factor of PV array
N^{PV}	20(years)	Life expectancy of PV array
i	4%	Market interest rate
R^{INV}	98%	Inverter efficiency rate

Table 3.7 Battery specifications

Parameter	Value	Description
B^{BAT}	3.3(kWh)	Basic battery capacity
C^{BAT}	539.11($)	AEC of basic battery capacity
F^{BAT}	0.2246	Capital recovery factor of battery
N^{BAT}	5(years)	Life expectancy of battery
i	4%	Market interest rate
S^{ISC}	50%	Initial amount of energy in the battery
S^{ESC}	30%	End amount of energy in the battery
S^{MIN}	5%	Minimum SOC
S^{MAX}	95%	Maximum SOC
R^{CHR}	99%	Charging efficiency
R^{DCH}	0.0139%	Self-discharging efficiency
R^{MCH}	5(kWh)	Maximum charging power
R^{MDC}	5(kWh)	Maximum discharging power

Table 3.8 Diesel generator specifications

Parameter	Value	Description
B^{DG}	15(kW)	Home backup diesel generator capacity
C^{DG}	1,031.80($)	AEC of diesel generator
F^{DG}	0.0947	Capital recovery factor of diesel generator
N^{PV}	14(years)	Life expectancy of diesel generator (operated max. 4 hrs/ day)
i	4%	Market interest rate
C^{F}	0.30($/kWh)	Cost of diesel fuel

3.5.3 Result

We run the model between Jan 1. 00AM and Dec 31. 12PM. The model is solved under 20 scenarios. It is assumed that the initial amount of energy in the battery equals 30% of the battery capacity and the amount of energy in the battery at the last period (T) of the day d is the same as

the first period of day d+1. We also assume that the amount of diesel fuel to generate 1kWh energy equals 0.099 gallons/kWh, the price of 1-gallon diesel fuel equals $3.05/gallon to calculate the expected annual diesel fuel cost.

In Table 3.9, we present the results of the model considering 20 scenarios. The optimal energy system consists of a 18.27kW PV array and 9.9kWh battery. The system has the AEC of $4,946.13 by taking into consideration the AEC of a diesel generator and expected diesel fuel cost.

Table 3.9 Experimental results

PV capacity	Battery capacity	Expected AEC				
		PV array	Battery	Diesel generator	Avg. diesel fuel	Total
18.27kW	9.9kWh	$1,877.81	$1,617.32	$1,031.80	$419.21	$4,946.13

We prove the effectiveness of the stochastic optimization model by comparing results to one scenario model. Firstly, we solve the model under one average scenario of 20 scenarios and obtain optimal capacities of 5.99kW PV array and 9.99kWh battery. We fix PV array and battery capacities by one average scenario, run the model under each scenario (1-20), respectively. However, the model represents infeasible solutions under every scenario. The reason is that fixed capacities of the PV array, battery and limited operation time of a diesel generator cannot provide sufficient energy under the worst day of each scenario. As a result, the stochastic model better estimates the optimal capacities of the PV array, battery and operation schedule of a diesel generator at minimum AEC of energy system since it considers many possible solar irradiance scenarios. If we consider few scenarios to estimate the capacity of the energy system, it would not satisfy energy demand under other possible solar irradiance scenarios.

In Table 3.10, we represent average energy usage under all scenarios. A total of 6,719.69kWh of energy is required by appliances. On average, 29,518.68kWh of energy is generated by the PV array, the PV array supplies 2,566.28kWh, the battery provides 2,760.37kWh and 1,393.03kWh

of energy is powered by a diesel generator. Notice that an average of 24,049.00kWh of unused energy is observed. It is the summation of PV energy loss ($e_{s,d,t}^{\text{loss\_pv}}$) after operating appliances and, charging the battery. It primarily occurs during daytime periods when generated solar energy is greater than the required energy by appliances and the battery.

Table 3.10 Annual energy usage under 20-scenario model

Scenario	Total energy generated by PV (kWh)	Appliances from PV and battery (kWh)	Appliances from diesel generator (kWh)	Conversion losses (kWh)	Unused energy (kWh)	Energy demand by appliances (kWh)
1	32,812.12	5,410.16	1,309.53	143.72	27,254.13	6,719.69
2	32,148.60	5,399.75	1,319.94	143.48	26,601.28	6,719.69
3	32,025.67	5,418.98	1,300.71	143.74	26,458.84	6,719.69
4	31,395.79	5,397.66	1,322.03	143.77	25,856.34	6,719.69
5	30,866.05	5,347.07	1,372.62	142.19	25,378.77	6,719.69
6	30,447.17	5,389.59	1,330.10	143.06	24,916.50	6,719.69
7	30,361.94	5,331.99	1,387.70	141.48	24,890.07	6,719.69
8	30,020.90	5,323.46	1,396.23	141.36	24,551.99	6,719.69
9	29,929.46	5,342.89	1,376.80	141.65	24,445.08	6,719.69
10	29,829.90	5,345.22	1,374.47	141.76	24,338.83	6,719.69
11	29,614.59	5,315.26	1,404.43	140.79	24,159.47	6,719.69
12	29,613.31	5,315.10	1,404.59	141.42	24,152.70	6,719.69
13	29,154.86	5,348.04	1,371.65	141.71	23,667.09	6,719.69
14	28,708.80	5,324.35	1,395.34	141.22	23,245.21	6,719.69
15	28,633.24	5,301.70	1,417.99	140.82	23,192.50	6,719.69
16	28,349.78	5,321.04	1,398.65	141.50	22,883.15	6,719.69
17	27,499.18	5,252.94	1,466.75	140.73	22,105.83	6,719.69
18	27,187.66	5,317.40	1,402.29	141.46	21,724.71	6,719.69
19	26,082.12	5,185.60	1,534.09	139.72	20,752.72	6,719.69
20	25,692.37	5,144.94	1,574.75	138.57	20,404.81	6,719.69

In Figures 3.10-3.13, the operation schedule of schedulable appliances represented by time period under the worst (best) day of the worst scenario and best scenario, for instance. Under all scenarios, we observe that all schedulable appliances are scheduled to operate based on the preferred operation period of each appliance.

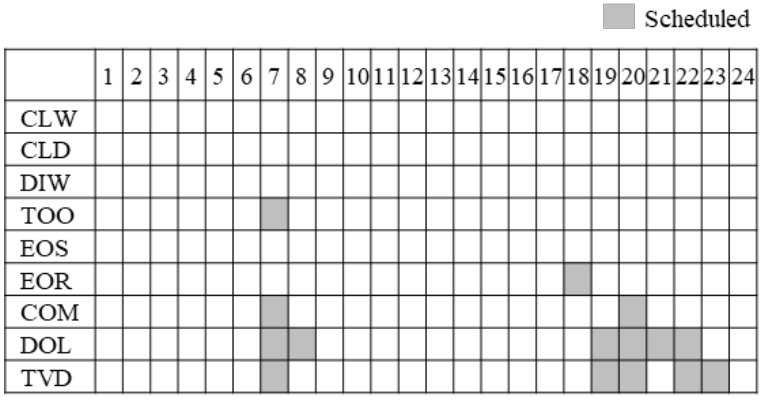

Figure 3.10 Operation schedule on worst day of best scenario (weekday)

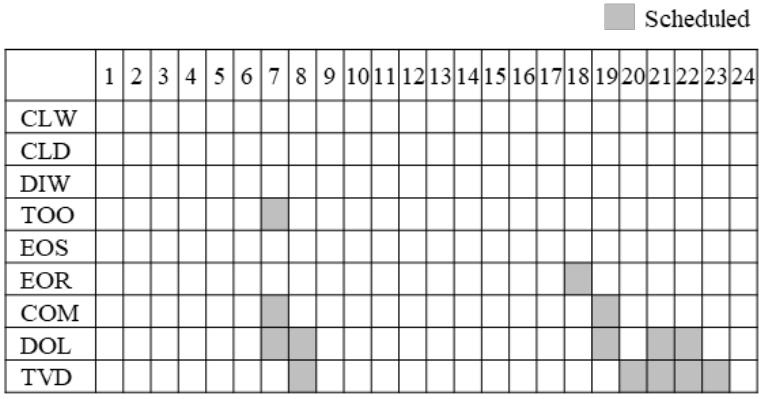

Figure 3.11 Operation schedule on best day of best scenario (weekday)

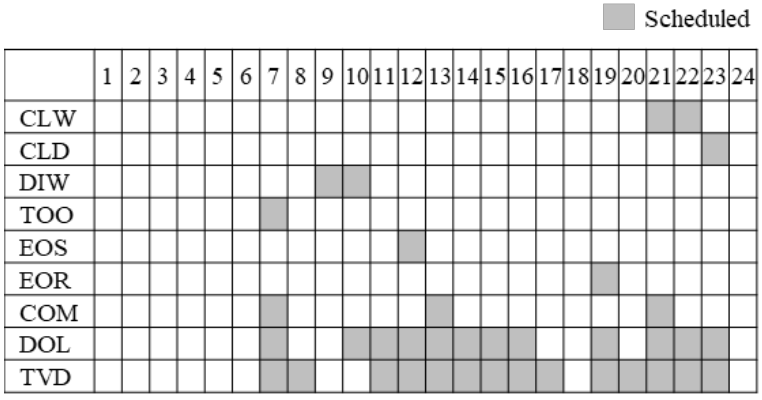

Figure 3.12 Operation schedule on worst day of worst scenario (weekend, even day)

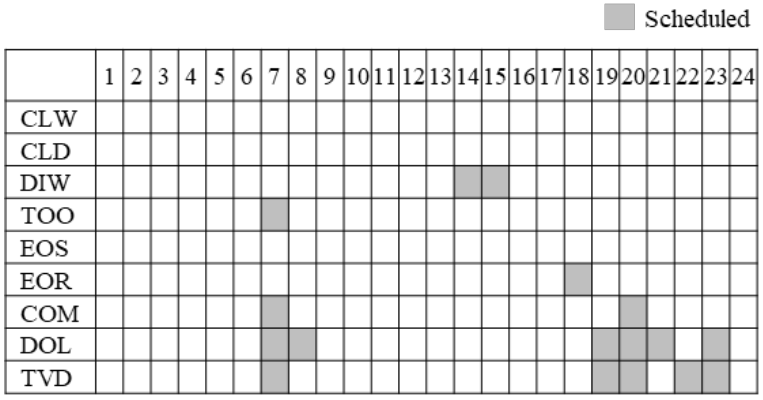

Figure 3.13 Operation schedule on best day of worst scenario (weekday, even day)

In Figure 3.14, we represent the average ratio of hourly energy generated by the diesel generator to daily energy generated by a diesel generator. The diesel generator operates the most between period 21 and period 23. Becasue there is not enough energy from the PV arrays and battery to operate all required appliances. Operating the diesel generator during these periods can prevent the battery from unnecessary increase in its capacity.

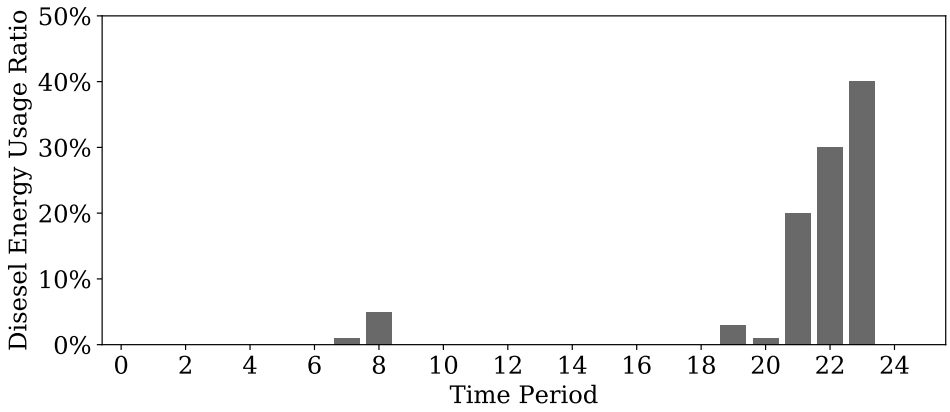

Figure 3.14 Average. ratio of hourly diesel fuel usage to daily diesel fuel usage

In Figure 3.15, we represent the average hourly SOC for the battery under all scenarios. We observe that the battery charges/discharges throughout the whole day, but the battery maintains a maximum SOC during period 18 to supply power to required appliances during the evening.

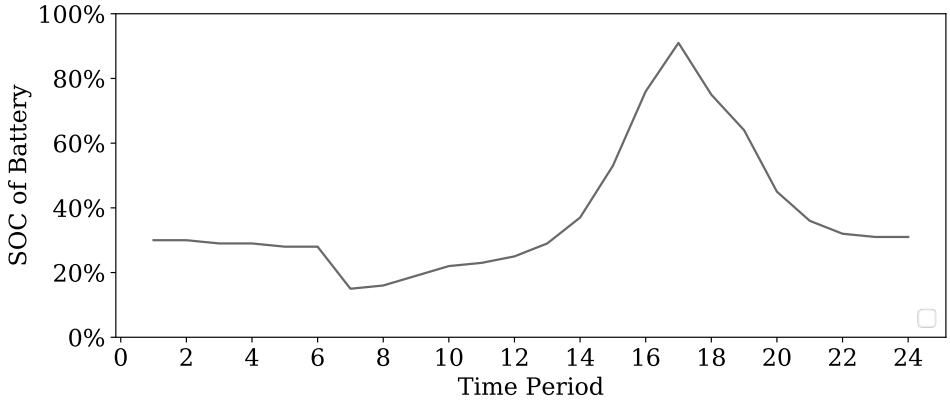

Figure 3.15 Average hourly SOC of the battery

3.5.4 Effect of energy consumption scheduling

To evaluate the effect of scheduling, we compare the results of the optimized versus the non-optimized case. It is assumed that the appliance operation preferences for the non-optimized case ($P_{s,d,a,t}^{non-opt.}$) are arbitrarily fixed and equal to the required operation period ($T_{d,a}$). Preferred operation periods for the non-optimized case are shown in Table 3.11.

Table 3.11 Appliance operation preference under non-optimized case

Preferred period (weekend only) Preferred period (all days)

Appliance	$T_{d,a}$		$P_{d,a,t}$																							
	Weekday	Weekend	1	2	3	4	5	6	7	8	9	10	11	12	13	14	15	16	17	18	19	20	21	22	23	24
CLW	2	2																								
CLD	1	1																								
DIW	2	2																								
TOO	1	1																								
EOS	-	1																								
EOR	1	1																								
COM	2	3																								
DOL	6	12																								
TVD	5	14																								

After running both cases, we obtain the results showing in Table 3.12. We observe that the optimized case satisfies energy demand at lower capacities of the PV array, battery and 4.34% less

diesel fuel cost. Notice that the AEC of the optimized case is 20.02% less than the non-optimized case.

Table 3.12 Energy system characteristics under the optimized case and non-optimized case under 20 scenarios

	PV capacity	Battery capacity	Avg. diesel fuel cost	AEC
Opt. case	18.27kW	9.9kWh	$419.21	$4,946.13
Non-opt. case	24.89kW	13.2kWh	$438.23	$6,184.15

3.5.5 Effect of number of scenarios

To assess how the number of scenarios affects the results of models, we change the number of scenarios considered from scenario 1 (best scenario) to scenario 20 (worst scenario) in increments of 5 scenarios. In Table 3.13, we obtained solutions for PV array and battery capacities under 1-scenario (scenario 1), 5-scenario (scenario 1-5), 10-scenario (scenario1-10), 15-scenario (scenario 1-15) and 20-scenario (scenario 1-20) models, respectively. In order to satisfy energy demand under an increased number of scenarios, more PV arrays are required, but the battery capacity remains at the optimal battery capacity 9.9kWh ensuring the minimum AEC of the energy system under all models.

Table 3.13 Energy system capacity under different number of scenarios

Model	PV capacity	Battery capacity
1-scenario	13.86kW	9.9kWh
5-scenario	14.18kW	9.9kWh
10-scenario	17.64kW	9.9kWh
15-scenario	17.64kW	9.9kWh
20-scenario	18.27kW	9.9kWh

We fix PV array and battery capacities and, solve the model under each scenario. In Table 3.14, some models represent infeasible solutions under particular scenarios except for the 20-scenario model since the energy system capacity cannot satisfy energy demand. Compared to other models,

it is demonstrated that the more-scenario model (i.e. 20-scenario model) meets energy demand better under various solar irradiance scenarios since it has optimal PV array and battery capacities considering variations in solar irradiance occurrence.

Table 3.14 Annual diesel fuel cost under each scenario

Scenario	1-scenario model	5-scenario model	10-scenario model	15-scenario model	20-scenario model
1	$429.02	$425.87	$398.23	$398.23	$394.08
2	$435.88	$432.43	$401.49	$401.49	$397.21
3	$433.03	$429.05	$396.12	$396.12	$391.43
4	$442.07	$437.97	$402.87	$402.87	$397.84
5	infeasible	$447.27	$417.63	$417.63	$413.06
6	$437.61	$434.31	$404.78	$404.78	$400.27
7	infeasible	infeasible	$421.82	$421.82	$417.61
8	infeasible	$457.16	$424.81	$424.81	$420.17
9	$451.80	$448.43	$418.81	$418.81	$414.32
10	$442.87	$440.35	$417.19	$417.19	$413.62
11	$460.26	$456.90	$427.10	$427.10	$422.64
12	$455.39	$452.70	$426.79	$426.79	$422.69
13	$450.77	$447.35	$417.26	$417.26	$412.77
14	infeasible	$453.60	$424.37	$424.37	$419.90
15	$472.96	$468.59	$431.74	$431.74	$426.72
16	$455.98	$452.91	$424.98	$424.98	$420.91
17	infeasible	infeasible	$445.97	$445.97	$441.40
18	$460.90	$458.35	$426.45	$426.45	$422.00
19	infeasible	infeasible	$465.85	$465.85	$461.65
20	infeasible	infeasible	infeasible	infeasible	$473.90
Expected diesel fuel cost	-	-	-	-	$419.21

3.6 Conclusion

We proposed a stochastic optimization model that determines PV array and battery capacities by considering solar irradiance uncertainty and appliance operation scheduling. Solar irradiance uncertainty was represented by 20 scenarios that were randomly chosen from the 12-year historical solar irradiance data. We integrated a diesel generator into an off-grid energy system to power appliances when there is not enough solar irradiance. A diesel generator also prevents the capacity

of the energy system depending on the worst solar irradiance day of the year. We tested the model in Auburn, AL. The model determined the optimal capacities of the PV array, battery and diesel fuel usage at the minimum AEC of the energy system under the probabilities of all-scenario occurrence. The contribution of the proposed optimization was demonstrated by comparing the results to one scenario model. Under the fixed capacity of the energy system obtained by an average scenario, one scenario model did not satisfy energy demand and represented infeasible solutions under every scenario. The effect of scheduling appliances was demonstrated through comparison of the results with a non-optimized case. Using optimization to schedule appliances satisfied the energy demand with less diesel energy usage and a more economical AEC than a non-optimized case. The effect of number of scenarios was evaluated by investigating models that consider the different number of scenarios. The results showed that the 20-scenario model was more effective than the less-scenario models since it has the optimal energy system capacity to satisfy energy demand under many possible solar irradiance occurrences.

References

[1] U.S. Energy Information Administration (EIA), (2019), International Energy Outlook 2019 with projections to 2050, Washington, DC. https://www.eia.gov/outlooks/ieo/pdf/ieo2019.pdf (accessed 25 November 2019)

[1] W. Zhou, C. Lou, Z. Li, L. Lu, H. Yang, (2010). Current status of research on optimum sizing of stand-alone hybrid solar wind power generation systems. Applied. Energy 87(2), 380-389.

[2] G.E. Ahmad, (2002). Photovoltaic-powered rural zone family house in Egypt. Renewable Energy 26(3), 379-390.

[3] M.M.H. Bhuiyan, M. Ali Asgar, (2003). Sizing of a stand-alone photovoltaic power system at Dhaka. Renewable Energy 28(6), 929-938.

[4] M. Lee, D. Soto, V. Modi, (2014). Cost versus reliability sizing strategy for isolated photovoltaic micro-grids in the developing world. Renewable Energy 69, 16-24.

[5] N.I.A. Aziz, S I. Sulaimana, S. Shaari, I. Musirin, K. Sopian, (2017). Optimal sizing of stand-alone photovoltaic system by minimizing the loss of power supply probability. Solar Energy 150, 220-228.

[6] N.D. Nordin, H.A. Rahman, (2016). A novel optimization method for designing stand alone photovoltaic system. Renewable Energy 89, 706-715.

[7] W. X. Shen, (2019). Optimally sizing of solar array and battery in a standalone photovoltaic system in Malaysia. Renewable Energy 34, 348-352.

[8] A. Mellit, (2010). ANN-based GA for generating the sizing curve of stand-alone photovoltaic systems. Advances in Engineering Software 41(5), 687-693.

[9] A. Bouabdallah, J.C. Olivier, S. Bourguet, M. Machmoum, E. Schaeffer, (2015). Safe sizing methodology applied to a standalone photovoltaic system. Renewable Energy 80, 266-274.

[10] P. Arun, R. Banerjee, S. Bandyopadhyay, (2009). Optimum sizing of photovoltaic battery systems incorporating uncertainty through design space approach. Solar Energy 83(7), 1013-1025.

[11] C.V.T. Cabral, D.O. Filho, A.S.A.C. Diniz, J.H. Martins, O.M. Toledo, L.V.B. M. Neto, (2010). A stochastic method for stand-alone photovoltaic system sizing. Solar Energy 84(9), 1628-1636.

[12] S.G. Chen, (2012). An efficient sizing method for a stand-alone PV system in terms of the observed block extremes. Applied Energy 9(1), 375-384.

[13] D.P.B. Iii, (2014). Optimal battery sizing for storm-resilient photovoltaic power island systems. Solar Energy 109, 165-173.

[14] National Centers for Environmental Information, (2012), National Solar Radiation Data Base: 1991–2010 Update [Online], Available: ftp://ftp.ncdc.noaa.gov/pub/data/nsrdb-solar/solar-only/.(accessed 3 February 2019)

[15] K.C. Sou, J. Weimer, H. Sandberg, K. H. Johansson, (2011). Scheduling smart home appliances using mixed integer linear programming. 50th IEEE Conference on Decision and Control and European Control Conference (CDC-ECC), 5144–5149.

[16] Hart, William E., Jean-Paul Watson, and David L. Woodruff, (2011). Pyomo: modeling and solving mathematical programs in Python. Mathematical Programming Computation 3(3), 219-260.

Conclusion

We proposed three optimization models for off-grid PV systems. First, we developed a daily energy consumption scheduling model of the residential stand-alone PV-battery system in an isolated area. The results showed that it is possible to optimize the use of available solar irradiance for powering appliances at home. In an off-grid situation, the battery capacity is more influential than the PV array capacity on satisfying the energy demand. In addition, under the same PV array capacity, results showed that using the optimized case to schedule appliances can fully satisfy energy demand with a smaller battery capacity than the non-optimized case.

Second, we studied an off-grid PV system design approach that considers energy consumption scheduling and system operation under solar irradiance uncertainty. The solution was obtained by integrating the Nelder-Mead algorithm, mixed-integer programming, and Monte Carlo simulation. The results showed that the N-M algorithm is able to determine cost-efficient PV array and battery capacity based on an available amount of solar irradiance. To meet the demand, the capacity of the battery is more influential than PV array capacity. The sensitivity analysis showed that the opportunity cost of non-served energy is a key factor in order to meet the demand with solar energy.

Third, we proposed a stochastic optimization model that determines PV array and battery capacity by considering solar irradiance uncertainty and appliance operation scheduling. We integrated a diesel generator into an off-grid energy system to power appliances when there was not enough solar irradiance. The model determined the optimal capacities of the PV array, battery

and expected diesel fuel usage at the minimum AEC of an energy system under the probabilities of all-scenario occurrence. The effect of scheduling was evaluated by comparing the results of the optimized with the non-optimized case. The result showed that the optimized case satisfies energy demand at lower capacities of the PV array, battery and less diesel fuel cost. The effect of number of scenarios is assessed by changing the number of scenarios considered. The result demonstrated that the more-scenario model meets energy demand better than less-scenario models under various solar irradiance scenarios.

Appendix A: Nomenclature for Chapter 1

Indices

a	Appliance (a = 1...A)
t	Time period (t = 1…T)

Parameters

A^{PV}	Area of PV array (m^2)
R^{PV}	PV array efficiency rate (%)
$\mathrm{R}^{\mathrm{INV}}$	Inverter efficiency rate (%)
$\mathrm{E}_t^{\mathrm{PV}}$	Forecasted PV array energy during period t (kWh)
$\mathrm{E}_t^{\mathrm{M}}$	Energy margin to operate occasionally used appliances during period t (kWh)
$\mathrm{S}_t^{\mathrm{PV}}$	Forecasted solar radiation incident on the PV array during period t ($\mathrm{kWh/m}^2$)
$\mathrm{R}^{\mathrm{DCH}}$	Battery self-discharging rate (%)
$\mathrm{R}^{\mathrm{CHR}}$	Battery charging efficiency rate (%)
$\mathrm{C}^{\mathrm{BAT}}$	Battery capacity (kWh)
$\mathrm{S}^{\mathrm{MAX}}$	Battery maximum SOC (%)
$\mathrm{S}^{\mathrm{ISC}}$	Battery initial SOC (%)
$\mathrm{S}^{\mathrm{ESC}}$	Battery end SOC (%)
$\mathrm{R}^{\mathrm{MCH}}$	Battery maximum charging energy (kWh)
$\mathrm{R}^{\mathrm{MDC}}$	Battery maximum discharging energy (kWh)
E_a	Energy consumption of appliance a (kWh)
T_a	Required number of periods to operate appliance a
W_a	Priority weight (1, 2, ...,10) of appliance a
$\mathrm{P}_{a,t}$	Time preference (0/1) to operate appliance a during period t
$\mathrm{P}_{a,t}^{\mathrm{non-opt.}}$	Time preference (0/1) to operate appliance a during period t in the non-optimized case
$\mathrm{P}_{a,t}^{\mathrm{opt.}}$	Time preference (0/1) to operate appliance a during period t in the optimized case

Sets

S	Set of all appliances that are preceded by at least one appliance
S_a	Set of all appliances that precede a
$\mathrm{U}^{\mathrm{app}}$	Set of all uninterruptible appliances

Variables

$e_t^{\text{app\_bat}}$	Energy discharged from the battery to operate the appliances during period *t* (kWh)
e_t^{chr}	Energy from the PV array used to charge the battery during period *t* (kWh)
$e_t^{\text{loss\_pv}}$	Energy loss from the PV array during period *t* (kWh)
$e_t^{\text{app\_pv}}$	Energy from the PV array to operate the appliances during period *t* (kWh)
s_t^{bat}	Battery SOC during period *t* (%)
y_t^{chr}	Binary variable to indicate that the battery is charging during period *t*
y_t^{dch}	Binary variable to indicate if the battery is discharging during period *t*
$x_{a,t}^{\text{app\_state}}$	Binary variable to indicate the operating state of appliance *a* during period *t*
$x_{a,t}^{\text{app\_end}}$	Binary variable to indicate that appliance *a* finished operation at the end of period *t*
z_a	Binary variable to determine the operation periods of uninterruptible appliance *a*

Appendix B: Nomenclature for Chapter 2

Indices

a	Appliance (a = 1...A)
t	Period (t = 1…T)

Parameters

C^{PV}	Capacity of PV array (kW) under Standard Test Condition (STC., i.e., for 1 kWh/m^2 of incident solar radiation)
C^{BAT}	Battery capacity (kWh)
INV^{E}	Inverter efficiency rate (%)
E_t^{PV}	Forecasted PV array energy during period t (kWh)
E_t^{R}	Reserved energy to operate occasionally used appliances during period t (kWh)
S_t^{PV}	Forecasted solar radiation incident on the PV array during period t (kWh/m^2)
R^{DCH}	Battery self-discharging rate (%)
R^{CHR}	Battery charging efficiency rate (%)
S^{MIN}	Battery minimum state of charge (%)
S^{MAX}	Battery maximum state of charge (%)
S^{ISC}	Battery initial state of charge (%)
S^{ESC}	Battery end state of charge (%)
R^{MCH}	Battery maximum charging energy (%)
R^{MDC}	Battery maximum discharging energy (%)
E_a	Energy consumption of appliance a (kWh)
T_a	Required number of periods to operate appliance a
W_a	Priority weight (1, 2, ...,10) of appliance a
$P_{a,t}$	Preference (0/1) to operate appliance a during period t
N^{PV}	Life expectancy of PV array (years)
N^{BAT}	Life expectancy of battery (Lithium-ion, years)
PV^{COST}	AEC of PV electricity per kW ($/kWh)
BAT^{COST}	AEC of battery energy per kWh ($/kWh)
NS^{COST}	Penalty cost of non-served energy ($)
PV^{CF}	Capital recovery factor of PV array
BAT^{CF}	Capital recovery factor of battery
i	Market interest rate (%)

Sets

S	Set of all appliances that are preceded by at least one appliance
S_a	Set of all appliances that precede *a*
$\mathrm{U}^{\mathrm{app}}$	Set of all uninterruptible appliances

Variables

x^{PV}	Capacity of PV array (kW) for the N-M algorithm under STC.
x^{BAT}	Battery capacity (kWh) of for the N-M algorithm
x^{NS}	Amount of non-served energy (kWh) for the N-M algorithm
$e_t^{\mathrm{app\_bat}}$	Energy discharged from the battery to operate the appliances during period *t* (kWh)
e_t^{chr}	Energy from the PV array used to charge the battery during period *t* (kWh)
$e_t^{\mathrm{loss\_pv}}$	Energy loss from the PV array during period *t* (kWh)
$e_t^{\mathrm{app\_pv}}$	Energy from the PV array to operate the appliances during period *t* (kWh)
s_t^{bat}	Battery state of charge during period *t* (%)
y_t^{chr}	Binary variable to indicate that the battery is charging during period *t*
y_t^{dch}	Binary variable to indicate if the battery is discharging during period *t*
$x_{a,t}^{\mathrm{app\_state}}$	Binary variable to indicate the operating state of appliance *a* during period *t*
$x_{a,t}^{\mathrm{app\_end}}$	Binary variable to indicate that appliance *a* finished operation at the end of period *t*
z_a	Binary variable to determine the operation periods of uninterruptible appliance *a*

Appendix C: Nomenclature for Chapter 3

Indices

s	Scenario (s = 1…S)
a	Appliance (a = 1…A)
d	Day (d = 1…D)
t	Time period (t = 1…T)

Parameters

C^{PV}	AEC of basic PV array capacity ($)
C^{BAT}	AEC of basic battery capacity ($)
C^{DG}	AEC of diesel generator ($)
C^{F}	Cost of diesel fuel ($/kWh)
B^{PV}	Basic PV array capacity (kW)
B^{BAT}	Basic battery capacity (kWh)
R^{INV}	Inverter efficiency rate (%)
$E^{R}_{d,t}$	Reserved energy to operate occasionally used appliances during period *t* of day *d* (kWh)
$S_{s,d,t}$	Forecasted solar radiation incident on the PV array during period *t* of day *d* under scenario *s* (kWh/m^2)
R^{DCH}	Battery self-discharging rate (%)
R^{CHR}	Battery charging efficiency rate (%)
S^{MIN}	Battery minimum SOC (%)
S^{MAX}	Battery maximum SOC (%)
S^{ISC}	Battery initial SOC (%)
S^{ESC}	Battery end SOC (%)
R^{MCH}	Battery maximum charging rate (kWh)
R^{MDC}	Battery maximum discharging rate (kWh)
$E_{d,a}$	Energy consumption of appliance *a* on day *d* (kWh)
$T_{d,a}$	Required number of periods to operate appliance *a* on day *d*
T^{DG}	Maximum allowable number of operation periods of diesel generator per day
$P_{d,a,t}$	Time preference (0/1) to operate appliance a during period *t* of day *d*
P_s	Probability of scenario *s* occurs

Sets

$\mathrm{S}^{\mathrm{app}}$	Set of all schedulable appliances
$\mathrm{NS}^{\mathrm{app}}$	Set of all non-schedulable appliances
$\mathrm{SQ}^{\mathrm{app}}$	Set of all appliances that are preceded by at least one appliance
$\mathrm{SQ}_{a}^{\mathrm{app}}$	Set of all appliances that precede appliance *a*
$\mathrm{U}^{\mathrm{app}}$	Set of all uninterruptible appliances

Variables

x^{PV}	Number of basic PV module (ea.)
x^{BAT}	Number of basic battery (ea.)
x_{s}^{F}	Annual amount of energy generated from diesel fuel under scenario *s* (kWh)
$\mathrm{E}_{\mathrm{s,d,t}}^{\mathrm{PV}}$	Forecasted PV array energy during period *t* of day *d* under scenario *s* (kWh)
$e_{s,d,t}^{\mathrm{app\_pv}}$	Energy from the PV array to operate the appliances during period *t* of day *d* under scenario *s* (kWh)
$e_{s,d,t}^{\mathrm{app\_bat}}$	Energy discharged from the battery to operate the appliances during period *t* of day *d* under scenario *s* (kWh)
$e_{s,d,t}^{\mathrm{chr}}$	Energy from the PV array used to charge the battery during period *t* of day *d* under scenario *s* (kWh)
$e_{s,d,t}^{\mathrm{loss\_pv}}$	Energy loss from the PV array during period *t* of day *d* under scenario *s* (kWh)
$e_{s,d,t}^{\mathrm{F}}$	Energy generated by a diesel fuel during period *t* of day *d* under scenario *s* (kWh)
$e_{s,d,t}^{\mathrm{bat}}$	Available energy in the battery during period *t* of day *d* under scenario *s* (kWh)
$y_{s,d,t}^{\mathrm{chr}}$	Binary variable to indicate that the battery is charging during period *t* of day *d* under scenario *s*
$y_{s,d,t}^{\mathrm{dch}}$	Binary variable to indicate if the battery is discharging during period *t* of day *d* under scenario *s*
$x_{s,d,a,t}^{\mathrm{app\_state}}$	Binary variable to indicate the operating state of appliance *a* during period *t* of day *d* under scenario *s*
$x_{s,d,a,t}^{\mathrm{app\_end}}$	Binary variable to indicate that appliance *a* finished operation at the end of period *t* of day *d* under scenario *s*
z_{s}^{DG}	Binary variable to determine if the diesel generator is operated or not under scenario *s*
$z_{s,d,t}^{\mathrm{DG}}$	Binary variable to determine if the generator is operated or not during period *t* of day *d* under scenario *s*